THE
PHYSICAL REVIEW
A Journal of Experimental and Theoretical Physics Established by E. L. Nichols in 1893

VOL. 55, NO. 5 MARCH 1, 1939 SECOND SERIES

On the Motion of Cosmic Rays in Interstellar Space

HANNES ALFVÉN
Forskningsinstitutet för Fysik, Stockholm, Sweden
(Received October 29, 1938)

The limitation of a current consisting of charged high energy particles (cosmic rays) passing through interstellar space is discussed. As interstellar matter is ionized, interstellar space is considered as a good conductor so that the electric field always equals zero. The motion of the particles is then governed by the magnetic fields produced by themselves. This sets a rather low upper limit to the currents through space so that a difference in intensity of cosmic rays in different points is smoothed out very slowly. This means that the intensity may vary considerably even within the galactic system. An explanation of the excess of positive particles in cosmic radiation is tentatively suggested. Arguments are given for the view that most of the rays we receive on the earth are generated within less than 1000 light years from us.

I

As the main part of the cosmic radiation very likely consists of positively charged particles an anisotropy of the radiation is equivalent to an electric current through space. As has been shown elsewhere[1] the magnetic field caused by such a current is strong enough to prevent the existence of a measurable anisotropy. Consequently, if in two adjacent volumes in space the intensity of the radiation has different values, the difference cannot be smoothed out very rapidly because a direct current from the high intensity volume to the low intensity one is limited by the magnetic field. The intensity of the cosmic radiation can therefore very well vary considerably in interstellar space. For example the intensity outside our galaxy may be very small although the intensity in our part of the galaxy is considerable.

In order to calculate the motion of cosmic rays in space we have to solve the following problem: *Suppose that cosmic rays of different energies are generated in certain parts of interstellar space* (e.g., at the double stars); *how will these rays move and what is the intensity of the radiation at a certain point?*

The general solution of the problem offers very great mathematical difficulties and no way of attack has as yet been found. We must therefore confine ourselves to a simple special case in which it is possible to estimate the factors limiting the free exchange of cosmic rays between different parts of space. It is clearly understood that there may be some danger in drawing too far-reaching general conclusions from such a special case. But on the other hand, as there no doubt always is an upper limit to a charged particle current through space, the treatment of a special case is very likely to give the right order of magnitude of this limit, and also to give a survey of the types of phenomena which must be taken into consideration.

II

The density of cosmic-ray particles in interstellar space in our neighborhood is of the order

[1] H. Alfvén, Phys. Rev. **54**, 97 (1938).

of magnitude of 10^{-10} or 10^{-11} cm^{-3}. The density of interstellar matter is of the order of magnitude of 10^{-25} g cm^{-3} and at least a considerable part of it consists of slow ions and electrons. Consequently, the number of slow ions in interstellar space can be supposed to be of the order of magnitude of 10^{-2} of 10^{-3} cm^{-3}, i.e., there are about 10^8 slow ions or electrons to every cosmic-ray particle. Any space charge set up by the cosmic rays will therefore be neutralized very

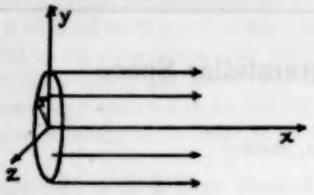

FIG. 1.

easily through a small displacement of the slow particles. In other words, as interstellar space can be assumed to be a good conductor no considerable electric field can be established. In the following we assume that *the electric field is zero* in a system where the interstellar matter is at rest, and that only magnetic forces act upon the cosmic rays. As the magnetic fields from celestial bodies are confined to their close neighborhood the motion of cosmic rays is governed by the magnetic fields produced by their own motion.

III

As an example we will treat the following special case. Suppose that we have an infinite conducting plane (y–z plane (Fig. 1)) in interstellar space. From a circular surface with the radius r_0 charged particles (for example positives) are emitted in the direction of the positive x axis, all of them having the same mass m and the same energy eV, the latter being of the same order of magnitude as that of the cosmic rays. We consider the state when the emission has been going on at a constant rate for a considerable time so that all transient phenomena have disappeared. The space charge of the emitted particles is then neutralized by slow ions so that the emitted particles travel under the influence of the magnetic field of the ray itself. (In order to close the current we can assume that the emitted charge is brought back to the surface through slow ions at a large distance from the x axis. Or we can assume that a corresponding number of negative rays is emitted from the surface in the direction of the negative x axis.)

Let i_0 be the current density of the emitted rays. If the total current $I=\pi r^2 i_0$ is very small ($\ll cV$, where c is the velocity of light), the beam is a circular cylinder and causes a magnetic field:

$$H=2Ir/cr_0^2; \quad r<r_0. \tag{1a}$$

$$H=2I/cr; \quad r>r_0. \tag{1b}$$

If I increases so that the magnetic field is considerable, the particles in the beam are deviated towards the axis. The radius of curvature of their path is

$$\rho=(V^2+2mc^2V/e)^{\frac{1}{2}}/H \tag{2}$$

or if $eV\gg mc^2$

$$\rho=V/H. \tag{2a}$$

As a first approximation we assume that (1) still holds. The equation of the motion is then

$$\rho=-\frac{[1+(dr/dx)^2]^{\frac{1}{2}}}{d^2r/dx^2}=\frac{cVr_0^2}{2Ir} \quad \text{if } r<r_0, \tag{3a}$$

$$=cVr/2I \quad \text{if } r>r_0. \tag{3b}$$

The Eq. (3a) can be integrated by means of elliptic functions. Fig. 2 shows the path of particles starting in the direction of the x axis at different distances from it and obeying (3a). It is evident that the particles on the paths $aa'a''$, $bb'b''$, $cc'c''$, and $dd'd''$ on the whole move in the positive direction so that they constitute a part of the beam. But the particles on the paths $ee'e''$ and $ff'f''$ go in the opposite direction. Consequently, only the particles up to a certain limit $r=r'$ situated between d and e will take part in the beam. If we put $r_0=r'$ and apply (3b) to the portion $r>r_0$, the paths $ee'e''$ and $ff'f''$ still go in the negative direction. The limit r_0' is reached when

$$I_0=1.65cV. \tag{4}$$

If we now try to calculate the motion of the particles not in the magnetic field given by (1) but in the real field produced by the particles themselves it is evident that the limit is changed, but it must still have the same order of magnitude. Consequently, *the maximum current in a*

direct beam through interstellar space is of the order of magnitude of

$$I_0 \sim cV \tag{5}$$

(or expressed in practical units

$$I_0 \sim V/30, \tag{5a}$$

where I_0 is the maximum current in amperes and V is the energy of the particles in electron volts).[2]

It is interesting that the limit does not depend upon the current density or cross section of the beam, but only on the energy. If $V=10^{19}$ ev and $i_0=0.5\times10^{-19}$ amp./cm^2 the radius of the beam is $r'\sim0.5\times10^{14}$ cm $=0.5\times10^{-4}$ light year.

IV

We have found that in a beam consisting of positive *or* negative particles the number of particles per second cannot surpass the order of magnitude of $I_0/e\sim cV/e$. But if we have a beam consisting of positive *and* negative particles to the same amount and equally distributed the magnetic field of the beam is zero and there seems to be no upper limit to the number of particles.

But as we have supposed interstellar space to be a good conductor, such a beam represents an *unstable* condition, and even a very small disturbance causes it to break up. Suppose that the beam passes through a very weak magnetic field in the direction of the z axis (Fig. 1). Then the positive particles are bent downwards and the negative particles upwards. The separation of the particles gives rise to a current in the direction of the positive x axis in the part of the beam below the x–z plane and a current in the opposite direction above the x–z plane. The magnetic fields of these currents increase the separation which causes a further increase of the magnetic field, so that the beam breaks up into a positive particle beam and a negative particle beam, traveling in opposite directions (parallel to the y axis).[3]

Consequently, even in this case the number of particles in a beam underlies the same limitation.

[2] If eV is not much larger than mc^2, the limit is $I_0\sim c(V^2+2mc^2V/e)^{\frac{1}{2}}$.

[3] Also, the isotropic emission of the same amount of positive and negative particles from the surface of a sphere is unstable, if the medium around the sphere is conducting.

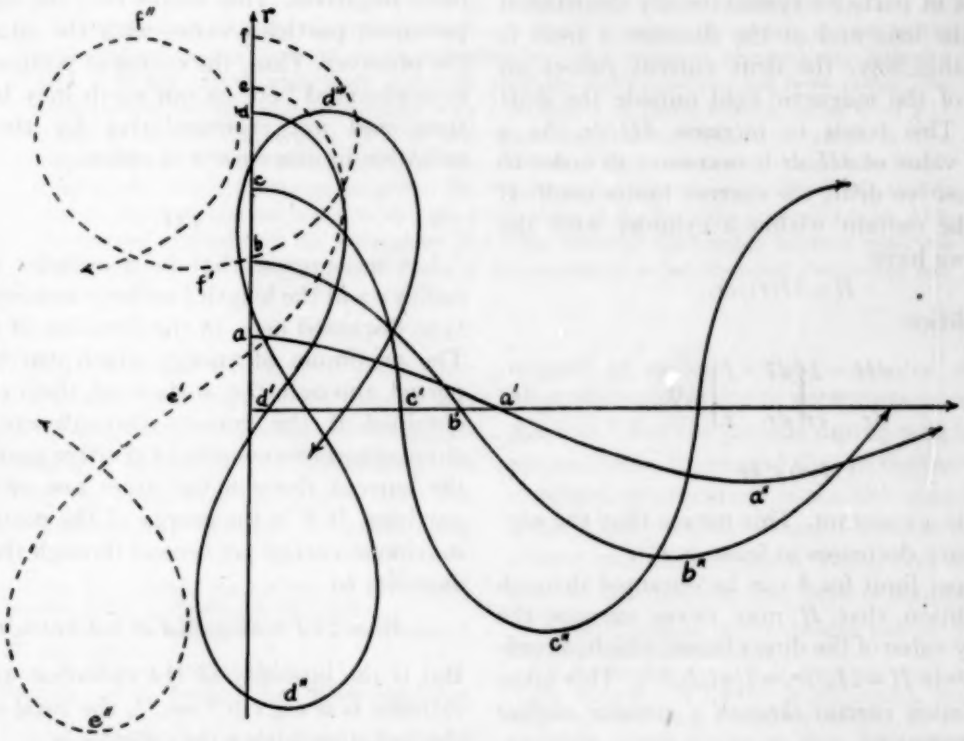

FIG. 2. Paths satisfying Eq. (3a) for particles starting in the direction of the x axis at different distances from it.

V

The upper limit to the current in a beam as found in Section III does not, however, represent the upper limit of the total current through a plane perpendicular to the x axis. Outside the beam the magnetic field decreases as r^{-1}. If a positive particle starts at g in Fig. 3 in the direction of the positive x axis, it follows the path $gg'g''g'''$. It is evident that upon the whole it moves in the direction of the positive x axis. It is

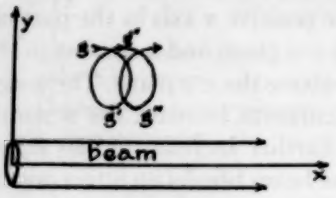

FIG. 3.

easy to show that all positive particles drift in this way if they move in regions where $dH/dr<0$. If $dH/dr>0$ they drift in the opposite directions and if $dH/dr=0$ they have no drift at all in the x direction.

If a lot of particles symmetrically distributed around the axis and at the distance r from it drift in this way, the drift current causes an increase of the magnetic field outside the drift current. This tends to increase dH/dr. As a negative value of dH/dr is necessary in order to give a positive drift, the current limits itself. If $I(r)$ is the current within a cylinder with the radius r we have

$$H=2I(r)/cr.$$

The condition

$$\frac{dH}{dr}=\frac{2}{cr}\left[\frac{dI}{dr}-\frac{I}{r}\right]<0 \qquad (6)$$

gives

$$I(r)<kr \qquad (7)$$

where k is a constant. This means that the current density decreases at least as r^{-1}.

An upper limit for k can be obtained through the condition that H may never surpass the boundary value of the direct beam, which according to (1) is $H=2I_0/cr_0=2(\pi i_0 I_0)^{\frac{1}{2}}/c$. This gives *the maximum current through a circular surface with the radius* r

$$I<(\pi i_0 I_0 r^2)^{\frac{1}{2}}, \qquad (8)$$

where i_0 is the current density in the direct beam and I_0 is given by (5).

It must be pointed out that except in the direct beam and its close neighborhood the anisotropy of the radiation is very small.

VI

It is interesting to observe that if a positive-particle current of the type described in Section V is established, a negative particle must drift in the opposite direction. Thus even in the drift-current region we have the same phenomenon as described in Section IV. Positive and negative particles have a tendency to travel in opposite directions. In the absence of electrostatic forces the magnetic forces between currents in wires tend to make the currents parallel. This is a phenomenon of the same type.

Thus it seems likely that if positive and negative cosmic-ray particles are generated in a certain volume, they will leave it in opposite directions. Consequently, an observer situated on one side of the generators finds an excess of positive particles, an observer on the other side receives more negatives. This means that the sign of the prevalent particles varies with the situation of the observer. Thus, the excess of positive cosmic rays observed here on our earth may be fortuitous, and not representative for the cosmic radiation in other parts of space.

VII

Let us suppose that in a cylinder with the radius r and the length l we have a current of the type discussed here, in the direction of the axes. The maximum of energy which can be transported through the surface of the cylinder is obtained if the current through one of the circular surfaces consists of positive particles and the current through the other one of negative particles. If V is the energy of the particles, the maximum energy per second through the surface amounts to

$$W_r=2VI=2V(\pi r^2 i_0 I_0)^{\frac{1}{2}}=2(\pi c)^{\frac{1}{2}} i_0^{\frac{1}{2}} r V^{\frac{1}{2}}.$$

But if the intensity of the radiation within the cylinder is w erg cm^{-2} sec.$^{-1}$, the total energy of the radiation within the cylinder is

$$W=3w\pi r^2 l/c.$$

The time necessary to empty or to fill the cylinder is (if $w=i_0V$)

$$T=W/W_r=(3\pi^{\frac{1}{2}}rl/2c^{\frac{1}{2}})(i_0/V)^{\frac{1}{2}}.$$

Putting $V=\frac{1}{3}\times10^{8}$ e.s.u. and $i_0=2\times10^{-10}$ e.s.u. (which corresponds to the intensity at the top of the atmosphere) and $l/2=r=1000$ light years (10^{21} cm), we find $T=10^{11}$ years, which is more than the age of the universe! Further, if we calculate the absorption in interstellar matter within the cylinder, we find that it is many times as large as W_r.

Let us now suppose that our earth is situated within the cylinder. We have found that unless the values of i_0 and V are *many* times larger at the surface of the cylinder than the values measured at the top of the earth's atmosphere (which is improbable), the current through the surface can neither fill the cylinder to the intensity measured here, nor compensate for the absorption losses. Consequently, *cosmic radiation must have been generated within the cylinder.*

This indicates that *most of the cosmic radiation we obtain here on earth has been generated within a distance of less than 1000 light years.*[4] (The thickness of the galactic system is about 10,000, the diameter about 100,000 light years.)

[4] Compare, H. Alfvén, Comptes rendus **204**, 1180 (1937).

MARCH 1, 1939 PHYSICAL REVIEW VOLUME 55

Long Period Variations of Cosmic Rays

PIARA S. GILL
University of Chicago, Chicago, Illinois

(Received November 14, 1938)

With the data from the Carnegie Institution's Model C cosmic-ray meters at four widely separated stations, a study of yearly variations and of a variation of cosmic-ray intensity with a 28-day period, apparently connected with the sun's rotation, has been made. The amplitude of the first annual harmonic with a maximum in colder months varies from 2.15 ±0.06 percent at Cheltenham, 38°.7 N to 0.15±0.03 percent at Huancayo, 12°.05 S. The amplitude of a 27.9-day period is 0.18 percent. Values of the atmospheric temperature coefficient at the different stations are given. The results give some support to Blackett's theory that the annual variation is due to changes in elevation of the barytron producing layer with the thermal expansion of the atmosphere. No other essential relationship between observed annual variation of cosmic-ray intensity and meteorological or astronomical phenomena has shown itself.

IN ADDITION to the well-known daily variation of cosmic-ray intensity, evidence has been given for the existence of seasonal variations and of variations following the rotation of the sun.[1–7] With the data that has come from the Carnegie Institution's Model C cosmic-ray meters[8] at various widely separated stations, a more thorough study of such variations has been possible.* For the periods during which the data are available, it is found that in the northern and southern temperature zones the cosmic-ray intensity has been significantly greater during the winter months. Seasonal variations occur likewise in the tropics, but here a six-month peri-

[1] J. Clay, Proc. Roy. Acad., Amsterdam **23**, 711 (1930).
[2] E. G. Steinke, Zeits. f. Physik **64**, 48 (1930).
[3] J. A. Priebsch and R. Steinmaurer, Gerlands Beitr. z. Geophys. **37**, 296 (1932).
[4] V. F. Hess, Terr. Mag. **41**, 345 (1936).
[5] J. A. Priebsch and W. Baldauf, Ber. Wien Akad. IIa, **145**, 583 (1936).
[6] A. H. Compton and R. N. Turner, Phys. Rev. **52**, 799 (1937).
[7] B. F. J. Schonland, B. Delatizky and J. Gaskell, Terr. Mag. **42**, 137 (1937).
[8] A. H. Compton, E. D. Wollan and R. D. Bennett, Rev. Sci. Inst. **5**, 415 (1934).

* *Note added in proof:* S. E. Forbush, has just published (Phys. Rev. **54**, 975 (1938)) an independent analysis of the same data, following a different method. He finds seasonal variations closely similar to those here reported, and in addition world-wide changes closely correlated between the various stations. Forbush pays slight attention to the variations following the solar rotation.

odicity becomes relatively prominent. There is likewise found a significant variation of cosmic-ray intensity with a 28-day period, which is probably to be associated with the time of the sun's rotation.

Earlier studies by Clay,[1] Steinke,[2] and Priebsch and Steinmaurer[3] indicated seasonal changes of several percent with a maximum in summer. The more extensive study made by Hess,[4] Priebsch and Baldauf,[5] with data obtained on the Hafelekar in Austria during 1932–34, however, showed changes of about the same magnitude but with the maximum in winter. This result was confirmed by Compton and Turner,[6] in their studies of the cosmic rays on the Pacific Ocean during 1936–37, where the maximum was found to occur in the winter in both hemispheres. The data of Compton and Turner were, however, of lower statistical weight, and obtained under considerably less favorable experimental conditions, than those used in the present investigation.

Significant evidence for a period of about 27 days in the cosmic-ray data collected on the Hafelekar has been presented by Hess[4] and Graziadei.[9] It has seemed worth while to extend this analysis, with a different method, to the more complete data now available. Their findings are definitely confirmed, and it has been shown that the effect is world-wide.

TABLE I. *Annual variation of cosmic rays at four stations in percent of mean ionization.*

Station	First Harmonic (12-mo. period)		Second Harmonic (6-mo. period)	
	Amp.	Phase	Amp.	Phase
Cheltenham, 38°.7 N. 76°.8 W. mean bar., 760 mm	2.15 ±0.06	84° ±2°	0.58 ±0.06	245° ±6°
Teoloyucan, 19°.75 N. 99°.2 W. mean bar., 585 mm	0.86 ±0.04	42° ±3°	0.53 ±0.04	265° ±5°
Huancayo, 12°.05 S. 75°.3 W. mean bar., 515 mm	0.15 ±0.03	163° ±13°	0.18 ±0.03	307° ±11°
Christchurch 43°.5 S. 172°.6 E. mean bar., 760 mm	0.27 ±0.04	205° ±9°	0.36 ±0.04	53° ±7°

[9] H. Th. Graziadei, Ber. Wien Akad. IIa, **145**, 495 (1936).

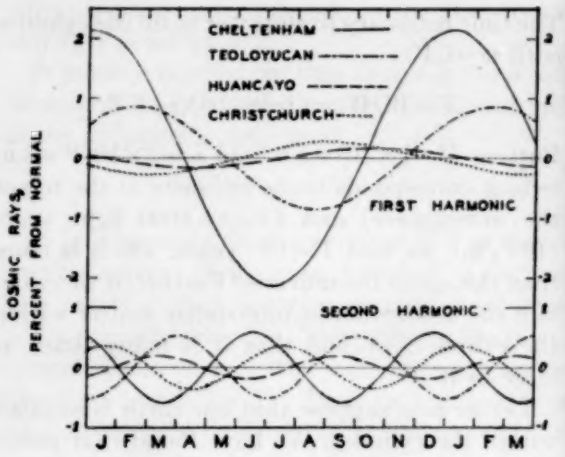

FIG. 1. First and second harmonics fitted to monthly mean ionization.

SEASONAL VARIATION OF COSMIC-RAY INTENSITY

The data used in this analysis were obtained from meters stationed at Cheltenham, Maryland; Teoloyucan, Mexico; Huancayo, Peru and Christchurch, New Zealand. They cover, respectively, the periods, from March, 1937 through February, 1938 at Teoloyucan, from July, 1936 through August, 1937 at Huancayo, and from April through December, 1936, and from April through June, 1937 at Christchurch. These meters measure the ionization in argon by cosmic rays that have been filtered through the equivalent of 12 cm of lead.

In analyzing the data, daily mean ionizations corrected to normal barometric pressure were tabulated, and monthly means were calculated. Previous studies had shown that no correction was required for the slightly variable temperature of the meter. Monthly mean ionizations, centered at mid-months, were used in obtaining the Fourier coefficients for the first and second harmonics. The calculations were made according to Duvall's formulae,[10] using for the probable error his function ϵ_y. Table I gives the amplitudes as thus obtained for the first and second harmonics, expressed in percentages of the total, or absolute, cosmic-ray ionization at each station. The tabulated probable errors for each place are the arithmetic means of those two months for which the probable errors were highest and lowest.

[10] C. R. Duvall, Terr. Mag. **32**, 151 (1927).

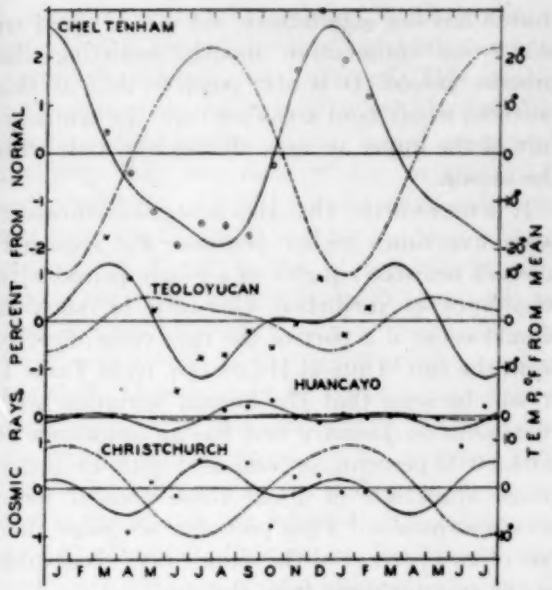

FIG. 2. Sum of first and second harmonics fitted to monthly mean ionization due to cosmic rays (heavy lines) and the sum of first and second harmonics fitted to monthly mean temperatures (broken lines).

At Huancayo the monthly mean ionization decreased almost linearly. Hence a least-squares line was fitted to the fourteen months data from July 1936 to August 1937, and the harmonic analysis was applied to the central twelve deviations from this line. For the other stations, no such adjustment was required.

Figure 1 shows the first and second harmonics at the various stations. In Fig. 2 are shown the sums of these two harmonics, and the datum points from which they are calculated. Likewise in this figure are given the sums of the first two harmonics of the mean temperature[11] at, or near, these stations.

COSMIC-RAY INTENSITY AND EXTERNAL TEMPERATURE

The maxima of the sum of the first and second harmonics at Cheltenham and Christchurch come approximately during the middle of the cold months at the respective places. At Teoloyucan and Huancayo, where the second harmonics play as important a part as the first, and where the seasonal temperature changes are small, the cosmic-ray maxima occur during the spring, i.e., about March 21, at Teoloyucan, and September 23 at Huancayo.

Nevertheless, except at Cheltenham, no significant correlation is found between the monthly mean cosmic-ray intensity and monthly mean atmospheric temperatures. The results of this correlation study are shown in Table II. In this table the calculation from Huancayo is omitted because the seasonal temperature variation is only about 0.5°C from the mean, so that any correlation with the temperature could only be fortuitous.

A comparison with Compton and Turner's[6] results from the Pacific Ocean shows that where the correlation coefficient is significant (Cheltenham) the magnitude of the atmospheric temperature coefficient agrees satisfactorily with their finding. It is apparent, from the present data however, as they had indeed suspected, that in other places the temperature of the atmosphere does not serve even as an approximate index of the cosmic-ray intensity. Moreover, though the temperature changes from week to week and from day to day at Cheltenham are quite large, Forbush[12] shows that over such short periods no significant correlation with temperature exists. It follows that neither local changes in temperature nor those associated with transient cyclones affect appreciably the cosmic-ray intensity. This conclusion is in no way contrary to the evidence here presented for a real temperature coefficient when the interval is extended over a month or a year.

TABLE II. *Atmospheric temperature coefficient of cosmic-ray ionization (reduced to standard barometer).*

LOCATION	COEFFICIENT PERCENT	CORRELATION COEFFICIENT
From the data of this paper		
Cheltenham	-0.15 ± 0.02	-0.90 ± 0.04
Teoloyucan	-0.08 ± 0.09	-0.19 ± 0.19
Christchurch	(-0.05 ± 0.02)	(-0.31 ± 0.20)
From the data of Compton-Turner		
Vancouver	-0.22 ± 0.02	-0.85 ± 0.04
Auckland	-0.16 ± 0.04	-0.47 ± 0.15
Sydney	-0.10 ± 0.02	-0.67 ± 0.10
At Sea	-0.18 ± 0.01	-0.68 ± 0.03

[11] Temperatures obtained at Cheltenham from U. S. Monthly Weather Review (monthly means from March 1936 to February 1937), Mexico City from Mexican Weather Reports (monthly means from 1878 to 1924), Arequipa, Peru (monthly means from 1892 to 1912), and Christchurch, New Zealand (monthly means from 1864 to 1923).

[12] S. E. Forbush, Terr. Mag. **42**, 1 (1937).

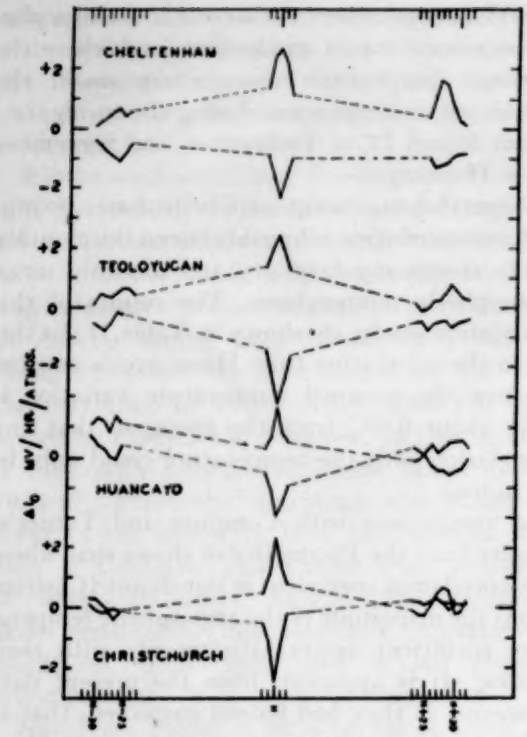

FIG. 3. Curves showing the occurrence of the first positive and negative pulses after an arbitrarily chosen pulse for highest or lowest values of daily mean cosmic-ray intensity at each station.

Blackett[13] has made a theoretical calculation of the temperature coefficient of the cosmic-ray intensity, using the hypothesis of the instability of the barytron as discussed by Euler and Heisenberg.[14] For the north temperate zone he estimates by two different methods, $\alpha=-0.16$ and $\alpha=-0.20$ percent per degree centigrade. Near the equator he mentions that the temperature coefficient should be considerably less. For the south temperate zone, because data regarding the temperature of the atmosphere at high altitudes for the various seasons are lacking, no quantitative prediction is made. It will be noted that these estimates are in good general agreement with the values listed in Table II. In addition to good quantitative agreement in the north temperate zone, we see an indication of the predicted decrease in α near the equator in the data from Teoloyucan. The value from Christchurch has low significance, since it is based on only nine consecutive months omitting the summer period. It is also possible that at this latitude, where land areas are rare, the temperature of the upper air may change but little with the season.

It is noteworthy that this analysis confirms to some five times higher precision the reported[6] absence near the equator of a yearly period with maximum at perihelion (January 1), such as should occur if a part of the rays come directly from the sun. Thus at Huancayo, from Table I, it will be seen that the annual variation with maximum on January first has an amplitude of 0.04 ± 0.03 percent, as compared with an anticipated amplitude of about three percent for a solar component.[6] Thus probably not more than one or two percent of the cosmic rays observable at the equator come from the sun.

Similarly, this analysis fails to reveal any evident affect ascribable to shielding by the action of the sun's magnetic field. This might have been expected to reduce the mean world intensity of cosmic rays when the earth is close to the sun on January first. The average of all data would be a very small change of opposite sign.

The result is that the present analysis shows definite seasonal variations at the locations and for the periods investigated. Though at Cheltenham there is a close correlation with atmospheric temperature, it is clear that there is no direct dependence of cosmic-ray intensity on transient changes of air temperature. The data give some support, however, to Blackett's view that this seasonal variation of cosmic rays is caused by the changing altitude of the barytron-producing layer with the thermal expansion of the atmosphere.

TWENTY-SEVEN-DAY PERIOD IN COSMIC-RAY INTENSITY

When the daily mean ionization as observed at the different stations was plotted against time, there occasionally appeared variations having a period of roughly a month which could be followed through several cycles and then gradually became confused with other variations. This suggested the search for a variation of a quasi-periodic type such as has been reported by Hess[4] and Graziadei.[9]

[13] P. M. S. Blackett, Phys. Rev. **54**, 973 (1938).
[14] H. Euler and W. Heisenberg, Ergebn. d. Exakt. Naturwiss. **17**, 1 (1938).

Chree's method,[15] developed in his studies of the 27-day period in international magnetic character numbers, was followed. This method consists in selecting in each month the five days showing the highest daily mean cosmic-ray intensity. Let the date of the maximum be indicated by n. Then the daily mean values for the dates $n+23, \cdots 32$ and for $n-23, \cdots 32$ are plotted. If a real period of roughly 27 days exists, the resulting graph should show greater than normal intensity, with a maximum near $n+27$ and $n-27$. If the period sought for does not exist, there should be equal probability of finding greater or less intensity than average for the month on the dates $n \pm 27$. Similarly, the five days having the lowest daily mean intensity during the month are selected, determining the date of observed minimum m. We should then anticipate less than normal intensity near $m \pm 27$ days if there is a true period of about 27 days.

Figure 3 shows the resulting values at dates near $n \pm 27$ and $m \pm 27$ as averaged over all the data available from our four stations. It is significant that in every one of the eight cases the intensity on the date $n \pm 27$ (or 28) is greater than on the date $m \pm 27$ (or 28). Had there been no periodicity of approximately this length, whether the former values would be the larger would be a matter of chance, with a probability for a favorable result eight times out of eight of one in 256. It is thus evident that the periodicity under investigation is a real one.

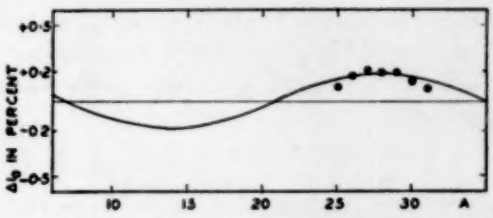

FIG. 4. Cosine curve drawn through the points $a=25$ to $a=31$ in order to determine the exact period of 27 or 28-day variation in cosmic-ray intensity.

In order to determine more exactly the length of the period, the departures ΔI_0 of the daily mean value of I_0 have been averaged over the a's for the dates $n+a$, $n-a$, $m+a$ and $m-a$, reversing the sign of the ΔI_0's for $m+a$ and $m-a$. Figure 4 shows the result. It will be noted that the points for $a=25$ to $a=31$ lie roughly on the first peak of a cosine curve whose period is about 27.9 days and whose amplitude is 0.18 percent.

The two prominent astronomical periods of approximately this length are (1) the sidereal month, of 27.32 days, and (2) the period of the sun's rotation relative to the earth.[16] This period varies from about 26 days at the equator to 32 days at 80°, with a mean value given as about 27.1 days. The lack of persistence of the quasi-periodic changes that we are discussing suggests that they should not be associated with something so definite as the revolution of the moon. On the other hand, this characteristic fits well with the view that they may be associated with some surface activity on the sun, such as sun spots. The known correlation between the appearance of sun spots and terrestrial magnetic disturbances lends support to this suggestion.

The writer wishes to express his sincere thanks to Professor A. H. Compton for his inspiring guidance and for his continuous interest in this investigation. The writer also wishes to acknowledge his indebtedness to Mrs. Ardis T. Monk for useful suggestions and help in calculations. Grateful acknowledgment is made to Dr. J. A. Fleming, Director of the Department of Terrestrial Magnetism, for supplying most of the records for this investigation.

[15] C. Chree, Phil. Trans. Roy. Soc. **A212**, 75 (1913); C. Chree and J. M. Stagg, Phil. Trans. **A227**, 21 (1927).

[16] Cf. *International Critical Tables* (1926), Vol. 1, p. 392.

Energy Production in Stars*

H. A. BETHE
Cornell University, Ithaca, New York

(Received September 7, 1938)

It is shown that the *most important source of energy in ordinary stars is the reactions of carbon and nitrogen with protons.* These reactions form a cycle in which the original nucleus is reproduced, *viz.* $C^{12}+H=N^{13}$, $N^{13}=C^{13}+\epsilon^+$, $C^{13}+H=N^{14}$, $N^{14}+H=O^{15}$, $O^{15}=N^{15}+\epsilon^+$, $N^{15}+H=C^{12}+He^4$. Thus carbon and nitrogen merely serve as catalysts for the combination of four protons (and two electrons) into an α-particle (§7).

The carbon-nitrogen reactions are unique in their cyclical character (§8). For all nuclei lighter than carbon, reaction with protons will lead to the emission of an α-particle so that the original nucleus is permanently destroyed. For all nuclei heavier than fluorine, only radiative capture of the protons occurs, also destroying the original nucleus. Oxygen and fluorine reactions mostly lead back to nitrogen. Besides, these heavier nuclei react much more slowly than C and N and are therefore unimportant for the energy production.

The agreement of the carbon-nitrogen reactions with observational data (§7, 9) is excellent. In order to give the correct energy evolution in the sun, the central temperature of the sun would have to be 18.5 million degrees while integration of the Eddington equations gives 19. For the brilliant star Y Cygni the corresponding figures are 30 and 32. This good agreement holds for all bright stars of the main sequence, but, of course, not for giants.

For fainter stars, with lower central temperatures, the reaction $H+H=D+\epsilon^+$ and the reactions following it, are believed to be mainly responsible for the energy production. (§10)

It is shown further (§5–6) that *no elements heavier than* He^4 *can be built up in ordinary stars.* This is due to the fact, mentioned above, that all elements up to boron are disintegrated by proton bombardment (α-emission!) rather than built up (by radiative capture). The instability of Be^8 reduces the formation of heavier elements still further. The production of neutrons in stars is likewise negligible. The heavier elements found in stars must therefore have existed already when the star was formed.

Finally, the suggested mechanism of energy production is used to draw conclusions about astrophysical problems, such as the mass-luminosity relation (§10), the stability against temperature changes (§11), and stellar evolution (§12).

§1. INTRODUCTION

THE progress of nuclear physics in the last few years makes it possible to decide rather definitely which processes can and which cannot occur in the interior of stars. Such decisions will be attempted in the present paper, the discussion being restricted primarily to main sequence stars. The results will be at variance with some current hypotheses.

The first main result is that, under present conditions, no elements heavier than helium can be built up to any appreciable extent. Therefore we must assume that the heavier elements were built up *before* the stars reached their present state of temperature and density. No attempt will be made at speculations about this previous state of stellar matter.

The energy production of stars is then due entirely to the combination of four protons and two electrons into an α-particle. This simplifies the discussion of stellar evolution inasmuch as the amount of heavy matter, and therefore the opacity, does not change with time.

The combination of four protons and two electrons can occur essentially only in two ways. The first mechanism starts with the combination of two protons to form a deuteron with positron emission, *viz.*

$$H+H=D+\epsilon^+. \tag{1}$$

The deuteron is then transformed into He^4 by further capture of protons; these captures occur very rapidly compared with process (1). The second mechanism uses carbon and nitrogen as catalysts, according to the chain reaction

$$\begin{aligned} &C^{12}+H=N^{13}+\gamma, && N^{13}=C^{13}+\epsilon^+\\ &C^{13}+H=N^{14}+\gamma,\\ &N^{14}+H=O^{15}+\gamma, && O^{15}=N^{15}+\epsilon^+\\ &N^{15}+H=C^{12}+He^4. \end{aligned} \tag{2}$$

The catalyst C^{12} is reproduced in all cases except about one in 10,000, therefore the abundance of carbon and nitrogen remains practically unchanged (in comparison with the change of the number of protons). The two reactions (1) and

* Awarded an A. Cressy Morrison Prize in 1938, by the New York Academy of Sciences.

(2) are about equally probable at a temperature of $16 \cdot 10^6$ degrees which is close to the central temperature of the sun ($19 \cdot 10^6$ degrees[1]). At lower temperatures (1) will predominate, at higher temperatures, (2).

No reaction other than (1) or (2) will give an appreciable contribution to the energy production at temperatures around $20 \cdot 10^6$ degrees such as are found in the interior of ordinary stars. The lighter elements (Li, Be, B) would "burn" in a very short time and are not replaced as is carbon in the cycle (2), whereas the heavier elements (O, F, etc.) react too slowly. Helium, which is abundant, does not react with protons because the product, Li^5, does not exist; in fact, the energy evolution in stars can be used as a strong additional argument against the existence of He^5 and Li^5 (§3).

Reaction (2) is sufficient to explain the energy production in very luminous stars of the main sequence as Y Cygni (although there are difficulties because of the quick exhaustion of the energy supply in such stars which would occur on any theory, §9). Neither of the reactions (1) or (2) is capable of accounting for the energy production in giants; if nuclear reactions are at all responsible for the energy production in these stars it seems that the only ones which could give sufficient energy are

$$H^2+H=He^3 \qquad (3)$$

$$Li^{6,7}+H=He^{3,4}+He^4.$$

It seems, however, doubtful whether the energy production in giants is due to nuclear reactions at all.[2]

We shall first calculate the energy production by nuclear reactions (§2, 4). Then we shall prove the impossibility of building up heavier elements under existing conditions (§5–6). Next we shall discuss the reactions available for energy production (§5, 7) and the results will be compared with available material on stellar temperatures and densities (§8, 9). Finally, we shall discuss the astrophysical problems of the mass-luminosity relation (§10), the stability of stars against temperature changes (§11) and stellar evolution (§12).

[1] B. Strömgren, Ergebn. d. Exakt. Naturwiss. **16**, 465 (1937).
[2] G. Gamow, private communication.

§2. Formula for Energy Production

The probability of a nuclear reaction in a gas with a Maxwellian velocity distribution was first calculated by Atkinson and Houtermans.[3] Recently, an improved formula was derived by Gamow and Teller.[4] The total number of processes per gram per second is[4]

$$p=\frac{4}{3^{5/2}}\frac{\rho x_1 x_2}{m_1 m_2}\frac{\Gamma}{\hbar}aR^2 e^{4(2R/a)^{\frac{1}{2}}}\tau^2 e^{-\tau}. \qquad (4)$$

Here ρ is the density of the gas, x_1x_2 the concentrations (by weight) of the two reacting types of nuclei, m_1m_2 their masses, Z_1e and Z_2e their charges, $m=m_1m_2/(m_1+m_2)$ the reduced mass, R the combined radius,

$$a=\hbar^2/me^2Z_1Z_2 \qquad (5)$$

the "Bohr radius" for the system, $\Gamma/\hbar$ the probability of the nuclear reaction, in sec.$^{-1}$, after penetration, and

$$\tau=3\left(\frac{\pi^2 me^4 Z_1^2 Z_2^2}{2\hbar^2 kT}\right)^{\frac{1}{3}}. \qquad (6)$$

If we measure ρ in g/cm^3, Γ in volts and T in units of 10^6 degrees, we have

$$p=5.3\cdot 10^{25}\rho x_1x_2\Gamma\varphi(Z_1,Z_2)\tau^2e^{-\tau}\ \text{g}^{-1}\text{sec.}^{-1}, \qquad (7)$$

$$\tau=42.7(Z_1Z_2)^{\frac{1}{3}}(A/T)^{\frac{1}{3}}, \qquad (8)$$

$$\varphi=\frac{1}{A_1A_2(Z_1Z_2A)^{\frac{1}{3}}}\left(\frac{8R}{a}\right)^2 e^{2(8R/a)^{\frac{1}{2}}}. \qquad (9)$$

where A_1A_2 are the atomic weights of the reacting nuclei ($A_i=m_i/m_H$), $A=m/m_H$, m_H = mass of hydrogen. For the combined radius of nuclei 1 and 2 we put

$$R=1.6\cdot 10^{-13}(A_1+A_2)^{\frac{1}{3}}\ \text{cm.} \qquad (10)$$

Then we obtain for φ the values given in Table I. The values of φ for isotopes of the same element differ only very slightly.

The values of Γ for reactions giving particles can be deduced from the *observed* cross sections

[3] R. d'E. Atkinson and F. G. Houtermans, Zeits. f. Physik **54**, 656 (1929).
[4] G. Gamow and E. Teller, Phys. Rev. **53**, 608 (1938), Eq. (3).

TABLE I. *Values of φ for various nuclear reactions.*

REACTION	R (10^{-13} CM)	φ	REACTION	R	φ
H^2+H	2.3	0.38	$Si^{30}+H$	5.0	29.3
H^3+H	2.5$_5$	0.48	$Cl^{37}+H$	5.4	75
He^4+H	2.7$_5$	0.81	H^2+H^2	2.5$_5$	0.67
Li^7+H	3.2	0.91	Be^7+H^2	3.3	1.18
Be^9+H	3.4$_5$	1.16	Be^7+He^3	3.4$_5$	7.9
$B^{11}+H$	3.6$_5$	1.52	He^4+H^2	2.9	0.57
$C^{12}+H$	3.7$_5$	2.00	He^4+He^3	3.0$_5$	1.09
$N^{14}+H$	3.9$_5$	2.78	He^4+He^4	3.2	1.29
$O^{16}+H$	4.1	3.80	Li^7+He^4	3.5$_5$	4.9
$F^{19}+H$	4.3$_5$	5.5	Be^7+He^4	3.5$_5$	13.2
$Ne^{22}+H$	4.5$_5$	7.7	Be^8+He^4	3.6$_5$	16.2
$Mg^{26}+H$	4.8	13.2	$C^{13}+He^4$	4.0	230

TABLE II. *Cross sections and widths for some nuclear reactions giving particles.*

REACTION	REF.	E KV	σ CM^2	R CM	Γ
$H^3+H^3=He^3+n^1$	5	100	$1.7\cdot10^{-28}$	$2.6\cdot10^{-13}$	$3\cdot10^5$
$Li^7+H^1=2He^4$	6	42	$1.7\cdot10^{-28}$	$3.2\cdot10^{-13}$	$4\cdot10^6$
$Li^6+H^1=He^4+He^3$	yield $\sim$ same as Li^7+H in natural Li target				$5\cdot10^5$
$Li^6+H^2=\{2He^4 \mid Li^7+H\}$	7	212	$1.9\cdot10^{-26}$	$3.2\cdot10^{-13}$	$4\cdot10^6$
$Li^7+H^2=2He^4+n$	7	212	$5.5\cdot10^{-26}$	$3.3\cdot10^{-13}$	10^7
$Be^9+H^1=\{Li^6+He^4 \mid Be^8+H^2\}$	7a	212	$1.1\cdot10^{-25}$	$3.5\cdot10^{-13}$	$1.7\cdot10^7$
$Be^9+H^2=\{Li^7+He^4 \mid Be^8+H^3 \mid Be^{10}+H^1\}$	7a	212	$5\cdot10^{-26}$	$3.6\cdot10^{-13}$	$6\cdot10^5$
$B^{11}+H^1=3He^4$	7b	212	$6\cdot10^{-25}$	$3.7\cdot10^{-13}$	$2\cdot10^6$

of such reactions with the use of the formula (cf. reference 4, Eq. (2))

$$\sigma=\frac{\pi R^2}{2E}\frac{A_1+A_2}{A_2}\Gamma\exp\left[\left(\frac{32R}{a}\right)^{\frac{1}{2}}-\frac{2\pi e^2}{\hbar v}Z_1Z_2\right] \quad (11)$$

where E is the absolute energy of the incident particle (particle 1). Table II gives the experimental results for some of the better investigated reactions. In each case, experiments with low energy particles were chosen in order to make the conditions as similar as possible to those in stars where the greatest number of nuclear reactions is due to particles of about 20 kilovolts energy. The cross sections were in each case calculated from the thick target yield with the help of the range-energy relation of Herb, Bellamy, Parkinson and Hudson.[8] The widths obtained (last column of Table II) are mostly between $3\cdot10^5$ and $2\cdot10^7$ ev, with the exception of the reaction $Li^7+H=2He^4$ which is known to be "improbable."[9]

The γ-ray widths Γ_γ can be obtained from observed resonance capture of protons. Table III gives the experimental results. Two of the older data were taken from Table XXXIX of reference 10; all the others are from more recent experiments on proton[11–14] and neutron[15] capture. Although the results of different investigators differ considerably (e.g., for $Li^7+H^1=Be^8$, Γ is between 4 and 40 volts the latter value being more likely) they seem to lie generally between about $\frac{1}{2}$ and 40 volts. Ordinarily, the width is somewhat larger for the more energetic γ-rays, as is expected theoretically. A not too bad approximation to the experiments is obtained by using the theoretical formula for dipole radiation (reference 10, Eq. (711b)) with an oscillator strength of 1/50. This gives

$$\Gamma_\gamma\sim0.1E_\gamma^2, \quad (12)$$

TABLE III. *γ-ray widths of nuclear levels.*

REACTION	REFERENCE	WIDTH (VOLTS)	γ-RAY ENERGY (MEV)
$Li^7+H^1=Be^8+\gamma$	10	4	17
	11	40	
$B^{11}+H^1=C^{12}+\gamma$	11	0.6	12, 16
$C^{12}+H^1=N^{13}+\gamma$	12	0.6	2
$C^{13}+H^1=N^{14}+\gamma$	13, 14	30	4, 8
$F^{19}+H^1=Ne^{20}+\gamma$	10	0.6, 8, 18	6
$C^{12}+n^1=C^{13}+\gamma$	15	<2.5	5
$O^{16}+n^1=O^{17}+\gamma$	15	<2.5	4

[5] R. Ladenburg and M. H. Kanner, Phys. Rev. **52**, 911 (1937).
[6] H. D. Doolittle, Phys. Rev. **49**, 779 (1936).
[7] J. H. Williams, W. G. Shepherd and R. O. Haxby, Phys. Rev. **52**, 390 (1937).
[7a] J. H. Williams, R. O. Haxby and W. G. Shepherd, Phys. Rev. **52**, 1031 (1937).
[7b] J. H. Williams, W. H. Wells, J. T. Tate and E. J. Hill, Phys. Rev. **51**, 434 (1937).
[8] D. B. Parkinson, R. G. Herb, J. C. Bellamy and C. M. Hudson, Phys. Rev. **52**, 75 (1937).
[9] M. Goldhaber, Proc. Camb. Phil. Soc. **30**, 560 (1934).
[10] H. A. Bethe, Rev. Mod. Phys. **9**, 71 (1937).
[11] W. A. Fowler, E. R. Gaerttner and C. C. Lauritsen, Phys. Rev. **53**, 628 (1938).
[12] R. B. Roberts and N. P. Heydenburg, Phys. Rev. **53**, 374 (1938).
[13] P. I. Dee, S. C. Curran and V. Petržilka, Nature **141**, 642 (1938). The γ-rays from C^{13} give about equally as many counts as those from C^{12}. The efficiency of the counter for C^{13} γ-rays is about twice that for C^{12}, because the cross section for production of Compton and pair electrons is smaller by a factor 2/3 while the range of these electrons is about 3 times longer. With an abundance of C^{13} of about 1 percent, the γ-width for this nucleus becomes 50 times that of C^{12}. I am indebted to Dr. Rose for these calculations.
[14] M. E. Rose, Phys. Rev. **53**, 844 (1938).
[15] O. R. Frisch, H. v. Halban and J. Koch, Nature **140**, 895 (1937); Danish Acad. Sci. **15**, 10 (1937).

where E_γ is the γ-ray energy in mMU (milli-mass-units), and Γ_γ the γ-ray width in volts. For quadrupole radiation, theory gives about

$$\Gamma_\gamma \sim 5 \cdot 10^{-4} E_\gamma^4 \quad \text{(quadrupole)}. \qquad (12a)$$

Formulae (12), and (12a) will be used in the calculations where experimental data are not available; they may, in any individual case, be in error by a factor 10 or more but such a factor is not of great importance compared with other uncertainties.

It should be noted that quite generally radiative processes are rare compared with particle emission. According to the figures given in Tables II and III, the ratio of probabilities is 10^4–10^5 in favor of particle reactions.

In a number of cases, the reaction of a nucleus A with a heavy particle (proton, alpha-) must compete with natural β-radioactivity of A or with electron capture. In those cases where the lifetime of radioactive nuclei is not known experimentally, we use the Fermi theory. According to this theory, the decay constant for β-emission is[16]

$$\beta = 0.9 \cdot 10^{-4} f(W) |G|^2 \text{ sec.}^{-1}. \qquad (13)$$

The matrix element G is about unity for strongly allowed transitions, and

$$f(W) = (W^2-1)^{\frac{1}{2}}\left(\frac{1}{30}W^4 - \frac{3}{20}W^2 - \frac{2}{15}\right) + \tfrac{1}{4}W \log\{W+(W^2-1)^{\frac{1}{2}}\}, \qquad (13a)$$

where W is the maximum energy of the β-particle, including its rest mass, in units of mc^2 (m = electron mass).

The probability of electron capture is

$$\beta_C = 0.9 \cdot 10^{-4} \pi^2 N (\hbar/mc)^3 W^2 |G|^2 \text{ sec.}^{-1}, \qquad (14)$$

where W is the energy of the emitted neutrino in units of mc^2 and N the number of electrons per unit volume. If the hydrogen concentration is x_H, we have (reference 1, p. 482) $N = 6 \cdot 10^{23} \rho \cdot \frac{1}{2}(1+x_H)$ (ρ the density), and

$$\beta_C = 1.5 \cdot 10^{-11} \rho (1+x_H) W^2 |G|^2 \text{ sec.}^{-1}. \qquad (14a)$$

[16] C. L. Critchfield and H. A. Bethe, Phys. Rev. **54**, 248, 862 (L) (1938).

§3. Stability of Unknown Isotopes

For the discussion of nuclear reactions it is essential to know whether or not certain isotopes exist (such as Li^4, Li^5, Be^6, Be^8, B^8, B^9, C^{10}, etc.). The criterion for the existence of a nucleus is its energetic stability against spontaneous disintegration into heavy particles (emission of a neutron, proton or alpha-particle). Whenever a light nucleus is energetically unstable against heavy particle emission, its life will be a very small fraction of a second (usually $\sim 10^{-20}$ sec.) even if the instability is slight (e.g., Be^8 will have a life of 10^{-13} sec. if it is by 50 kv heavier than two α-particles[17]).

For the question of the lifetime of radioactive nuclei, it is also necessary to know the mass difference between isobars. Similar information is required for estimating the γ-ray width in capture reactions (cf. Eqs. (12), (12a)).

H^3 and He^3

The most recent determination[18] of the reaction energy in the reaction $H^2+H^2=He^3+n^1$ yielded 3.29 Mev as compared with 3.98 in $H^2+H^2=H^3+H^1$. With a mass difference of 0.75 Mev between neutron and hydrogen atom,[19] this makes He^3 more stable than H^3 by 0.06 Mev. This would be in agreement with the experimental fact that no H^3 is present in natural hydrogen to more than 1 part in 10^{12}. Even if He^3 should turn out to be heavier than H^3, the difference cannot be greater than about 0.05 Mev = 0.1 mc^2 which would make the life of He^3 exceedingly long ($\sim$2000 years at the center of the sun, (Eq. (14a)), 3000 years in the complete atom, on earth).

H^4 and Li^4

As was first pointed out by Bothe and Gentner,[20] it is definitely possible that H^4 is stable. Li^4 is, of course, less stable because of the Coulomb repulsion between its three protons. If it is stable, Li^4 would be formed when He^3 captures a proton and would thus play an important role in stars (cf. §5). The only possible estimate of the stability seems to be a comparison

[17] H. A. Bethe, Rev. Mod. Phys. **9**, 167 (1937).
[18] T. W. Bonner, Phys. Rev. **52**, 685 (1938).
[19] H. A. Bethe, Phys. Rev. **53**, 313 (1938).
[20] W. Bothe and W. Gentner, Naturwiss. **24**, 17 (1936).

of Li^6Li^8 to the analogous pair B^8B^9. Reasonable estimates[21] make B^9 just unstable (0.3–0.7 mMU), while B^8 comes out at the limit of stability (binding energy between -0.4 and $+0.4$ mMU), i.e., B^8 about 0.3 to 0.7 mMU more stable than B^9. Li^5 (see below) is unstable by 1.4–1.8 mMU; if one assumes the same difference, Li^4 is found to be unstable by ~ 1 mMU. However, this argument is very uncertain and the possibility of a stable Li^4 cannot be excluded at present. H^4 would, from a similar argument, turn out stable by 0.6 mMU.

He^5 and Li^5

The instability of He^5 is shown directly by the experiments of Williams, Shepherd and Haxby[22] on the reaction

$$Li^7+H^2=He^5+He^4. \qquad (15)$$

From a measurement of the range of the α-particles, the mass of He^5 is found (reference 23, Table 73, p. 373) to be 5.0137 whereas the combined mass of an α-particle plus a neutron would be only $4.003\,86+1.008\,93=5.012\,8$. Thus He^5 is unstable by 0.9 mMU (milli-mass-units) which is far outside the experimental error (about 0.1–0.2 mMU). It might be argued that the α-particle group observed in reaction (15) might correspond to an excited state of He^5. However, this is extremely improbable because a nucleus of such a simple structure as He^5 (α-particle plus neutron) should not have any low-lying excited levels.[24] (This holds both in the α-particle and the Hartree model of nuclear structure.) Moreover, it would be difficult to explain why the α-particle group corresponding to the ground state of He^5 should not have been observed.

The conclusion that the mass of 5.0137 found by W. S. and H. really corresponds to the ground state of He^5 is supported by considerations of mass defects. In fact, the instability of He^5 was first predicted by Atkinson[25] on the basis of such considerations. Considering analogous nuclei, consisting of α-particles plus one neutron, we find that the last neutron is bound with a binding energy of 5.3 mMU in C^{13} and with only 1.8 mMU in Be^9. A binding energy of -0.9 mMU in He^5 fits very well into this series while a positive binding energy would not.

If He^5 is unstable, this is *a fortiori* true of Li^5 since the binding energies of these two nuclei should differ by just the Coulomb repulsion between proton and alpha in Li^5. This repulsion will be about 0.6–1 mMU, so that Li^5 is unstable by 1.4–1.8 mMU.

Thus all the nuclear evidence[25a] points to the nonexistence of both He^5 and Li^5. Even if there were no such evidence, astrophysical data themselves would force us to this conclusion, because at a temperature of $2\cdot 10^7$ degrees (central temperature of sun) the energy production from the combination of He^4 and H forming Li^5 would be of the order of 10^{10} ergs/g sec. (cf. §4), as against an observed energy production of 2 ergs/g sec. Only the nonexistence of Li^5 prevents this enormous production of energy.

Be^6

This nucleus is certainly unstable, as can be shown by comparing it with the known nucleus He^6 from which it differs by the interchange of protons and neutrons. The Coulomb energy which is the only difference between the binding energies of the two nuclei can be calculated rather accurately.[21] The instability against disintegration into He^4+2H is between 1 and 2.6 mMU.

Be^7

This nucleus has been observed by Roberts, Heydenburg and Locher.[26] It decays with a

[21] H. A. Bethe, Phys. Rev. **54**, 436, 955 (1938).

[22] J. H. Williams, W. G. Shepherd and R. O. Haxby, Phys. Rev. **51**, 888 (1937).

[23] M. S. Livingston and H. A. Bethe, Rev. Mod. Phys. **9**, 247 (1937).

[24] With the possible exception of a doublet structure of the ground state, similar to Li^7. However, the doublet separation should probably be much smaller than in Li^7 because of the loose binding of He^5, and presumably both components of the doublet are already contained in the rather broad α-particle group observed by Williams, Shepherd and Haxby.

[25] R. d'E. Atkinson, Phys. Rev. **48**, 382 (1935).

[25a] *Note added in proof:*—Recently, F. Joliot and I. Zlotowski (J. de phys. et rad. **9**, 403 (1938)) reported the formation of stable He^5 from the reaction $He^4+H^2=He^5+H^1$. The evidence is based upon the emission of singly charged particles of long range when heavy paraffin is bombarded by α-particles. However, the number of such particles observed was exceedingly small (only 6 out of a total of 126 tracks). Furthermore, the mass given for He^5 by Joliot and Zlotowski (5.0106) is irreconcilable with the stability (against neutron emission) of the well-known nucleus He^6.

[26] R. B. Roberts, N. P. Heydenburg and G. L. Locher, Phys. Rev. **53**, 1016 (1938).

TABLE IV. *Corrected and additional nuclear masses, and binding energies.*

NUCLEUS	MASS	BINDING ENERGY (MMU)	REFERENCE
n^1	1.008 93		19
He^3	3.016 99	5.87	18
H^4	4.025 4	0.6 ±1	
He^4	4.003 86		29
Li^4	4.026 9	−1 ±1	
He^5	5.013 7	−0.9 ±0.2	23
Li^5	5.013 6	−1.6 ±0.3	
Be^6	6.021 9	−1.8 ±0.8	21
Be^7	7.019 28	5.7	26
Be^8	8.007 80	−0.08±0.04	28
B^8	8.027 4	0.0 ±0.4	21
B^9	9.016 4	−0.5 ±0.2	21
C^{10}	10.020 2	3.8	21
N^{12}	12.022 5 −24 3	0.0 ±0.9	21
N^{13}	13.010 08	2.03	19
O^{14}	14.013 1	5.1	21

half-life of 43 days (mean life 60 days) and probably only captures K electrons. Calculations of the Coulomb energy,[21] on the other hand, would make positron emission just possible (positron energy ~ 0.1 mMU). As a compromise, we assume that the mass of Be^7 is just equal to Li^7 plus two electrons, i.e., 7.019 28.

Be^8

The instability of Be^8 against disintegration into two α-particles has been definitely established by Paneth and Glückauf[27] who have shown that the Be^8 formed in the photoelectric disintegration of Be^9 disintegrates into 2 He^4. Kirchner and Neuert[28] have confirmed this conclusion by investigating the products of the disintegration $B^{11}+H=Be^8+He^4$. They found that frequently two α-particles enter the detecting apparatus simultaneously, with a small angle (less than 50°) between their respective directions of flight; this is just what should be expected if the Be^8 formed breaks up into two α-particles on its way to the detector. From the average angle between the two alphas, the disintegration energy of Be^8 (difference Be^8-2He^4) was estimated as between 40 and 120 kev.[28a]

B^8

The existence is doubtful; calculation[21] by comparison with its isobar Li^8 gives a binding energy between −0.4 and +0.4 mMU. This nucleus is not very important for astrophysics.

B^9

B^9 is almost certainly unstable, as can be shown by calculating[21] the difference in binding energy (Coulomb energy) between it and its isobar Be^9. The theoretical instability is between 0.3 and 0.7 mMU, 0.3 being almost certainly a lower limit. However, in view of the smallness of this instability, we shall at least discuss what would happen if B^9 were stable (§6). It will turn out that this would make almost no difference at "ordinary" temperatures ($2\cdot 10^7$ degrees) and not much even at higher ones (10^8 degrees). For these calculations, we shall assume B^9 to be stable with 0.2 mMU which seems generous.

C^{10}

C^{10} is stable with 4 mMU against Be^8+2H.

N^{12}

N^{12} is doubtful, mainly because the binding energy of its isobar, B^{12}, is known only very inaccurately (between 2 and 3.3 mMU). Assuming 2 mMU, N^{12} would probably be instable, with 3.3 stable.

Table IV summarizes the binding energies of doubtful nuclei, and also gives some nuclear masses supplementary to and correcting those given in reference 23, p. 373.

§4. REACTION RATES AT $2\cdot 10^7$ DEGREES

We are now prepared to actually calculate the rate of nuclear reactions under the conditions prevailing in stars. We choose a temperature of twenty million degrees, close to the temperature at the center of the sun. In order to have a figure independent of density and chemical composition, we calculate (cf. 7)

$$P=(m_2/x_2)p/\rho x_1, \qquad (16)$$

$P\rho x_1$ gives the probability (per second) that a given nucleus of kind 2 undergoes a reaction with any nucleus of kind 1. If there are no other reactions destroying or producing nuclei of kind 2, $1/P\rho x_1$ will be the mean life of nuclei of kind 2 in the star.

[27] F. A. Paneth and E. Glückauf, Nature **139**, 712 (1937).
[28] F. Kirchner and H. Neuert, Naturwiss. **25**, 48 (1937).
[28a] *Note added in proof:*—These conclusions are compatible with the new measurements of S. K. Allison, E. R. Graves, L. S. Skaggs and N. M. Smith, Jr. (Phys. Rev. **55**, 107 (1939)) on the reaction energy of $Be^9+H=Be^8+H^2$.
[29] K. T. Bainbridge, Phys. Rev. **53**, 922(A) (1938).

TABLE V. *Probability of nuclear reactions at $2 \cdot 10^7$ degrees.*[**]

REACTION	Q (MMU)	Γ (EV)	τ	P (SEC.$^{-1}$)	LIFE, FOR $\rho x_1 = 30$
$H+H=H^2+\epsilon^+$	1.53	Ref. 16	12.5	$8.5 \cdot 10^{-21}$	$1.2 \cdot 10^{11}$ yr.
$H^2+H=He^3$	5.9	1 E	13.8	$1.3 \cdot 10^{-2}$	2 sec.
$H^3+H=He^4$	21.3	10 E	14.3	$1.7 \cdot 10^{-1}$	0.2 sec.
$He^3+H=Li^{4*}$	(0.5)	0.02 D	22.7	$3 \cdot 10^{-7}$	1 day
$He^4+H=Li^{5*}$	(0.2)	0.005 D	23.2	$6 \cdot 10^{-8}$	6 days
$Li^6+H=He^4+He^3$	4.1	$5 \cdot 10^5$ X	31.1	$7 \cdot 10^{-2}$	5 sec.
$Li^7+H=2\ He^4$	18.6	$4 \cdot 10^4 X$	31.3	$6 \cdot 10^{-4}$	1 min.
$Be^7+H=B^{8}$?	(0.5)	0.02 D	38.1	$6 \cdot 10^{-12}$	2000 yr.
$Be^9+H=Li^6+He^4$	2.4	10^6 X	38.1	$4 \cdot 10^{-6}$	15 min.
$B^9+H=C^{10*}$	3.5	2 D	44.6	$2 \cdot 10^{-13}$	5000 yr.
$B^{10}+H=C^{11}$	9.2	10 D	44.6	10^{-12}	1000 yr.
$B^{11}+H=3\ He^4$	9.4	10^6 E	44.6	$1.2 \cdot 10^{-7}$	3 days
$C^{11}+H=N^{12}$	(0.4)	0.02 D	50.6	10^{-17}	10^8 yr.
$C^{12}+H=N^{13}$	2.0	0.6 X	50.6	$4 \cdot 10^{-16}$	$2.5 \cdot 10^8$ yr.
$C^{13}+H=N^{14}$	8.2	30 X	50.6	$2 \cdot 10^{-14}$	$5 \cdot 10^4$ yr.
$N^{14}+H=O^{15}$	7.8	5 D	56.3	$2 \cdot 10^{-17}$	$5 \cdot 10^7$ yr.
$N^{15}+H=C^{12}+He^4$	5.2	10^6 E	56.3	$5 \cdot 10^{-13}$	2000 yr.
$O^{16}+H=F^{17}$	0.5	0.02 D	61.6	$8 \cdot 10^{-22}$	10^{12} yr.
$F^{19}+H=O^{16}+He^4$	8.8	10^6 E	66.9	$4 \cdot 10^{-17}$	$3 \cdot 10^7$ yr.
$Ne^{22}+H=Na^{22}$	10.7	10 D	71.7	$5 \cdot 10^{-23}$	$2 \cdot 10^{13}$ yr.
$Mg^{26}+H=Al^{27}$	8.0	10 D	81.3	10^{-26}	10^{17} yr.
$Si^{30}+H=P^{31}$	7.0	10 D	90.4	$4 \cdot 10^{-30}$	$3 \cdot 10^{20}$ yr.
$Cl^{37}+H=A^{38}$	12.0	10 D	103.1	$5 \cdot 10^{-26}$	$2 \cdot 10^{25}$ yr.
$H^2+H^2=He^3+n$	3.5	$3 \cdot 10^5$ X	15.7	10^3	
$Be^7+H^2=B^{9*}$	18.5	10 D'	45.9	$2 \cdot 10^{-13}$	
$Be^7+H^2=B^9+n^*$	11.9	10^6 E	50.7	$2 \cdot 10^{-10}$	
$Be^7+He^3=C^{10}$	16.2	1 D'	80.5	$3 \cdot 10^{-28}$	
$H^2+He^4=Li^6$	1.7	$4 \cdot 10^{-3}$ Q	27.5	$3 \cdot 10^{-10}$	
$He^3+He^4=Be^7$	1.6	0.02 D'	47.3	$3 \cdot 10^{-17}$	$3 \cdot 10^7$ yr.
$He^4+He^4=Be^{8*}$	(0.05)	$5 \cdot 10^{-9}$ Q	50.0	10^{-24}	
$Li^7+He^4=B^{11}$	9.1	1 D'	71.0	$2.5 \cdot 10^{-24}$	
$Be^7+He^4=C^{11}$	8.0	1 D'	86	$3 \cdot 10^{-30}$	$3 \cdot 10^{20}$ yr.
$C^{13}+He^4=O^{16}$	7.8	1 Q'	119	$7 \cdot 10^{-43}$	

[**] The letters in the column giving the level width mean: X = experimental value; D = calculated for dipole radiation, from Eq. (12); D' = dipole radiation with small specific charge, 1/4 to 1/20 of Eq. (12); Q = quadrupole radiation, Eq. (12a); and E = estimate.

* These reactions are not believed to occur since their product or one of the reactants is unstable. They are listed merely for the sake of discussion.

Table V gives the results of the calculations, based on Eqs. (7) to (9). In the first column, the nuclear reactions are listed. All reactions which seemed of importance in the interior of stars were considered; in addition, some reactions with heavier elements (O^{16} to Cl^{37}) were included in order to show the manner in which the reaction rate decreases. Moreover, seven reactions were listed in spite of the fact that their products or reactants are believed to be (§3) unstable (starred) or doubtful (question mark); these reactions are included in order to discuss the consequences if they did occur.

The second column gives the energy evolution Q in the reaction, calculated from the masses (reference 23, Table LXXIII, and this paper, Table IV). In the third column, the width Γ determining the reaction rate (cf. §2) is tabulated. Wherever possible, this was taken from experiments (Tables II and III) or from the "empirical formulae" (12), (12a) for the radiation width. For the radiative combination of two nuclei of equal specific charge (H^2+He^4, He^4+He^4, $C^{12}+He^4$) quadrupole radiation was assumed, otherwise dipole radiation.[30] For almost equal specific charge (e.g., Be^7+He^4), the dipole formula with an appropriate reduction was used. In some instances, the width was estimated by analogy (e.g., $N^{15}+H=C^{12}+He^4$) or from approximate theoretical calculations ($H^2+H=He^3$).[31] The way in which Γ was obtained was indicated by a letter in each instance.

The fourth column contains τ, as calculated from (8), the fifth P from (16). The wide variation of P is evident, also the smallness of P for α-particle as compared with proton reactions.

[30] If the combined initial nuclei and the final nucleus have the same parity (as may be the case, e.g., for $O^{16}+H=F^{17}$), it is still possible to have a dipole transition if only the incident particle has orbital momentum one. This does not materially affect its penetrability if $R>a$ (cf. (4), (5)) which is true in every case where the parities are expected to be the same.

[31] L. I. Schiff, Phys. Rev. **52**, 242 (1937).

E.g., the reaction between He^4 and a nucleus as light as Be is as improbable as between a proton and Si. This arises, of course, from the greater charge and mass of the α-particle both of which factors reduce its penetrability. The reaction $He^4+He^4=Be^8$ has an exceedingly small probability because of the small frequency and the quadrupole character of the emitted γ-rays. Thus this reaction would not be important even if Be^8 were stable. On the other hand, the reaction $He^4+H=Li^5$ would be extremely probable if Li^5 existed. The helium in the sun would be "burnt up" completely in about six days, even if rather unfavorable assumptions are made about the probability of the reaction. Similarly, if the energy evolution per process is 0.2 mMU $=3\cdot10^{-7}$ ergs, the energy produced per gram of the star would be

$$(6\cdot10^{23}/4)\rho x_H x_{He}\cdot3\cdot10^{-7}\cdot6\cdot10^{-8}.$$

With $\rho=80$, $x_H=0.35$ and $x_{He}=0.1$, this would give about 10^{10} ergs/g sec. as against 2 ergs/g sec. observed. This is a very strong additional argument against the existence of Li^5.

In the last column of Table V, the mean life is calculated for the various nuclei reacting with protons, by assuming a density $\rho=80$ and hydrogen content $x_1=35$ percent, which correspond to the values at the center of the sun.[1] It is seen that, with the exception of H, the lifetimes of all nuclei up to boron are quite short, ranging from a fraction of a second for H^3 to 1000 years for B^{10}. (The life of B^{10} may actually be slightly shorter because of the reaction $B^{10}+H=Be^7+He^4$. See §6.) Of the two lives longer than 1000 years listed, one refers to B^9 which probably does not exist (§3), the other to Be^7 which decays by positron emission with a half-life of 43 days.[26] We must conclude that *all the nuclei between* H *and* C, *notably* H^2, H^3, Li^6, Li^7, Be^9, B^{10}, B^{11}, *can exist in the interior of stars only to the extent to which they are continuously re-formed by nuclear reactions.* This conclusion does not apply to He^4 because Li^5 does not exist. To He^3 it probably applies whether Li^4 exists or not, because He^3 will also be destroyed by combination with He^4 into Be^7, although with a considerably longer period ($3\cdot10^7$ years instead of the 1 day for the reaction giving Li^4).

The actual lifetime of carbon and nitrogen is much longer than it would appear from the table because these nuclei are reproduced by the nuclear reactions themselves (§7). This makes their actual lifetime of the order of 10^{12} (or even 10^{20}, cf. §7) years, i.e., long compared with the age of the universe ($\sim2\cdot10^9$ years). Protons, and all nuclei heavier than nitrogen, also have lives long compared with astronomical times.

§5. The Reactions Following Proton Combination

In the last section, it has been shown that all elements lighter than carbon, with the exception of H^1 and He^4, have an exceedingly short life in the interior of stars. Such elements can therefore only be present to the extent to which they are continuously produced in nuclear reactions from elements of longer life. This is in accord with the small abundance of all these elements both in stars and on earth.

Of the two more stable nuclei, He^4 is too inert to play an important rôle. It combines neither with a proton nor with another α-particle since the product would in both cases be an unstable nucleus. The only way in which He^4 can react at all, is by triple collisions. These will be discussed in the next section and will be shown to be very rare, as is to be expected.

As the only primary reaction between elements lighter than carbon, there remains therefore the reaction between two protons,

$$H^1+H^1=H^2+\epsilon^+. \qquad (1)$$

According to Critchfield and Bethe,[16] this process gives an energy evolution of 2.2 ergs/g sec. under "standard stellar conditions" ($2\cdot10^7$ degrees, $\rho=80$, hydrogen content 35 percent). The reaction rate under these conditions is (cf. Table V) $2.5\cdot10^{-19}$ sec.$^{-1}$, corresponding to a mean life of $1.2\cdot10^{11}$ years for the hydrogen in the sun. This lifetime is about 70 times the age of the universe as obtained from the red shift of nebulae.

According to the foregoing, any building up of elements out of hydrogen will have to start with reaction (1). The deuteron will capture another proton,

$$H^2+H^1=He^3. \qquad (17)$$

This reaction follows almost instantaneously upon (1), with a delay of only 2 sec. (Table V). There is, therefore, always statistical equilibrium between protons and deuterons, the concentrations (by number of atoms) being in the ratio of the respective lifetimes. This makes the concentration of deuterons (by weight) equal to

$$x(H^2) = x(H^1) \cdot \frac{2 \cdot 8.5 \cdot 10^{-21}}{1.3 \cdot 10^{-2}} = 1.3 \cdot 10^{-18} x(H^1) \quad (18)$$

(cf. Table V). The relative probability of the reaction

$$H^2 + H^2 = He^3 + n^1 \quad (19)$$

as compared with (17), is then

$$p_n = \frac{1}{4} \cdot \frac{P(H^2+H^2=He^3+n^1)}{P(H^2+H=He^3)} \cdot \frac{x(H^2)}{x(H^1)} = \frac{10^3 \cdot 1.3 \cdot 10^{-18}}{4 \cdot 1.3 \cdot 10^{-2}} = 2 \cdot 10^{-14}. \quad (19a)$$

(One factor $\frac{1}{2}$ comes from the fact that in (19) two nuclei of the same kind interact; another is the atomic weight of H^2.) Thus one neutron is produced for about $5 \cdot 10^{13}$ proton combinations.

The further development of the He^3 produced according to (17) depends on the question of the stability of Li^4 and of the relative stability of H^3 and He^3.

Assumption A: Li^4 stable

In this case, the He^3 will capture another proton, *viz.*:

$$He^3 + H^1 = Li^4. \quad (20)$$

With the assumptions made in Table V, the mean life of He^3 would be 1 day. The Li^4 would then emit a positron:

$$Li^4 = He^4 + \epsilon^+. \quad (20a)$$

With an assumed stability of Li^4 of 0.5 mMU compared with He^3+H^1, the maximum energy of the positrons in (20a) would be 20.8 mMU = 19.4 Mev (including rest mass) which would be by far the highest β-ray energy known. The lifetime of Li^4 may accordingly be expected to be a small fraction of a second (half-life = 1/500 sec. for an allowed transition in the Fermi theory).

The most important consequence of the stability of Li^4 would be that only a fraction of the mass difference between four protons and an α-particle would appear as usable energy. For in the β-emission (20a) the larger part of the energy is, on the average, given to the neutrino which will in general leave the star without giving up any of its energy (see below). According to the Konopinski-Uhlenbeck theory, which is in good agreement with the observed energy distribution in β-spectra, the neutrino receives on the average 5/8 of the total available energy if the latter is large. In our case, this would be 13.0 mMU. Adding 0.2 mMU for the neutrino emitted in process (1), we find that altogether 13.2 mMU energy is lost to neutrinos, of a total of 28.7 mMU developed in the formation of an α-particle out of four protons and two electrons. Thus the observable energy evolution is only 15.5 mMU, i.e., 54 percent of the total. Therefore, if Li^4 is stable, process (1) would give only 1.2 ergs/g sec. instead of 2.2 (under "standard" conditions).[16]

The neutrinos emitted will have some chance of producing neutrons in the outer layers of the star. It seems reasonable to assume that a neutrino has no other interaction with matter than that implied in the β-theory. Then a free neutrino (ν) will cause only "reverse β-processes"[22] of which the simplest and most probable is

$$H + \nu = n^1 + \epsilon^+. \quad (21)$$

This process is endoergic with 1.9 mMU and is therefore caused only by fast neutrinos such as those from Li^4. The cross section is according to the Fermi theory

$$\sigma = \pi^2(\hbar/mc)^2 \cdot 0.9 \cdot 10^{-4} c^{-1} W(W^2-1)^{\frac{1}{2}} = 1.7 \cdot 10^{-43} W(W^2-1)^{\frac{1}{2}} \text{ cm}^2, \quad (22)$$

where W is the energy of the emitted positron, including rest mass, in units of mc^2. In reaction (21), this is the neutrino energy minus 1.35 mMU. For the Li^4 neutrinos, the average cross section comes out to be

$$\sigma_{Av} = 2.5 \cdot 10^{-43} \text{ cm}^2 \quad (22a)$$

per proton, and the probability of process (21) for a neutrino starting from the center of the star

$$p = 6 \cdot 10^{23} \cdot \sigma_{Av} x_H \int_0^R \rho dr = 1.5 \cdot 10^{-19} x_H \int_0^R \rho dr, \quad (22b)$$

where $\rho(r)$ is the density (in g/cm^3) at the distance r from the center of the star. For the sun, $p = 1.6 \cdot 10^{-7}$. This means that $1.6 \cdot 10^{-7}$ of the neutrinos emitted will cause reaction (21) before leaving the sun, and that the number of neutrons formed is $1.6 \cdot 10^{-7}$ times the number of proton combinations (1).

A further consequence of (20, 20a) would be that ordinarily no nuclei heavier than 4 mass units are formed at all, even as intermediate products. Such nuclei would only be produced in the rare cases when H^2 or He^3 capture an α-particle rather than a proton, according to the reactions

$$H^2 + He^4 = Li^6 \quad (23)$$

and

$$He^3 + He^4 = Be^7. \quad (24)$$

Under the favorable assumption that the concentration of He^4 is the same as of H^1 (by weight), the fraction of H^2 forming Li^6 is (cf. Table V)

$$p(Li^6) = 3 \cdot 10^{-10}/1.3 \cdot 10^{-2} = 2 \cdot 10^{-8} \quad (23a)$$

the fraction of He^3 giving Be^7 is

$$p(Be^7) = 3 \cdot 10^{-17}/3 \cdot 10^{-7} = 10^{-10}. \quad (24a)$$

[22] H. A. Bethe and R. Peierls, Nature **133**, 689 (1934).

Most of the Li^6 will give rise to the well-known reaction

$$Li^6+H=He^3+He^4 \tag{23b}$$

and most of the Be^7 will go over into Li^7 which in turn reacts with a proton to give two α-particles. Only occasionally, Li^6, Be^7 or Li^7 will capture an α-particle and thus form heavier nuclei. It can be shown (cf. assumption B) that Li^7 is the most efficient nucleus in this respect. Therefore, the amount of heavier elements formed is determined by Be^7, the mother substance of Li^7, and is thus 10^{-10} times the amount formed with assumption B.

Assumption B: Li^4 unstable, He^3 more stable than H^2

This assumption seems to be the most likely according to available evidence. The *only* reaction which the He^3 can undergo, is then (24), i.e., each proton combination leads to the formation of a Be^7 nucleus. The most probable mode of decay of this nucleus is by electron capture, leading to Li^7. The lifetime of Be^7 (half-life) is 43 days[36] in the complete atom, and 10 months at the center of the sun (cf. 14, 14a). This makes the mean life = 14 months and the reaction rate $2.8\cdot10^{-8}$ sec.$^{-1}$. The capture of a proton by Be^7 would, even if the product B^8 is stable, be 2000 times slower (Table V). Each electron capture by Be^7 is accompanied by the emission of a neutrino of energy $\sim 2mc^2 = 1.1$ mMU (when Li^7 is left in its excited state, which happens rather rarely, the neutrino receives only 0.6 mMU). The total energy lost to neutrinos (including process 1) will therefore be very small in this case ($\sim$1.3 mMU per α-particle formed, i.e., 4½ percent of the total energy evolution) and practically the full mass energy will be transformed into heat radiation. The Li^7 formed by electron capture of Be^7 will cause the well-known reaction

$$Li^7+H=2\ He^4 \tag{25}$$

and have (Table V) a mean life of only 1 minute at $2\cdot10^7$ degrees.

The reaction chain described leads, as in the case of assumption A, to the building up of one α-particle out of four protons and two electrons, for each process (1). No nuclei heavier than He^4 are formed permanently. Such nuclei can be produced only by branch reactions alternative to the main chain described. These will be discussed in the following.

a. Reactions with protons.—When Li^7 reacts with slow protons, the result is not always two α-particles, but, in one case out of about[22] 5000, radiative capture, giving Be^8. However, Be^8 will disintegrate again into two α-particles (§3), and during its life of about 10^{-12} sec., the probability of its reacting with another particle (e.g., capture of another proton) is exceedingly small ($\sim10^{-24}$). Similarly, Be^7 will, in one out of about 2000 cases (see above) capture a proton and form B^8 if that nucleus exists. However, B^8 will again go over into Be^8, by positron emission, and two alphas will again be the final result.

At this place, obviously, stability of Be^8 would increase the yield of heavy nuclei. Then one stable Be^8 would be formed for 5000 proton combinations; and, if B^9 is also assumed to be stable, every Be^8 goes over into B^9. Since about one out of $3\cdot10^8$ B^9 gives a C^{12} (§6), the number of heavy nuclei (C^{12}) formed would be $\sim10^{-12}$ per α-particle. This would be the highest yield obtainable. However, Be^8 is known to be unstable (§3).

b. Reactions with α-particles.—The only abundant light nucleus other than the proton is He^4. The only reaction possible between an α-particle and Li^7 or Be^7 is radiative capture, *viz.*

$$Li^7+He^4=B^{11}, \tag{26}$$

$$Be^7+He^4=C^{11}. \tag{26a}$$

The probability of formation of B^{11} and C^{11} is (Table V)

$$p(B^{11})=\frac{P(Li^7+He^4)}{P(Li^7+H)}=\frac{2.5\cdot10^{-24}}{6\cdot10^{-4}}=4\cdot10^{-21}, \tag{26b}$$

$$p(C^{11})=\frac{P(Be^7+He^4)}{P(Be^7+\epsilon=Li^7)}=\frac{14\text{ months}}{3\cdot10^{20}\text{ yr.}}=4\cdot10^{-21}. \tag{26c}$$

Thus the formation of B^{11} is about as probable as that of C^{11}; the effect of the lower potential barrier of Li^7 for α-particles is compensated by its shorter life. The C^{11} will, of course, also give B^{11} by positron emission.

The B^{11} will react with protons in two ways, *viz.*

$$B^{11}+H^1=3\ He^4, \tag{27}$$

$$B^{11}+H^1=C^{12}. \tag{27a}$$

The branching ratio is about 10^4 : 1 in favor of (27) (calculated from experimental data). Thus there will be one C^{12} nucleus formed for about 10^{24} α-particles. The building up of heavier nuclei, even in this most favorable case, is therefore exceedingly improbable.

c. Reactions with He^3.—Since He^3 has a rather long life ($3\cdot10^7$ years, Table V) and penetrates more easily through the potential barrier than the heavier He^4, it may be considered as an alternative possibility. However, the probability of formation of C^{10} from Be^7+He^3 is only 100 times greater than that of C^{11} from Be^7+He^4 (Table V) if the concentrations of He^3 and He^4 are equal. Actually, that of He^3 is only about $3\cdot10^{-4}$ (life of He^3 divided by life of protons) so that this process is 1/30 as probable as (26a). For Li^7+He^3, the situation is even less favorable.

d. Reactions with H^2.—Deuteron capture by Be^7 would lead to B^9 whose existence is very doubtful. The probability per second would be (cf. Table V and Eq. (18))

$$2\cdot10^{-12}\rho x(H^2)=2\cdot10^{-12}\cdot30\cdot1.3\cdot10^{-18}=10^{-29}, \tag{28}$$

which is only 1/10 of the probability of (26a) (Table V). Moreover, most of the B^9 formed reverts to He^4 (§6) so that the contribution of this process is negligible.

e. Reactions with He^4 in statu nascendi.—The process (25) produces continuously fast α-particles which need not penetrate through potential barriers. These α-particles have a range of 8 cm each in standard air, corresponding to 16 cm = 0.02 g/cm^2 for both. In stars, with their large hydrogen content, a somewhat smaller figure must be used

[22] It was assumed that radiative capture takes place only through the resonance level at 440 kv proton energy. The proton width of this level was taken as 11 kv, the radiation width as 40 ev.

since hydrogen has a greater stopping power per gram; we take 0.01 g/cm². The cross section for fast particles is about

$$\sigma = \pi R^2 \frac{\Gamma}{h^2/MR^2}. \quad (29)$$

With $\Gamma = 1$ volt (Table V) and $R = 3.6 \cdot 10^{-13}$ cm (Eq. (10)), this gives $\sigma = 1.3 \cdot 10^{-31}$ cm². The number of Be^7 atoms per gram is

$$6 \cdot 10^{23} x(Be^7) = 6 \cdot 10^{23} \cdot \frac{14 \text{ months}}{1.2 \cdot 10^{11} \text{ yr}} x(H) = 2 \cdot 10^{12} \quad (29a)$$

with $x(H) = 0.35$. This gives for the number of processes (26a) per proton combination:

$$0.01 \cdot 2 \cdot 10^{12} \cdot 1.3 \cdot 10^{-31} = 2.5 \cdot 10^{-21}, \quad (29b)$$

which is about the same as the formation of C^{11} or B^{11} by capture of *slow* alphas (cf. 26b, c).

Returning to the main reaction chain in the case of our assumption B, we note that the formation of Be^7 (Eq. (24)) is a very slow reaction, requiring $3 \cdot 10^7$ years at "standard" conditions ($2 \cdot 10^7$ degrees). At lower temperatures, the reaction will be still slower and, finally, it will take longer than the past life of the universe ($\sim 2 \cdot 10^9$ years). In this case, the amount of He^3 present will be much smaller than its equilibrium value (provided there was no He^3 "in the beginning") and the energy production due to reactions (24), (25) will be reduced accordingly. Ultimately, at very low temperatures ($< 12 \cdot 10^6$ degrees), the reaction H+H will lead only to He^3, and will therefore give an energy production of only 7.2 mMU, i.e., only one-quarter of the high temperature value, 27.4 mMU.

Assumption C: H^3 more stable than He^3

In this case, He^3 will be able to capture an electron,

$$He^3 + \epsilon^- = H^3. \quad (30)$$

Under the assumption that a difference in mass of 0.1 electron mass exists between He^3 and H^3, the probability of (30) is, according to (14a),

$$p(H^3) = 1.5 \cdot 10^{-11} \text{ sec.}^{-1} \quad (30a)$$

for a density $\rho = 80$ and 35 percent hydrogen content. This corresponds to a mean life of ~ 2000 years. The electron capture is therefore about 10^4 times more probable than the formation of Be^7 according to (24). This ratio will be reversed at temperatures $> 4 \cdot 10^7$ since (30) is independent of T and the probability of (24) increases as T^{15}.

H^3 will capture a proton and form He^4,

$$H^3 + H = He^4$$

with a mean life of about 0.2 seconds. This way of formation of He^4 from reaction (1) is probably the most direct of all. As in *B*, practically no energy is lost to neutrinos.

The formation of heavier elements goes as in *B*, but now there is only one Be^7 formed for 10^4 proton combination processes. This reduces the probability of formation of C^{12} by another factor 10^4, to one C^{12} in 10^{28} alphas.

The H^3 itself does not contribute appreciably to the building up of elements. It is true that the reaction $Be^7 + H^3 = B^9 + n^1$ is about 100 times as probable as $Be^7 + H^2 = B^9$ (considering the shorter life of H^3), and therefore 10 times as probable as (26a). However, most of the B^9 reverts to He^4 (cf. §6) so that (26) and (26a) remain the most efficient processes for building up C^{12}.

Summarizing, we find that the formation of nuclei heavier than He^4 can occur only in negligible amounts. One C^{12} in 10^{24} α-particles and one neutron in 10^{14} α-particles are the yields when Li^4 is unstable, one C^{12} in 10^{34} alphas and one neutron in 10^7 alphas when Li^4 is stable. The reason for the small probability of formation of C^{12} is twofold: First, any nonradioactive nucleus between He and C, i.e., $Li^{6,7}$, Be^9, $B^{10,11}$, reacting with protons will give α-particle emission rather than radiative capture so that a disintegration takes place rather than a building up. This will no longer be the case for heavier nuclei so that for these a building up is actually possible. Second, the instability of Be^8 causes a gap in the list of stable nuclei which is the harder to bridge because Be^8 is very easily formed in nuclear reactions (small mass excess). On the other hand, the instability of He^5 and Li^5 is of no influence because Be^7 and Li^7 are stages in the ordinary chain of nuclear reactions.

§6. Triple Collisions of Alpha-Particles

In the preceding section, we have shown that collisions with protons alone lead practically always to the formation of α-particles. In order that heavier nuclei be formed, use must therefore certainly be made of the α-particles themselves. However, collisions of an α-particle with one other particle, proton or alpha, do not lead to stable nuclei. Therefore we must assume triple collisions, of which three types are conceivable:

$$He^4 + 2H = Be^6, \quad (31)$$

$$2He^4 + H = B^9, \quad (32)$$

$$3He^4 = C^{12}. \quad (33)$$

The first of these reactions leads to a nucleus which is certainly unstable (Be^6). Even if it were stable, it would not offer any advantages over Be^7 which is formed as a consequence of the proton combination (1). The second reaction leads to B^9 which is probably also unstable. However, since this is not absolutely certain, we

[34] G. Breit and E. Wigner, Phys. Rev. **49**, 519 (1936).

shall discuss this process in the following. The last process leads directly to C^{12}, but since it involves a rather large potential barrier for the last α-particle, it is very improbable at $2\cdot10^7$ degrees (see below).

The formation of B^9

The probability of this process is enhanced by the well-known resonance level of Be^8, which corresponds to a kinetic energy of about $E=50$ kev of two α-particles. The formation of B^9 occurs in two stages,

$$2\ He^4 = Be^8, \quad Be^8+H=B^9 \tag{32a}$$

with a time interval of about 10^{-12} sec. (life of Be^8). The process can be treated with the usual formalism for resonance disintegrations, the compound nucleus being Be^8. This nucleus can "disintegrate" in two ways, (a) into two α-particles, (b) with proton capture. We denote the respective widths of the Be^8 level by Γ_a and Γ_H; the latter is given by the ordinary theory of thermonuclear processes, i.e.,

$$\Gamma_H = hpm_2/x_2, \tag{34}$$

where p is given by (4), and the subscripts 1 and 2 denote H^1 and Be^8, respectively.

The cross section of the resonance disintegration becomes then

$$\sigma = \pi\lambda^2\frac{\Gamma_a\Gamma_H}{(E-E_r)^2+\frac{1}{4}(\Gamma_a+\Gamma_H)^2}. \tag{35}$$

E_r is the resonance energy. Γ_a is much larger than Γ_H (corresponding to about 10^{13} and 10^{-11} sec.$^{-1}$, respectively) but very small compared with E_r (about 10^{-8} against $5\cdot10^4$ volts). The resonance is thus very sharp, and, integrating over the energy, we obtain for the total number of processes per cm^3 per sec. simply

$$\rho p = B(E_r)v_r\pi\lambda_r^2 2\pi\Gamma_H. \tag{36}$$

Here $B(E)dE$ is the number of pairs of α-particles with relative kinetic energy between E and $E+dE$ per cm^3, *viz.*

$$B(E) = \tfrac{1}{2}\left(\frac{\rho x_a}{m_a}\right)^2\frac{2}{\pi^{\frac{1}{2}}}\frac{E^{\frac{1}{2}}}{(kT)^{\frac{3}{2}}}e^{-E/kT} \tag{36a}$$

(x_a = concentration of He^4 by weight). Combining (36), (36a) and (34), (4), we find

$$p(B^9) = \frac{16\pi^{3/2}}{3^{5/2}}\frac{\rho^2x_a^2x_H}{m_a^{7/2}m_H}\frac{h^2\Gamma_{rad}}{(kT)^{3/2}}aR^2\tau^2 \times\exp\{4(2R/a)^{\frac{1}{2}}-\tau-E_r/kT\}, \tag{37}$$

where Γ_{rad} is the radiation width for the process $Be^8+H=B^9$. Numerically, (37) gives for the decay constant of hydrogen the value

$$pm_H/x_H = 1.00\cdot10^{-4}(\rho x_a)^2\Gamma\varphi T^{-\frac{1}{2}}e^{-11.7E_r/T}\tau^2e^{-\tau}, \tag{37a}$$

where T is measured in millions of degrees, the resonance energy E_r of Be^8 in kilo-electron-volts and Γ in ev. The quantities Γ, φ and τ refer to the process $Be^8+H=B^9$. If there were no resonance level of Be^8, (37) would be replaced by

$$p(B^9) = \frac{8}{243}\frac{\rho^2x_a^2x_H}{m_a^2m_H}\frac{\Gamma_{rad}}{\hbar}aR^2a'R'^2\tau^2\tau'^2 \times\exp\{(32R/a)^{\frac{1}{2}}+(32R'/a')^{\frac{1}{2}}-\tau-\tau'\}, \tag{38}$$

where the primed quantities refer to the reaction $2\ He^4=Be^8$, the unprimed ones to $Be^8+H=B^9$. Numerically, (38) gives

$$pm_H/x_H = 2.0\cdot10^{-11}(\rho x_a)^2\Gamma\varphi\tau^2e^{-\tau}\varphi'\tau'^2e^{-\tau'}. \tag{38a}$$

Assuming $T=20$, $\rho=80$, $x_a=0.25$, $\Gamma=0.02$ electron-volts, we obtain for the probability of formation of B^9 per proton per second:

$$\begin{aligned} pm_H/x_H = 2\cdot10^{-28} &\text{ for resonance, } E_r=25 \text{ kev}\\ 10^{-31} &\text{ for resonance, } E_r=50 \text{ kev}\\ 4\cdot10^{-38} &\text{ for resonance, } E_r=75 \text{ kev}\\ 2\cdot10^{-44} &\text{ for resonance, } E_r=100 \text{ kev}\\ 5\cdot10^{-42} &\text{ for nonresonance.}\end{aligned}$$

The value 25 kev for the resonance level must probably be excluded on the basis of the experiments of Kirchner and Neuert.[28] But even for this low value of the resonance energy, the probability of formation of B^9 is only 10^{-6} times that of the proton combination $H+H=H^2+\epsilon^+$ (Table V, $\rho x_1=30$). With $E_r=50$ kev which seems a likely value, the ratio becomes $4\cdot10^{-12}$. On the other hand, the building up of B^9 (if this nucleus exists) would still be the most efficient process for obtaining heavier elements (see below).

Reactions of B^9

It can easily be seen[21] that B^9 cannot be positron-active but can only capture electrons if it exists at all. If B^9 is stable by 0.3 mMU, the energy evolution in electron capture would be just one electron mass. The decay constant of B^9 (for β-capture) is then, according to (14a), $1.5\cdot10^{-9}$ sec.$^{-1}$ ($\rho=80$, $x_H=0.35$) corresponding to a lifetime of about 20 years. On the other hand, the lifetime with respect to proton capture (Table V) is 5000 years. Therefore, ordinarily B^9 will go over into Be^9. This nucleus, in turn, will in general undergo one of the two well-known reactions:

$$Be^9+H=Be^8+H^2, \tag{39}$$
$$Be^9+H=Li^6+He^4. \tag{39a}$$

Only in one out of about 10^5 cases, B^{10} will be formed by radiative proton capture. Therefore the more efficient way for building up heavier elements will be the direct proton capture by B^9, leading to C^{10}, which occurs in one out of about 300 cases.

The C^{10} produced will go over into B^{10} by positron emission. B^{10} may react in either of the following ways:

$$B^{10}+H=C^{11}, \tag{40}$$
$$B^{10}+H=Be^7+He^4. \tag{40a}$$

The reaction energy of (40a) is (cf. Table VII, §8) 1.2 mMU; the penetrability of the outgoing alphas about 1/40 (same table), therefore the probability of the particle reaction (40a) will be about 100 times that of the capture reaction (40).

The C^{11} from (40) will emit another positron. The resulting B^{11} reacts with protons as follows:

$$B^{11}+H=C^{12}, \tag{41}$$
$$B^{11}+H=3\,He^4. \tag{41a}$$

Both reactions are well-known experimentally. Reaction (41) has a resonance at 160 kev. From the width of this resonance and the experimental yields, the probability of (41) with low energy protons is about 1 in 10,000 (i.e., the same as for nonresonance). Altogether, about one B^9 in $3\cdot10^8$ will transform into C^{12}.

With a resonance energy of Be^8 of 50 kev, and $2\cdot10^7$ degrees, there will thus be about one C^{12} formed for 10^{21} α-particles if B^9 is stable. This is better than any other process but still negligibly small.

At higher temperatures, the formation of B^9 will become more probable and will, for $T>10^8$, exceed the probability of the proton combination. At these temperatures (actually already for $T>3\cdot10^7$) the B^9 will rather capture a proton (giving C^{10}). Even then, there remain the unfavorable branching ratios in reactions (40), (40a) and (41), (41a),[35] so that there will still be only one C^{12} formed in 10^6 alphas. Thus even with B^9 stable and granting the excessively high temperature, the amount of heavy nuclei formed is extremely small.

Direct formation of C^{12}

C^{12} may be formed directly in a collision between 3 α-particles. The calculation of the probability is exactly the same as for the formation of B^9. The nonresonance process gives about the same probability as a resonance of Be^8 at 50 kev. With $\rho=80$, $x_\alpha=\frac{1}{4}$, $\Gamma=0.1$ electron-volt, $T=2\cdot10^7$ degrees, the probability is 10^{-56} per α-particle, i.e., about 10^{-37} of the proton combination reaction (1). This gives an even smaller yield of C^{12} than the chains described in this and the preceding section. The process is strongly temperature-dependent, but it requires temperatures of $\sim10^9$ degrees to make it as probable as the proton combination (1).

The considerations of the last two sections show that there is no way in which nuclei heavier than helium can be produced permanently in the interior of stars under present conditions. We can therefore drop the discussion of the building up of elements entirely and can confine ourselves to the energy production which is, in fact, the only observable process in stars.

§7. The Carbon-Nitrogen Group

In contrast to lighter nuclei, C^{12} is not permanently destroyed when it reacts with protons; instead the following chain of reactions occurs

$$C^{12}+H^1=N^{13}, \tag{42}$$
$$N^{13}=C^{13}+\epsilon^+, \tag{42a}$$
$$C^{13}+H^1=N^{14}, \tag{42b}$$
$$N^{14}+H^1=O^{15}, \tag{42c}$$
$$O^{15}=N^{15}+\epsilon^+, \tag{42d}$$
$$N^{15}+H^1=C^{12}+He^4. \tag{42e}$$

Thus the C^{12} nucleus is reproduced. The reason is that the alternative reactions producing α-particles, *viz.*

$$C^{12}+H^1=B^9+He^4, \tag{43}$$
$$C^{13}+H^1=B^{10}+He^4, \tag{43a}$$
$$N^{14}+H^1=C^{11}+He^4, \tag{43b}$$

are all strongly forbidden energetically (Table VII, §8). This in turn is due to the much greater stability of the nuclei in the carbon-nitrogen group as compared with the beryllium-boron group, and is in contrast to the reactions of Li, Be and B with protons which all lead to emission of α-particles.

The cyclical nature of the chain (42) means that practically no carbon will be consumed. Only in about 1 out of 10^4 cases, N^{15} will capture a proton rather than react according to (42e). In this case, O^{16} is formed:

$$N^{15}+H^1=O^{16}. \tag{44}$$

However, even then the C^{12} is not permanently destroyed, because except in about one out of $5\cdot10^7$ cases, O^{16} will again return to C^{12} (cf. §8). Thus there is less than one C^{12} permanently consumed for 10^{12} protons. Since the concentration of carbon and nitrogen, according to the evidence from stellar spectra, is certainly greater than 10^{-12} this concentration does not change noticeably during the evolution of a star. *Carbon and nitrogen are true catalysts; what really takes place is the combination of four protons and two electrons into an α-particle.*

A given C^{12} nucleus will, at the center of the sun, capture a proton once in $2.5\cdot10^6$ years (Table V), a given N^{14} once in $5\cdot10^7$ years. These times are short compared with the age of the sun. Therefore the cycle (42) will have re-

[35] The reaction $C^{11}+H=N^{12}$ becomes more probable than $C^{11}=B^{11}+\epsilon^+$ only at $T>3\cdot10^8$ degrees. The branching ratio in (40), (40a) may perhaps be slightly more favorable because the effect of the potential barrier in (40a) may be stronger.

TABLE VI. *Central temperatures necessary for giving observed energy production in sun, with various nuclear reactions.*

REACTION	T (MILLION DEGREES)
$H^2+H=He^3$	0.36
$He^4+H=Li^5$	2.1
$Li^7+H=2He^4$	2.2
$Be^9+H=Li^6+He^4$	3.3
$B^{10}+H=C^{11}$	9.2
$B^{11}+H=3He^4$	5.5
$C^{12}+H=N^{13}$	15.5
$N^{14}+H=O^{15}$	18.3
$O^{16}+H=F^{17}$	32
$Ne^{22}+H=Na^{23}$	37

peated itself many times in the history of the sun, so that statistical equilibrium has been established between all the nuclei occurring in the cycle, *viz.* $C^{12}C^{13}N^{13}N^{14}N^{15}O^{15}$. In statistical equilibrium, the concentration of each nucleus is proportional to its lifetime. Therefore N^{14} should have the greatest concentration, C^{12} less, and $C^{13}N^{15}$ still less. (The concentration of the radioactive nuclei N^{13} and O^{15} is, of course, very small, about 10^{-12} of N^{14}). A comparison of the observed abundances of C and N is not very conclusive, because of the very different chemical properties. However, a comparison of the isotopes of each element should be significant.

In this respect, the result for the carbon isotopes is quite satisfactory. C^{13} captures slow protons about 70 times as easily as C^{12} (experimental value!), therefore C^{12} should be 70 times as abundant. The actual abundance ratio is 94 : 1. The same fact can be expressed in a more "experimental" way: In equilibrium, the number of reactions (42) per second should be the same as of (42b). Therefore, if a natural sample of terrestrial carbon (which is presumed to reproduce the solar equilibrium) is bombarded with protons, equally many captures should occur due to each carbon isotope. This is what is actually found experimentally;[35] the equality of the γ-ray intensities from C^{12} and C^{13} is, therefore, not accidental.[36]

The greater abundance of C^{12} is thus due to the smaller probability of proton capture which in turn appears to be due to the smaller $h\nu$ of the capture γ-ray. Thus the great energetic stability of C^{12} actually makes this nucleus abundant. However, it is not because of a Boltzmann factor as has been believed in the past, but rather because of the small energy evolution of the proton capture reaction.

In nitrogen, the situation is different. Here N^{14} is energetically less stable (has higher mass excess) than N^{15} but is more abundant in spite of it (abundance ratio $\sim 500:1$). This must be due to the fact that N^{15} can give a $p-\alpha$ reaction while N^{14} can only capture a proton; particle reactions are always much more probable than radiative capture. Thus the greater abundance of N^{14} is due not to its own small mass excess but to the large mass excess of C^{11} which would be the product of the $p-\alpha$ reaction (43b).

Quantitative data on the nitrogen reactions (42c), (42e) are not available, the figures in Table V are merely estimates. If our theory about the abundance of the nitrogen isotopes is correct, the ratio of the reaction rates should be 500 : 1, i.e., either $N^{14}+H=O^{15}$ must be more probable[36a] or $N^{15}+H=C^{12}+He^4$ less probable than assumed in Table V. Experimental investigations would be desirable.

Turning now to the energy evolution, we notice that the cycle (42) contains two radioactive processes (N^{13} and O^{15}) giving positrons of 1.3_5 and 1.8_5 mMU maximum energy, respectively. If we assume again that $\frac{2}{3}$ of the energy is, on the average, given to neutrinos, this makes 2.0 mMU neutrino energy per cycle, which is 7 percent of the total energy evolution (28.7 mMU). There are therefore $4.0\cdot10^{-5}$ ergs available from each cycle. (It may be mentioned that the neutrinos emitted have too low energy to cause the transformation of protons into neutrons according to (21).)

The duration of one cycle (42) is equal to the sum of the lifetimes of all nuclei concerned, i.e., practically to the lifetime of N^{14}. Thus each N^{14} nucleus will produce $4.0\cdot10^{-5}$ erg every $5\cdot10^7$ years, or $3\cdot10^{-20}$ erg per second. Under the

[35] It would be tempting to ascribe similar significance to the equality of intensity of the two α-groups from natural Li bombarded by protons ($Li^6+H=He^4+He^3$, $Li^7+H=2He^4$). However, the lithium isotopes do not seem to be genetically related as are those of carbon.

[36a] *Note added in proof:*—In this case, the life of N^{14} in the sun might actually be shorter, and its abundance smaller than that of C^{12}. Professor Russell pointed out to me that this would be in better agreement with the evidence from stellar spectra. Another consequence would be that a smaller abundance of N^{14} would be needed to explain the observed energy production.

TABLE VII. *p–α reactions.*

Initial Nucleus	Product Nucleus	Energy Evolution Q (MU)	Potential Barrier B (MU)	Penetrability P
Li^6	He^3	4.14		1
Li^7	He^4	18.59		1
Be^9	Li^6	2.45	2.6	1
B^{10}	Be^7	1.2	3.4	0.027
B^{11}	$2He^4$	9.4		1
C^{12}	B^9	−8.1		0
C^{13}	B^{10}	−4.4		0
N^{14}	C^{11}	−3.5		0
N^{15}	C^{12}	5.2	4.6	1
O^{16}	N^{13}	−5.8		0
O^{17}	N^{14}	1.3	5.1	$1.7\cdot10^{-4}$
O^{18}	N^{15}	3.1	5.0	0.2
F^{19}	O^{16}	8.8		1
Ne^{20}	F^{17}	−4.5		0
Ne^{21}	F^{18}	−1.6		0
Ne^{22}	F^{19}	−1.6		0
Na^{23}	Ne^{20}	1.6	6.7	$6\cdot10^{-6}$
Mg^{24}	Na^{21}	<-3.0		0
Mg^{25}	Na^{22}	−2.1		0
Mg^{26}	Na^{23}	−2.0		0
Al^{27}	Mg^{24}	1.8	7.6	$1.1\cdot10^{-6}$
Si^{28}	Al^{25}	<-2.9		0
Si^{29}	Al^{26}	−2.0		0
Si^{30}	Al^{27}	−2.4		0
P^{31}	Si^{28}	2.0	8.5	$2.5\cdot10^{-7}$
S^{32}	P^{29}	<0		0
S^{33}	P^{30}	−2		0
S^{34}	P^{31}	−2.0		0
Cl^{35}	S^{32}	2.3	9.3	$5\cdot10^{-8}$
Cl^{37}	S^{34}	4.2	9.1	$2.5\cdot10^{-2}$

assumption of a N^{14} concentration of 10 percent by weight, this gives an energy evolution of

$$\frac{6\cdot10^{23}\cdot0.1}{14}\cdot3\cdot10^{-20}\approx100 \text{ ergs/g sec.} \quad (45)$$

at "standard stellar conditions," i.e., $T=2\cdot10^7$, $\rho=80$, hydrogen concentration 35 percent.

This result is just about what is necessary to explain the observed luminosity of the sun. Since the nitrogen reaction depends strongly on the temperature (as T^{18}) and the temperature, as well as the density, decrease rapidly from the center of the sun outwards, the average energy production will be only a fraction, perhaps 1/10 to 1/20, of the production at the center.[36b] This means that the average production is 5 to 10 ergs/g sec., in excellent agreement with the observed luminosity of 2 ergs/g sec.

[36b] *Added in proof:*—According to calculations of R. Marshak, the correct figure is about 1/30.

Thus we see that the reaction between nitrogen and protons which we have recognized as the logical reaction for energy production from the point of view of nuclear physics, also agrees perfectly with the observed energy production in the sun. This result can be viewed from another angle: We may ignore, for the moment, all our nuclear considerations and ask simply which nucleus will give us the right energy evolution in the sun? Or conversely: Given an energy evolution of 20 ergs/g sec. at the center of the sun, which nuclear reaction will give us the right central temperature ($\sim19\cdot10^6$ degrees)?

This calculation has been carried out in Table VI. It has been assumed that the density is 80, the hydrogen concentration 35 percent and the concentration of the other reactant 10 percent by weight. The "widths" were assumed the same as in Table V. Given are the necessary temperatures for an energy production of 20 ergs/g sec. It is seen that all nuclei up to boron require extremely low temperatures in order not to give too much energy production; these temperatures ($<10^7$ degrees) are quite irreconcilable with the equations of hydrostatic and radiation equilibrium. On the other hand, oxygen and neon would require much too high temperatures. Only carbon and nitrogen require nearly, and nitrogen in fact exactly, the central temperature obtained from the Eddington integrations ($19\cdot10^6$ degrees). Thus from stellar data alone we could have predicted that the capture of protons by N^{14} is the process responsible for the energy production.

§8. Reactions with Heavier Nuclei

Mainly for the sake of completeness, we shall discuss briefly the reactions of nuclei heavier than nitrogen. For the energy production, these reactions are obviously of no importance because the higher potential barrier of the heavier nuclei makes their reactions much less probable than those of the carbon-nitrogen group.

The most important point for a qualitative discussion is the question whether a $p-\alpha$ reaction is energetically possible for a particular nucleus, and, if possible, whether it is impeded by the potential barrier. In Table VII are listed the energy evolution in $p-\alpha$ reactions for all stable

(nonradioactive) nuclei up to chlorine. In the first column, the reacting nucleus is given, in the second, the product of a $p-\alpha$ reaction. The third column contains the reaction energy Q; when Q is negative, the reaction is energetically impossible so that the initial nucleus can only capture protons with γ-emission. In the fourth column, the height of the nuclear potential barrier is given for all reactions with positive Q. In the last column, the penetrability of the potential barrier is calculated according to standard methods (reference 10, p. 166). If $Q>B$, the penetrability is 1; if Q is negative, $P=0$ was inserted.

The *a priori* probability of a $p-\alpha$ reaction is roughly 10^4 times that of radiative capture. Therefore the emission of α-particles will be preferred when $P>10^{-4}$. It is seen from the table that for all nuclei up to boron the $p-\alpha$ reaction is strongly preferred, a fact which we recognized as the main reason for the impossibility of building up heavier elements than He^4 (§5). Furthermore, in the carbon group, only proton capture is possible for $C^{12}C^{13}N^{14}$ while for N^{15} the $p-\alpha$ reaction will strongly predominate (cf. §7).

The oxygen-fluorine group shows intermediate behavior. O^{16} can only capture protons, for O^{17} the capture and the α-emission will have roughly equal probability while for O^{18} and F^{19} the $p-\alpha$ reaction will be much more probable. With a ratio 10^4 for the *a priori* probabilities, about 40 percent of the O^{17} will become F^{18} (and then O^{18} by positron emission) while 60 percent will revert to N^{14}. Of the O^{18}, only 1 part in 2000 will become F^{19}, and of the F^{19}, only 1 in 10,000 will transform into Ne^{20}. Thus, under continued proton bombardment, about one O^{16} nucleus in $5\cdot10^7$ will ultimately transform into Ne^{20}, the rest will become nitrogen.

Actually, these considerations are somewhat academic because in general the supply of protons will be exhausted long before all the O^{16} initially present in the star will have captured a proton. Because of the small energy evolution in the reaction $O^{16}+H=F^{17}$, this reaction is extremely slow ($\sim10^{12}$ years) so that equilibrium in the oxygen group will not be reached in astronomical times.

Among the nuclei heavier than fluorine, the $p-\alpha$ reaction is in general energetically permitted only for those with mass number $4n+3$. But even for these, the energy evolution is so much less than the height of the barrier that the penetrabilities are extremely small. Thus for all these elements only proton capture will occur (with the possible exception of Cl^{37}).

These considerations demonstrate the uniqueness of the carbon-nitrogen cycle.

§9. Agreement with Observations

In Table VIII, we have made a comparison of our theory (carbon-nitrogen reaction) with observational data for five stars for which such data are given by Strömgren.[1] The first five columns are taken from his table, the last contains the necessary central temperature to give the correct energy evolution with the carbon-nitrogen reactions (cf. Table VI). As in §7, we have assumed a N^{14} content of 10 percent, and an energy production at the center of ten times the average energy production (listed in the second column).

The result is highly satisfactory: The temperatures necessary to give the correct energy evolution (last column) agree very closely with the temperatures obtained from the Eddington integration (second last column). The only exception from this agreement is the giant Capella: This is not surprising because this star has greater luminosity than the sun at smaller density and temperature; such a behavior cannot possibly be explained by the same mechanism which ac-

Table VIII. *Comparison of the carbon-nitrogen reaction with observations.*

Star	Luminosity erg/g sec.	Central Density	H content (per cent)	Central Temperature (Million degrees)	
				Integration	Energy Production
Sun	2.0	76	35	19	18.5
Sirius A	30	41	35	26	22
Capella	50	0.16	35	6	32
U Ophiuchi (bright)	180	12	50	25	26
Y Cygni (bright)	1200	6.5	80	32	30

[37] A. S. Eddington, *The Internal Constitution of the Stars* (Cambridge University Press, 1926).

counts for the main sequence. We shall come back to the problem of energy production in giants at the end of this section.

For the main sequence we observe that the small increase of central temperature from the sun to Y Cygni (19 to $33 \cdot 10^6$ degrees) is sufficient to explain the much greater energy production (10^4 times) of the latter. The reason for this is, of course, the *strong temperature dependence of our reactions* ($\sim T^{18}$, cf. §10). We may say that *astrophysical data themselves would demand such a strong dependence* even if we did not know that the source of energy are nuclear reactions. The small deviations in Table VIII can, of course, easily be attributed to fluctuations in the nitrogen content, opacity, etc.

In judging the agreement obtained, it should be noted that the "observational" data in Table VIII were obtained by integration of an Eddington model,[1, 37] i.e., the energy production was assumed to be almost constant throughout the star. Since our processes are strongly temperature dependent, the "point source" model should be a much better approximation. However, it seems that the results of the two models are not very different so that the Eddington model may suffice until accurate integrations with the point source model are available.[37a]

Since our theory gives a definite mechanism of energy production, it permits decisions on questions which have been left unanswered by astrophysicists for lack of such a mechanism. The first is the question of the "model," which is answered in favor of one approximating a point source model. The second is the problem of chemical composition. The equilibrium conditions permit for the sun a hydrogen content of either 35 or 99.5 percent when there is no helium, and intermediate values when there is helium. The central temperature varies from $19 \cdot 10^6$ to $9.5 \cdot 10^6$ when the hydrogen content increases from 35 to 99.5 percent. It is obvious that the latter value can be definitely excluded on the basis of our theory: The energy production due to the carbon-nitrogen reaction would be reduced by a factor of about 10^8 (100 for nitrogen concentration, 10^6 for temperature). The proton combination (1) would still supply about 5 percent of the observed luminosity; but apart from the fact that a factor 20 is missing, the proton combination does not depend sufficiently on temperature to explain the larger energy production in brighter stars of the main sequence. Thus it seems that only a small range of hydrogen concentrations around 35 percent is permitted; what this range is, depends to some extent on the N^{14} concentration and also requires a more accurate determination of the distribution of temperature and density.

Next, we want to point out a rather well-known difficulty about the energy production of very heavy stars such as Y Cygni. With an energy production of 1200 ergs/g sec., and an available energy of $1.0 \cdot 10^{-5}$ erg per proton (formation of α-particles!), *all* the energy will be consumed in $1.7 \cdot 10^8$ years. Since at present Y Cygni still has a hydrogen content of 80 percent, its past life should be less than $3.5 \cdot 10^7$ years. We must therefore conclude that Y Cygni and other heavy stars were "born" comparatively recently—by what process, we cannot say. This difficulty, however, is not peculiar to our theory of stellar energy production but is inherent in the well-founded assumption that nuclear reactions are responsible for the energy production.[38]

Finally, we want to come back to the problem of stars outside the main sequence. The white dwarfs presumably offer no great difficulty. The internal temperature of these stars is probably rather low,[1, 39] because of the low opacity (degeneracy!) so that the small energy production may be understandable. Quantitative calculations are, of course, necessary. For the giants, on the other hand, it seems to be rather difficult to account for the large energy production by nuclear reactions. If the Eddington (or the point

[37a] Mr. Marshak has kindly calculated the central temperature and density of the sun for the point source model, using Strömgren's tables for which we are indebted to Professor Strömgren. With an average atomic weight $\mu = 1$, Marshak finds

for the point source model $T_c = 20.3 \cdot 10^6$, $\rho_c = 50.2$
for the Eddington model $T_c = 19.6 \cdot 10^6$, $\rho_c = 72.2$

Not only is the temperature difference very small (3½ percent) but it is, for the sake of the energy production, almost compensated by a density difference in the opposite direction. The product $\rho_c T_c^{18}$ is only 20 percent greater for the point source model.

[38] Even if the most stable nuclei (Fe, etc.) are formed rather than He, the possible life will only increase by 30 percent.

[39] S. Chandrasekhar, Monthly Not. **95**, 207, 226, 676 (1935).

TABLE IX. *Relations between stellar constants.*

QUANTITY	$\gamma=18$ $\alpha=1/2$ $\beta=2\frac{3}{4}$ $\delta=19\frac{3}{4}$	$\gamma=18$ $\alpha=1$ $\beta=3\frac{1}{2}$ $\delta=20\frac{1}{2}$	$\gamma=15$ $\alpha=1/2$ $\beta=2\frac{3}{4}$ $\delta=16\frac{3}{4}$	$\gamma=4.5$ $\alpha=1/2$ $\beta=2\frac{3}{4}$ $\delta=6\frac{1}{4}$
Radius R	$M^{0.75}\mu^{0.57}(yz)^{0.05}$	$M^{0.71}\mu^{0.51}(yz)^{0.05}$	$M^{0.70}\mu^{0.49}(yz)^{0.06}$	$M^{0.20}\mu^{-0.38}(yz)^{0.16}$
Temperature T	$M^{0.25}\mu^{0.43}(yz)^{-0.05}$	$M^{0.29}\mu^{0.49}(yz)^{-0.05}$	$M^{0.30}\mu^{0.51}(yz)^{-0.06}$	$M^{0.80}\mu^{1.38}(yz)^{-0.16}$
Density ρ	$M^{-1.25}\mu^{-1.71}(yz)^{-0.15}$	$M^{-1.13}\mu^{-1.53}(yz)^{-0.15}$	$M^{-1.10}\mu^{-1.47}(yz)^{-0.18}$	$M^{0.40}\mu^{1.08}(yz)^{-0.48}$
Luminosity L	$M^{4.22}\mu^{6.94}y^{-1.06}z^{-0.06}$	$M^{3.15}\mu^{7.24}y^{-1.02}z^{-0.02}$	$M^{4.27}\mu^{6.13}y^{-1.07}z^{-0.07}$	$M^{3.06}\mu^{7.20}y^{-1.20}z^{-0.20}$
Surf. temp. T_S	$M^{0.70}\mu^{1.22}y^{-0.28}z^{-0.04}$	$M^{0.59}\mu^{1.55}y^{-0.28}z^{-0.03}$	$M^{0.74}\mu^{1.29}y^{-0.30}z^{-0.05}$	$M^{1.25}\mu^{1.98}y^{-0.38}z^{-0.13}$

source) model is used, the central temperatures and densities are exceedingly low, e.g., for Capella $T=6\cdot10^6$, $\rho=0.16$. Only a nuclear reaction going at very low temperature is therefore at all possible; $Li^7+H=2He^4$ would be just sufficient. But it seems difficult to conceive how the Li^7 should have originated in *all* the giants in the first place, and why it was not burned up long ago. The only other source of energy known is gravitation, which would require a core model[40] for giants.[41] However, any core model seems to give small rather than large stellar radii.

§10. THE MASS-LUMINOSITY RELATION

In this section, we shall use our theory of energy production to derive the relation between mass and luminosity of a star. For this purpose, we shall employ the well-known homology relations (reference 1, p. 492). This is justified because we assume that all stars have the same mechanism of energy evolution and therefore follow the same model. Further, it is assumed that the matter throughout the star is non-degenerate which seems to be true for all stars except the white dwarfs. (For all considerations in this and the following two sections, cf. reference 1.)

We shall consider the mass of the star M, the mean molecular weight μ, the concentration of "Russell Mixture" y and the product of the concentrations of hydrogen and nitrogen, z, as independent variables. In addition, we introduce for the moment the radius R which, however, will be eliminated later. Then, obviously, we have for the density (at each point)

$$\rho\sim M/R^3. \tag{46}$$

From the equation of hydrostatic equilibrium

$$dp/dr=-GM_r\rho/r^2 \tag{47}$$

(G = gravitational constant) and the gas equation

$$p=RT\rho/\mu \tag{47a}$$

(R the gas constant, radiation pressure neglected), we find

$$T\sim M\mu/R. \tag{48}$$

Finally, we must use the equation of radiative equilibrium:

$$aT^3\frac{dT}{dr}=-\frac{3}{4}\frac{k}{c}\rho\frac{L_r}{4\pi r^2}, \tag{49}$$

where a is the Stefan-Boltzmann constant, c the velocity of light, k the opacity, and L_r the luminosity (energy flux) at distance r from the center.

For the opacity, we assume

$$k\sim y\rho^\alpha T^{-\beta} \tag{50}$$

(y concentration of heavy elements). Usually, α is taken as 1 and $\beta=3.5$ (Kramers' formula). However, the Kramers formula must be divided by the "guillotine factor" τ which was calculated from quantum mechanics by Strömgren.[42] For densities between 10 and 100, and temperatures between 10^7 and $3\cdot10^7$, Strömgren's numerical results can be fairly well represented by taking $\tau\sim\rho^{\frac{1}{2}}T^{-1}$. Therefore we adopt $\alpha=\frac{1}{2}$, $\beta=2.75$ in (50).

The luminosity may be written

$$L\sim M\rho zT^\gamma. \tag{51}$$

That the energy production per unit mass, L/M, contains a factor ρ follows from the fact that it is due to two-body nuclear reactions; this factor is

[40] L. Landau, Nature **141**, 333 (1938).

[41] This suggestion was made by Gamow in a letter to the author.

[42] Cf. reference 1, Table 6, p. 485.

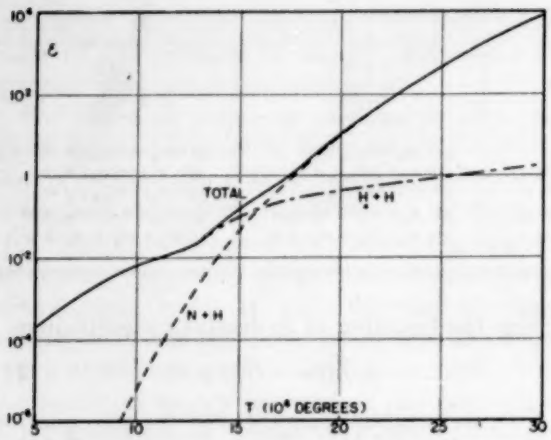

FIG. 1. The energy production in ergs/g sec. due to the proton-proton combination (curve H+H) and the carbon-nitrogen cycle (N+H), as a function of the central temperature of the star. Solid curve: total energy production caused by both reactions. The following assumptions were made: central density = 100, hydrogen concentration 35 percent, nitrogen 10 percent; average energy production 1/5 of central production for H+H, 1/10 for N+H.

apparent from all our formulae, e.g., (4). $z = x_1 x_2$ is the product of the concentrations of the reacting nuclei (N^{14} and H). For γ we obtain from (4), (6)

$$\gamma = \frac{d \log (\tau^2 e^{-\tau})}{d \log T} = \tfrac{1}{3}(\tau - 2). \tag{52}$$

For N^{14}+H and $T = 2 \cdot 10^7$, this gives $\gamma = 18$. For $T = 3.2 \cdot 10^7$ (Y Cygni), $\gamma = 15.5$; generally, $\gamma \sim T^{-\frac{1}{3}}$. $\gamma = 18$ will be a good approximation over most of the main sequence.

Inserting (50), (51) in (49), we have

$$T^{4+\beta-\gamma} \sim yz M \rho^{2+\alpha} R^{-1}. \tag{53}$$

Combining this with (46), (48), and introducing the abbreviation

$$\delta = \gamma + 3 + 3\alpha - \beta \tag{54}$$

we find

$$R \sim M^{1-2(2+\alpha)/\delta} \mu^{1-(7+3\alpha)/\delta} (yz)^{1/\delta}, \tag{55}$$

$$T \sim M^{2(2+\alpha)/\delta} \mu^{(7+3\alpha)/\delta} (yz)^{-1/\delta}, \tag{56}$$

$$\rho \sim M^{-2+6(2+\alpha)/\delta} \mu^{-3+3(7+3\alpha)/\delta} (yz)^{-3/\delta}, \tag{57}$$

$$L \sim M^{3+2\alpha+2(2+\alpha)(\beta-3\alpha)/\delta} \mu^{4+3\alpha+(7+3\alpha)(\beta-3\alpha)/\delta} \times y^{-1} (yz)^{-(\beta-3\alpha)/\delta}. \tag{58}$$

Furthermore, the surface temperature may be of interest, we have

$$T_S \sim L^{\frac{1}{4}} R^{-\frac{1}{2}} \sim M^{\frac{1}{4}+\frac{1}{2}\alpha+\frac{1}{2}(2+\alpha)(\beta-3\alpha+2)/\delta} \times \mu^{\frac{1}{4}+\frac{1}{2}\alpha+\frac{1}{2}(7+3\alpha)(\beta-3\alpha+2)/\delta} y^{-\frac{1}{4}} \times (yz)^{-\frac{1}{2}(\beta-3\alpha+2)/\delta}. \tag{59}$$

In Table IX, these formulas are given explicitly, for four different sets of constants.

The most important result is that the central *temperature* depends only slightly on the mass of the star, *viz.* as $M^{0.25}$ and $M^{0.30}$ for $\gamma = 18$ and 15. The reason for this is the strong temperature dependence of the reaction rate: The exponent of M in (56) is inversely proportional to δ which is mainly determined (cf. (54)) by the exponent γ in formula (51) for the temperature dependence of the reaction rate. The integration of the Eddington equations with the use of observed luminosities, radii, etc., gives, in fact, only a small dependence of the central temperature on the mass. This can *only* be explained by a strong temperature dependence of the source of stellar energy, a fact which has not been sufficiently realized in the past. Theoretically, the central temperature increases somewhat with increasing mass of the star, more strongly with the mean molecular weight, and is practically independent of the chemical composition, i.e., of y and z.

The *radius* of the star is larger for heavy stars and for high molecular weight. The density behaves, of course, in the opposite way. Both these results are in qualitative agreement with observation. The product of mass and density which occurs in Eq. (51) for the luminosity, is almost independent of the mass; therefore, for constant concentrations z, the luminosity is determined by the central temperature alone. Both radius and density are almost independent of the chemical composition, except insofar as it affects μ.

The *luminosity* increases slightly faster than the fourth power of the mass and the sixth power of the mean molecular weight. This increase is considerably less than that usually given ($M^{5.5}\mu^{7.5}$) and agrees better with observation. The difference from the usual formula is mainly due to the different dependence of the opacity on density and temperature; in fact, with the usual assumption ($\alpha = 1$, $\beta = 3\frac{1}{2}$), we obtain $M^{3.15}\mu^{7.24}$.

The remaining difference is that the dependence on the radius is carried as a separate factor in the usual formula while we have expressed R in terms of M and μ. The observations show, for bright stars, an even slower increase than M^4; this seems to be due to the lower average molecular weight (higher hydrogen content) of most very bright stars. It may be that these stars become unstable because of excessive energy production when their hydrogen content becomes too low (cf. §12).—The luminosity is inversely proportional to the concentration y of heavy elements (Russell mixture) because y determines the opacity. However, L is almost independent of the nitrogen concentration, as are R, T and ρ.

All these considerations are valid for bright stars, down to about three magnitudes fainter than the sun. For fainter stars, with lower central temperatures, the proton combination $H+H = D+\epsilon^+$ should become more probable than the carbon-nitrogen reactions, because this reaction depends less on temperature. In discussing the energy production from H+H, we must take into account that (cf. §5) at low temperatures, this reaction leads only to He^3 rather than He^4, because of the slowness of the reaction $He^4+He^3 = Be^7$. (Assumption B of §5 is made, *viz.* that He^3 is more stable than H^3, and Li^4 unstable.) This causes a rather sudden drop in the energy evolution from H+H around $14 \cdot 10^6$ degrees (cf. Fig. 1), i.e., just below the temperature at which the proton combination becomes important ($\sim 16 \cdot 10^6$ degrees, see Fig. 1). Therefore, the temperature exponent γ stays fairly large (~ 13, cf. Fig. 2) down to about $13 \cdot 10^6$ degrees which corresponds to an energy production of about one percent of that of the sun (five magnitudes fainter). For still fainter stars, γ drops to very low values, reaching a minimum of about 4.5 near 10^7 degrees.

The relations between central temperature, radius, luminosity and mass for this case ($\gamma = 4.5$) are given in the last column of Table IX. The temperature is seen to depend much more strongly on the mass (as $M^{0.80}$) while the radius becomes almost independent of M and the density decreases with decreasing mass. The luminosity decreases faster with the mass (as M^5) than for the bright stars. Unfortunately, little material is available for these fainter stars. This is the more regrettable as it is rather important for nuclear physics to decide whether the H+H reaction is really as probable as assumed in this paper: There is some possibility that it is forbidden by selection rules (cf. reference 16, p. 250) in which case it would be about 10^6 times *less* probable. Then the carbon-nitrogen reactions would furnish the energy even for faint stars, and the central temperature of these stars would not depend much on their mass.

Figure 1 gives the energy production due to the proton combination (H+H) and to the carbon-nitrogen reactions (N+H) as a function of the central temperature, on a logarithmic scale. The great preponderance of H+H at low and N+H at high temperatures is evident. The following assumptions were made: Hydrogen concentration 35 percent, nitrogen 10 percent, central density $\rho = 100$, average energy production = $\frac{1}{3}$ of central production for H+H, $\frac{1}{10}$ for N+H reaction. He^3 is supposed to be more stable than H^3, and Li^4 unstable (assumption B of §5).

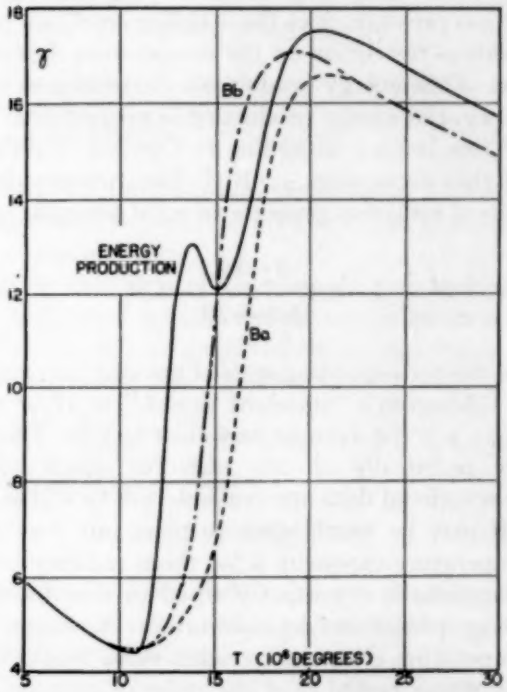

FIG. 2. The exponent γ in the relation $L \sim T^\gamma$ between luminosity L and temperature T, as a function of T. Solid curve: γ for total energy production (logarithmic derivative of solid curve in Fig. 1). Dotted curves: γ for stability against temperature changes (curve Ba for times less than 14 months, Bb for more than 14 months).

Figure 2, solid curve, gives the exponent γ in the *total* energy production. It is low at low temperatures ($\sim$4–5, hydrogen reaction) and has a minimum of 4.44 at 11 million degrees. Between 11 and 14 million degrees, γ rises steeply as the reaction $He^4+He^3=Be^7$ sets in (§5); then it falls again from 13 to 12 when this reaction reaches saturation. From $T=15$, the carbon-nitrogen reactions set in, causing a rise of γ to a maximum of 17.5 at $T=20$, while at higher temperatures γ decreases again as $T^{-\frac{1}{3}}$.

§11. Stability Against Temperature Changes

Cowling[43] has investigated the stability of stars against vibration. This stability is determined mostly by the ratio γ of the specific heats at constant pressure and constant volume. If the radiation pressure in the star is negligible compared with the gas pressure ($\gamma=5/3$) then the star will be stable for any value of the temperature exponent n in the energy production (38), up to $n\approx 450$. Only for very heavy stars, for which the radiation pressure is comparable with the gas pressure, does the stability condition put a serious restriction on the temperature dependence of the energy production. According to our theory, the energy production is proportional to T^{17} (see below); according to Cowling, stability will then occur when $\gamma>10/7$. The corresponding ratio of radiation pressure to total pressure is

$$1-\beta=\frac{5-3\gamma}{3(7\gamma-9)}=0.24 \qquad (60)$$

and the corresponding mass of the star, according to Eddington's "standard model," is $17/\mu^2\ \odot$, where μ is the average molecular weight. Therefore practically all the stars for which good observational data are available will be stable.

It may be worth while to point out that the temperature exponent n for these stability considerations is not exactly equal to that for the energy production in equilibrium. A change of temperature gives rise to radial vibrations of the star whose period is of the order of days or, at most, a few years. On the other hand, when the temperature is raised or lowered, the equilibrium between carbon and nitrogen will be disturbed and it takes a time of the order of the lifetime of C^{12} ($\sim 10^6$ years) to restore equilibrium at the new temperature. Thus we must take the concentrations of carbon and nitrogen corresponding to the *original* temperature.

At $T=2\cdot 10^7$ degrees, the carbon reactions have a $\tau=50.6$ (Table V) and therefore a temperature exponent $\gamma_C=16.2$ (cf. 52); the nitrogen reactions have $\tau=56.3$ and $\gamma_N=18.1$. The number of reactions per second is, in equilibrium, the same for each of the reactions in the chain (42). The energy evolution in the first three reactions together is 11.7 mMU, after subtracting 0.8_5 mMU for the neutrino emitted by N^{13}. These three reactions are carbon reactions, the remaining three, with an energy evolution of 15.0 mMU, are nitrogen reactions. Thus the effective temperature exponent for stability problems becomes

$$\gamma=\frac{11.7\gamma_C+15.0\gamma_N}{26.7}=17.3 \qquad (60a)$$

at $2\cdot 10^7$ degrees. γ is approximately proportional to $T^{-\frac{1}{3}}$ (cf. 52, 6).

For the proton combination, we have to distinguish the three possibilities discussed in §5. The simplest of these is assumption C.

Assumption C: Li^4 unstable, H^2 more stable than He^3

In this case, there are two "slow" processes, *viz.* (a) the original reaction H+H and (b) the transformation of He^2 into H^2 by electron capture ($\sim$2000 years). (a) depends on temperature approximately as $T^{3.5}$, (*b*) is independent of T. The energy evolution up to the formation of He^3 is 7.2 mMU, from He^3 to He^4 21.3 mMU. Thus

$$\gamma=\frac{7.2\cdot 3.5+21.3\cdot 0}{28.5}=0.9. \qquad (61C)$$

This would be a very slight dependence indeed.

Assumption A: Li^4 stable

According to Table V, the transformation of He^3 into Li^4 takes about one day.

(a) For times *shorter than one day*, the reactions up to He^3 and from then on are independent of each other. The first group again has $\gamma_H=3.5$ and gives 7.2 mMU, the second group now gives only 8.3 mMU because the remaining 13.0 are lost to the neutrino from Li^4 (cf. §5) and has (Table V) $\gamma_{He}=6.9$. Therefore

$$\gamma=\frac{7.2\cdot 3.5+8.3\cdot 6.9}{15.5}=5.3. \qquad (61Aa)$$

[43] T. G. Cowling, Monthly Not. **94**, 768 (1934); **96**, 42 (1935).

(b) For times *longer than one day*, the proton combination determines the whole chain of reactions so that

$$\gamma = 3.5. \qquad (61Ab)$$

Assumption B. Li^4 unstable, He^3 more stable than H^3 (most probable assumption)

As was pointed out in §5, the reaction $He^4+He^3=Be^7$ is so slow ($3\cdot10^7$ years, Table V) that the concentration of He^3 will remain unaffected by the temperature fluctuation. Be^7 has a mean life of 14 months at the center of the sun so that there are again two cases:

(a) *For times less than 14 months*, there are three groups of reactions, (a) those up to He^3, giving again 7.2 mMU with $\gamma_H=3.5$, (b) the reaction $He^4+He^3=Be^7$, giving (Table V) 1.6 mMU with $\gamma_{H_e}=15.1$, and (c) the electron capture by Be^7, followed by $Li^7+H=2He^4$. This last reaction does not depend on temperature ($\gamma_{Be}=0$) and gives 18.6 mMU. Therefore the effective γ becomes

$$\gamma=\frac{7.2\cdot3.5+1.6\cdot15.1+18.6\cdot0}{27.4}=1.8. \qquad (61Ba)$$

(b) *For times longer than 14 months*, the reaction $He^4+He^3=Be^7$ governs all the energy evolution from He^3 on, so that

$$\gamma=\frac{7.2\cdot3.5+20.2\cdot15.1}{27.4}=12.1 \qquad (61Bb)$$

at $2\cdot10^7$ degrees.

At low temperatures, the reaction $He^4+He^3=Be^7$ stops altogether (cf. §5) so that then the γ of the H+H reaction itself determines the radial stability. From 12 to $16\cdot10^6$ degrees we have a transition region in which the importance of the He^4+He^3 reaction (and the consequent ones) is reduced.

In Fig. 2, curves Ba and Bb, we have plotted the effective γ for the radial stability, by taking into account both C+N and H+H reactions, and making the same assumptions about the concentrations of hydrogen and nitrogen as in Fig. 1 (cf. end of §10). Assumption B was made regarding the stability of Li^4 and He^3; the curves Ba and Bb refer to the short time and long time formulas (61Ba) and (61Bb). At high temperatures, the two curves coincide because then the proton combination is unimportant compared with the carbon-nitrogen reactions. The combined γ is seen to reach a maximum of 17 (for the long time curve).

§12. Stellar Evolution[44]

We have shown that the concentrations of heavy nuclei (Russell mixture) and, therefore, also of nitrogen, cannot change appreciably during the life of a star. The only process that occurs is the transformation of hydrogen into helium, regardless of the detailed mechanism. The state of a star is thus described by the hydrogen concentration x, and by a *fixed* parameter, y, giving the concentration of Russell mixture. The rest, $1-x-y$, is the helium concentration. Without loss of generality, we may fix the zero of time so that the helium concentration is zero. (Then the actual "birth" of the star may occur at $t>0$).

It has been shown (Table IX) that the luminosity depends on the chemical composition practically only[45] through the mean molecular weight μ. This quantity is given by

$$1/\mu=2x+\tfrac{3}{4}(1-x-y)+\tfrac{1}{2}y=(5/4)(x+a), \qquad (62)$$

$$a=0.6-0.2y, \qquad (62a)$$

taking for the molecular weights of hydrogen, helium and Russell mixture the values $\frac{1}{2}$, 4/3 and 2, respectively.[1]

Now the rate of decrease of the hydrogen concentration is proportional to the luminosity, which we put proportional to μ^n. According to Table IX, n is about 6. Then

$$dx/dt\sim-(x+a)^{-n}. \qquad (63)$$

Integration gives

$$(x+a)^{n+1}=A(t_0-t), \qquad (64)$$

where A is a constant depending on the mass and other characteristics of the star. Since $x=1-y$ at $t=0$, we have

$$At_0=(1.6-1.2y)^{n+1}. \qquad (64a)$$

---

[44] Most of these considerations have already been given by G. Gamow, Phys. Rev. **54**, 480(L) (1938).

[45] Except for the factor y^{-1} which, however, does not change with time.

It is obvious from (63) and (64) that the hydrogen concentration decreases slowly at first, then more and more rapidly. E.g., when the concentration of heavy elements is $y=\frac{1}{2}$, the first half of the hydrogen in the star will be consumed in 87 percent of its life, the second half in the remaining 13 percent. If the concentration of Russell mixture is small, the result will be even more extreme: For $y=0$, it takes 92 percent of the life of the star to burn up the first half of the hydrogen. Consequently, very few stars will actually be found near the end of their lives even if the age of the stars is comparable with their total lifespan t_0 (cf. 64a). In reality, the lifespan of all stars, except the most brilliant ones, is long compared with the age of the universe as deduced from the red-shift ($\sim 2\cdot 10^9$ years): E.g., for the sun, only one percent of the total mass transforms from hydrogen into helium every 10^9 years so that there would be only 2 percent He in the sun now, provided there was none "in the beginning." The prospective future life of the sun should according to this be $12\cdot 10^9$ years.

It seems to us that this comparative youth of the stars is one important reason for the existence of a *mass*-luminosity relation—if the chemical composition, and especially the hydrogen content, could vary absolutely at random we should find a greater variability of the luminosity for a *given* mass.

It is very interesting to ask what will happen to a star when its hydrogen is almost exhausted. Then, obviously, the energy production can no longer keep pace with the requirements of equilibrium so that the star will begin to contract. (This is, in fact, indicated by the factor $z^{1/3}$ in Eq. (55) for the stellar radius; z is proportional to the hydrogen concentration.) Gravitational attraction will then supply a large part of the energy. The contraction will continue until a new equilibrium is reached. For "light" stars of mass less than $6\mu^{-2}$ sun masses (reference 1, p. 507), the electron gas in the star will become degenerate and a white dwarf will result. In the white dwarf state, the necessary energy production is extremely small so that such a star will have an almost unlimited life. This evolution was already suggested by Strömgren.[1]

For heavy stars, it seems that the contraction can only stop when a neutron core is formed. The difficulties encountered with such a core[46] may not be insuperable in our case because most of the hydrogen has already been transformed into heavier and more stable elements so that the energy evolution at the surface of the core will be by gravitation rather than by nuclear reactions. However, these questions obviously require much further investigation.

These investigations originated at the Fourth Washington Conference on Theoretical Physics, held in March, 1938 by the George Washington University and the Department of Terrestrial Magnetism. The author is indebted to Professors Strömgren and Chandrasekhar for information on the astrophysical data and literature, to Professors Teller and Gamow for discussions, and to Professor Konopinski for a critical revision of the manuscript.

[46] G. Gamow and E. Teller, Phys. Rev. **53**, 929(A), 608(L) (1938).

Radioactive Isotopes of Zinc

J. J. LIVINGOOD,*
Radiation Laboratory, Physics Department, University of California, Berkeley, California

AND

G. T. SEABORG,
Chemistry Department, University of California, Berkeley, California

(Received December 15, 1938)

The existence of zinc radioactivities with half-lives 57 minutes and 13.8 hours is confirmed, by deuteron activation of zinc. In addition, it is found that both these activities are produced by deuteron and by fast neutron irradiation of gallium, so that the two periods must be due to isomers of Zn^{69}. Both emit negative electrons and the properties of their radiations are given. It is shown that Zn^{65}, produced through deuteron bombardment of zinc, has a half-life of 250 days, agreeing with the period found by others after proton and deuteron bombardment of copper. This isotope appears to decay by K electron capture and also, to a lesser extent, by positron emission. No evidence has been found for radioactive Zn^{71}. All previously reported zinc activities are discussed and the following table contains all the known periods that are believed to be genuine.

Reaction	Half-Life	Particle Range Grams/cm² Al	Gamma-Ray Half-Thickness Grams/cm² Pb
$Zn^{64}(\gamma, n)Zn^{63}$ $Zn^{64}(n, 2n)Zn^{63}$ $Cu^{63}(p, n)Zn^{63}$ $Ni^{60}(\alpha, n)Zn^{63}$	38±2 min. (+)	?	?
$Zn^{68}(d, p)Zn^{69}$ $Zn^{68}(n, \gamma)Zn^{69}$ $Ga^{71}(d, \alpha)Zn^{69}$ $Ga^{69}(n, p)Zn^{69}$	57±2 min. (−) and 13.8±0.4 hr. (−)	~0.4 0.40	None 3.7
$Zn^{64}(d, p)Zn^{65}$ $Cu^{65}(d, 2n)Zn^{65}$ $Cu^{65}(p, n)Zn^{65}$	250±5 days (+, and K electron capture)	0.20	9.6

THE study of the radioactive isotopes of zinc has been replete with confusion and contradiction. There is but one point upon which all observers have agreed: that Zn^{63} is positron-active with a half-life of 37 to 40 minutes. This activity has been produced by 17-Mev gamma-rays[1] on zinc through $Zn^{64}(\gamma, n)Zn^{63}$; by fast neutrons[2–5] on zinc through $Zn^{64}(n, 2n)Zn^{63}$; by helium ions on nickel[6] through $Ni^{60}(\alpha, n)Zn^{63}$, and by proton bombardment of copper[7, 7a, 8, 8a] through $Cu^{63}(p, n)Zn^{63}$. These experiments in themselves limit the choice of the isotope responsible to either Zn^{63} or Zn^{65}, but since slow neutron or deuteron bombardment of zinc has never produced the activity, one can be certain that it belongs to Zn^{63}.

Early work on the bombardment of zinc with neutrons was confused because of the production of an active nickel as well as an active zinc, in addition to two easily recognized copper periods. The half-life and chemical identity of this nickel (2.6 hours, Ni^{63} or Ni^{65}) has now been established,[9] so that it is possible to interpret reasonably the pseudo-periods that were obtained without benefit of a chemical separation of zinc from nickel. (The report by Rotblat[10] of a chemically identified nickel with 60 minutes half-life, produced by fast neutrons on zinc, has

* Now at Harvard University, Cambridge, Massachusetts.

[1] W. Bothe and W. Gentner, Naturwiss. **25**, 191 (1937).
[2] M. L. Pool, J. M. Cork and R. L. Thornton, Phys. Rev. **52**, 239 (1937).
[3] F. A. Heyn, Physica **IV**, 1224 (1937).
[4] R. Sagane, Phys. Rev. **53**, 212(A) (1938), **55**, 31 (1938).
[5] R. L. Thornton, Phys. Rev. **53**, 326 (1938).
[6] L. N. Ridenour and W. J. Henderson, Phys. Rev. **52**, 139 (1937).
[7] L. N. Ridenour, L. A. Delsasso, M. G. White and R. Sherr, Phys. Rev. **53**, 770 (1938).
[7a] L. A. Delsasso, L. N. Ridenour, R. Sherr, M. G. White, Phys. Rev. **55**, 113 (1939).
[8] C. V. Strain and J. H. Buck, Phys. Rev. **53**, 943(A) (1938).
[8a] C. V. Strain, Phys. Rev. **54**, 1021 (1938).
[9] See J. J. Livingood and G. T. Seaborg, Phys. Rev. **53**, 765 (1938) for bibliography and discussion.
[10] J. Rotblat, Nature **139**, 1110 (1937).

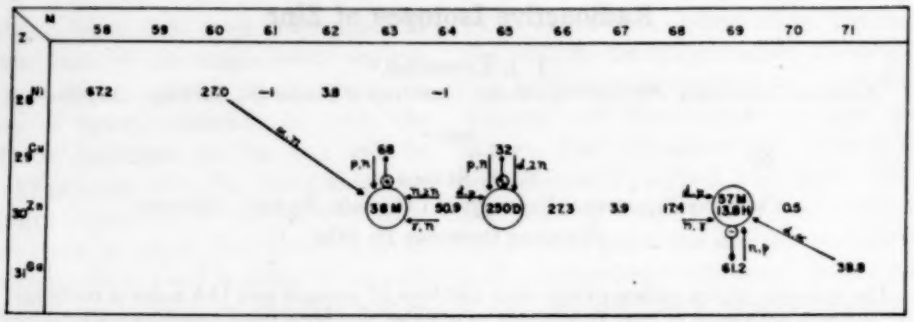

FIG. 1. Percent abundance of the stable isotopes in the neighborhood of zinc. The half-lives of radioactive forms of zinc are shown in circles; arrows indicate known transmutations.

not been confirmed and in our opinion must be considered to be in error.)

There is now some unanimity on the existence of a zinc isotope with half-life about one hour. This has been reported as produced by slow neutron[3, 4, 5, 11] and deuteron[5] bombardment of zinc and by deuteron activation of copper[5] (we will show that this last transmutation is probably erroneous). The emitted particles have been observed to be negative electrons by Sagane[4] and by Heyn.[11] The thickness of aluminum to reduce them to half-value is given by these authors as 0.06 and 0.04 gram per cm², respectively. This activity has been ascribed at various times both to Zn^{69} and Zn^{65}; the alternative choice of Zn^{71} is very improbable because of the low abundance of stable Zn^{70} (0.4 percent).

A weak zinc activity of 10 hours half-life has been found by Thornton[5] after slow neutron activation of zinc; this is probably the same as a stronger 14-hour zinc period obtained by him following bombardment of zinc with fast neutrons and also after deuteron bombardment of zinc and of gallium. This activity has been assigned to Zn^{69}, since the $Ga(d, \alpha)Zn$ reaction could lead but to this one beta-particle emitting zinc isotope.

Thornton has also reported[5] a weak 4-day zinc period after activating zinc with deuterons. This has been shown by Alvarez[12] actually to be Ga^{67}, formed by $Zn^{66}(d, n)Ga^{67}$; the same gallium period has been obtained by Mann[13] through $Zn^{64}(\alpha, p)Ga^{67}$ and by Strain and Buck[8] through $Zn^{67}(p, n)Ga^{67}$ or $Zn^{66}(p, \gamma)Ga^{67}$. We also have confirmed this identification, after deuteron activation of zinc (unpublished).

Thornton also states[5] that a weak zinc activity with 30 days half-life is produced by deuteron bombardment of zinc and suggests that it be due to Zn^{71}.

Perrier, Santangelo and Segrè[14] have reported a zinc activity with 245 days half-life from deuteron activated copper. Barnes and Valley[15] quote a 7-month period from proton activated copper. We have reported[16] a 7-month zinc period from zinc bombarded with deuterons. In our opinion, for which we will give evidence further on, Thornton's 30-day figure is to be interpreted as an indication of this longer period and not as a separate activity.

In this paper we propose to show conclusively that the 7-month activity is due to Zn^{65} and that the one-hour and 14-hour periods are isomers of Zn^{69}. To aid in understanding the arguments, the known stable isotopes[17] in the pertinent region are displayed in Fig. 1, with the radioactive forms of zinc shown in circles. The bombardments were made with the Berkeley cyclotron, with deuteron currents up to 100 microamperes at eight Mev. The activities were observed with an air-filled quartz-fiber electroscope with a thin window of 0.0001 inch aluminum. For deuteron bombardments, C.P. sticks or sheets of zinc were soldered to a water-cooling pipe and activated in vacuum; the surface was

[11] F. A. Heyn, Nature **138**, 723 (1936).
[12] L. W. Alvarez, Phys. Rev. **53**, 606 (1938).
[13] W. B. Mann, Phys. Rev. **54**, 649 (1938).
[14] C. Perrier, M. Santangelo and E. Segrè, Phys. Rev. **53**, 104 (1938).
[15] S. W. Barnes and G. Valley, Phys. Rev. **53**, 946(A) (1938).
[16] J. J. Livingood and G. T. Seaborg, Phys. Rev. **54**, 239 (1938).
[17] M. S. Livingston and H. A. Bethe, Rev. Mod. Phys. **9**, 380 (1937).

then filed to obtain the radioactive metal. For gallium, the deuterons were passed through a thin aluminum window into the air where they struck a puddle of molten gallium (melting point 30.1°C) supported in a depression in a carbon block. To obtain high intensities of fast neutrons, metallic lithium was pressed into a corrugated and water-cooled copper plate which was bombarded in helium at reduced pressure, the deuterons entering this subsidiary target chamber[18] through a thin aluminum foil.

All of the measurements were made upon chemically separated samples. The zinc was separated last, after the removal of other radioactive elements produced by the bombardments. The zinc from the Zn+D activations was dissolved in a mixture of dilute HCl and HNO_3 and small amounts of $GaCl_3$ and $CuCl_2$ were added to serve as carriers for the transmutation products copper and gallium. The solution was then adjusted to 6.0 *N* in HCl and the $GaCl_3$ was extracted with ether, according to the method of Noyes and Bray.[19] Complete removal of the $GaCl_3$ was insured by several additional shakings with fresh portions of ether. The HCl solution was then adjusted to a concentration one *N* and the copper was precipitated as CuS by introducing H_2S. After removal of the CuS by filtration, the filtrate was made alkaline with NH_4OH and the zinc was precipitated as ZnS upon the further addition of H_2S.

Essentially the same procedure was followed to separate zinc after the bombardments of gallium with neutrons. After deuteron bombardment of gallium, the gallium was dissolved in a mixture of HCl and HNO_3 following the addition of carrier $GeCl_4$ and $ZnCl_2$. The volatile $GeCl_4$ was distilled off and the $GaCl_3$ was extracted with ether in the manner described above. The zinc was then removed by precipitation as ZnS with H_2S from an alkaline solution.

Radioactive Isotope Zn^{69}: From Zn+D, Zn+n, Ga+D and Ga+n: Half-Lives 57±2 Minutes (−) and 13.8±0.4 Hours (−)

Figure 2 shows the decay of radioactive zinc separated from a bombardment of zinc for a few minutes with several microamperes of eight-Mev deuterons. The half-lives are 57 minutes and 13.8 hours; both activities emit negative electrons, as found by magnetic deflection. They must therefore be assigned to either Zn^{69} or Zn^{71} or to both. The initial activities, extrapolated back to the end of the bombardment, are 30 and 1.1 divisions per second, respectively; when corrected to infinite bombardment time these figures become 494 and 263 divisions per second, so that their ratio is 1.88. This number at once suggests the isomerism of the two periods, since the abundances of the stable isotopes Zn^{68} and Zn^{70} (17.8 percent and 0.4 percent) would lead one to expect a ratio of 44.5 if the activities were associated one with Zn^{69} and one with Zn^{71}.

In accord with the results of Thornton, we find that eight-Mev deuterons on gallium yield the 13.8-hour activity in the zinc precipitate. In addition, we find also the 57-minute period in the zinc. (See Fig. 2.) Both these activities have again been found to be electron emitters. This proves conclusively that the two periods are associated with one isotope and that this must be Zn^{69} since no other beta-particle emitting

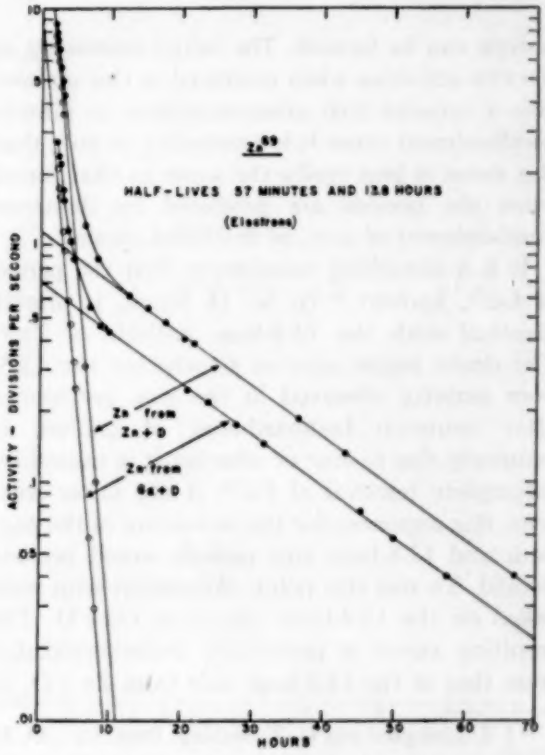

Fig. 2. Decay curves of Zn^{69}.

[18] F. N. D. Kurie, J. App. Phys. **9**, 691 (1938).
[19] A. A. Noyes and W. C. Bray, *Qualitative Analysis for the Rare Elements* (Macmillan Company, 1927).

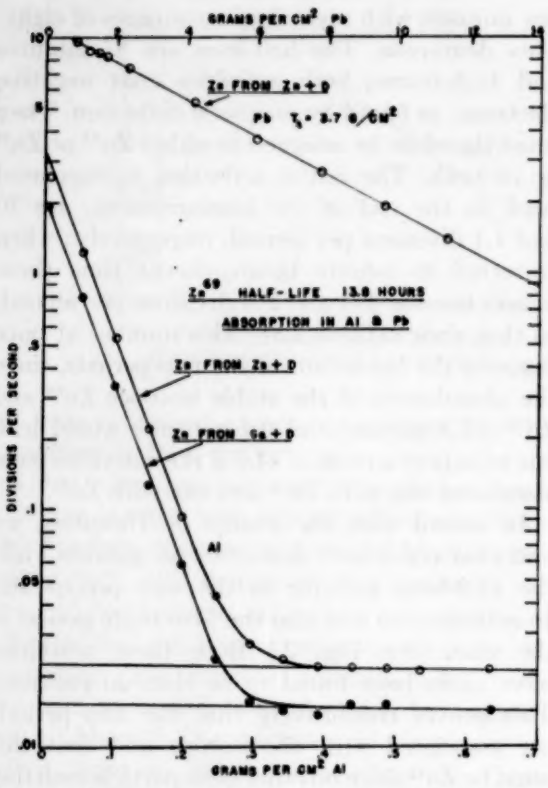
GRAMS PER CM² Pb
Zn FROM Zn + D
Pb $T_{\frac{1}{2}}$ = 2.7 G/CM²
Zn⁶⁹ HALF-LIFE 13.8 HOURS
ABSORPTION IN Al & Pb
Zn FROM Zn + D
Zn FROM Ga + D
Al
DIVISIONS PER SECOND
GRAMS PER CM² Al

FIG. 3. Absorption curves of 13.8-hour period of Zn^{69}.

isotope can be formed. The initial intensities of the two activities when produced in this manner give a ratio of 2.00 after correction to infinite bombardment time. It is interesting to note that this value is practically the same as that found when the periods are produced by deuteron bombardment of zinc, as described above.

It is a disturbing coincidence that the period of Ga^{72}, known[4, 20] to be 14 hours, is almost identical with the 13.8-hour half-life of Zn^{69}. The doubt might arise as to whether the 13.8-hour activity observed in the zinc precipitate after deuteron bombardment of gallium is genuinely due to zinc or whether it is caused by incomplete removal of Ga^{72}; if the latter were true, this argument for the isomerism of the one-hour and 13.8-hour zinc periods would become invalid. To test this point, absorption data were taken on the 13.8-hour zinc from Ga+D. The resulting curve is practically indistinguishable from that of the 13.8-hour zinc from Zn+D, as is shown in Fig. 3; furthermore, the range and half-thickness of the electrons from the 14-hour Ga^{72} are unquestionably different, as we will show in a subsequent paper.

As a final check, we have bombarded gallium with the fast neutrons from Li+D and again have found in the zinc precipitate the 57-minute and 13.8-hour periods, both negative electron emitters. (The neutrons released during the deuteron bombardment of gallium may have enough energy to cause the Ga(n, p)Zn reaction, so that part of the intensity of the 57-minute and 13.8-hour periods observed after a Ga+D activation may be due to this mechanism; however, intensity arguments show that practically all the activities in this case must be due to the Ga(d, α)Zn reaction.)

We therefore feel that it has been demonstrated positively that both the 57-minute and 13.8-hour activities belong to Zn^{69}, and the modes of production are:

$$
\begin{aligned}
&{}_{30}Zn^{68}+{}_{1}D^{2}\rightarrow{}_{30}Zn^{69}+{}_{1}H^{1},\\
&{}_{30}Zn^{68}+{}_{0}n^{1}\rightarrow{}_{30}Zn^{69}+\gamma,\\
&{}_{31}Ga^{71}+{}_{1}D^{2}\rightarrow{}_{30}Zn^{69}+{}_{2}He^{4},\\
&{}_{31}Ga^{69}+{}_{0}n^{1}\rightarrow{}_{30}Zn^{69}+{}_{1}H^{1},
\end{aligned}
$$

which are followed in each case by

$$
{}_{30}Zn^{69}\rightarrow{}_{31}Ga^{69}+{}_{-1}e^{0}\quad 57\text{ min. and }13.8\text{ hr.}
$$

The only published report inconsistent with the above interpretation is that of Thornton, who reports[5] a 65-minute zinc isotope produced by bombarding copper with deuterons; this activity would have to be placed with Zn^{65} or Zn^{63} through Cu^{65}(d, $2n$)Zn^{65}, Cu^{63}(d, γ)Zn^{65} or Cu^{63}(d, $2n$)Zn^{63}. We have repeated this bombardment but have not been able to confirm Thornton's findings; any one-hour activity in the zinc precipitate was certainly less than one part in 10,000 of that of the 12.8-hour Cu^{64} period in the copper precipitate. If Thornton's yield of one-hour zinc was of this order of magnitude perhaps it could be accounted for by an impurity of stable zinc in the copper used by him.

An early report by one of us[21] that the bombardment of zinc with 3.2-Mev deuterons gives activities with half-lives one hour, 12 hours, 25 hours and 97 hours (without chemical

[20] J. J. Livingood and G. T. Seaborg, Phys. Rev. **54**, 51 (1938).

[21] J. J. Livingood, Phys. Rev. **50**, 425 (1936).

analysis) can now be interpreted reasonably as due to the formation of the 57-minute Zn^{69}, 66-minute Ga^{68}, 13.8-hour Zn^{69} (and possibly 12.8-hour Cu^{64}) and the 4-day Ga^{67} activities; the 25-hour period was probably a spurious apparent component of the complex decay curve.

Absorption data for the 13.8-hour activity from Zn+D and Ga+D are shown in Fig. 3. The electrons have a range of 0.40 ± 0.03 gram per cm^2 Al, corresponding to an energy of 1.1 Mev through the relation of Widdowson and Champion:[22]

$$E(\text{Mev}) = [\text{Range}(\text{grams/cm}^2) + 0.165]/0.536.$$

The gamma-ray is absorbed to half-value by 3.7 grams per cm^2 Pb, which indicates an energy of 0.4 Mev through the correlation of Gentner.[23]

Absorption data for the 57-minute activity, both from Zn+D and Ga+D bombardments, are shown in Fig. 4. These curves are the result of differences of data taken when both the 57-minute and 13.8-hour periods were present and when only the latter was left. Correction for decay was applied. It may be seen that no gamma-ray is present in the 57-minute activity. The electrons show a half-thickness of 0.033 gram per cm^2 Al and an estimated range of about 0.35 gram per cm^2, corresponding to an energy of roughly one Mev.

There is no evidence that there exists a genetic relationship between the two activities of this isomer of the type recently studied by Pontecorvo[24] in rhodium and by Segrè, Halford and Seaborg[24a] in bromine, because the absorption curves give no definite indication of the presence of a line spectrum of soft electrons.[25] This might make it appear that the two activities, arising from two different states of Zn^{69}, each decay by beta-emission to stable Ga^{69}. If there is a transition between the two levels of Zn^{69}, it has not been observed as a line of electrons in these experiments. However, the active samples were covered with Cellophane of three mg per cm^2 thickness (to protect the electroscope from contamination), so that very soft electrons would have been missed.

[22] E. E. Widdowson and F. C. Champion, Proc. Phys. Soc. **50**, 192 (1938).
[23] W. Gentner, J. de phys. et rad. **6**, 274 (1935).
[24] B. Pontecorvo, Phys. Rev. **54**, 542 (1938).
[24a] E. Segrè, R. S. Halford and G. T. Seaborg, Phys. Rev. **55**, 321 (1939).
[25] M. H. Hebb and G. E. Uhlenbeck, Physica **V**, 607 (1938).

Radioactive Isotope Zn^{65}: From Zn+D, Cu+D and Cu+H; Half-Life 250±5 Days (+ and K Electron Capture)

Perrier, Santangelo and Segrè have obtained[14] a radioactive zinc isotope with half-life 245 days from deuteron activated copper, by using filings from the copper deflector plate of the Berkeley cyclotron. The sign of the particles was not determined but they suggested the reaction $Cu^{63}(d, \gamma)Zn^{65}$; alternative possibilities for the transmutation are $Cu^{65}(d, 2n)Zn^{65}$ or $Cu^{63}(d, 2n)Zn^{63}$, with positron emission or K electron capture postulated in all cases.

Barnes and Valley have found[15] an activity in proton bombarded copper, the half-life of which was about seven months. Both positrons and electrons were observed, with a high γ/β ratio.

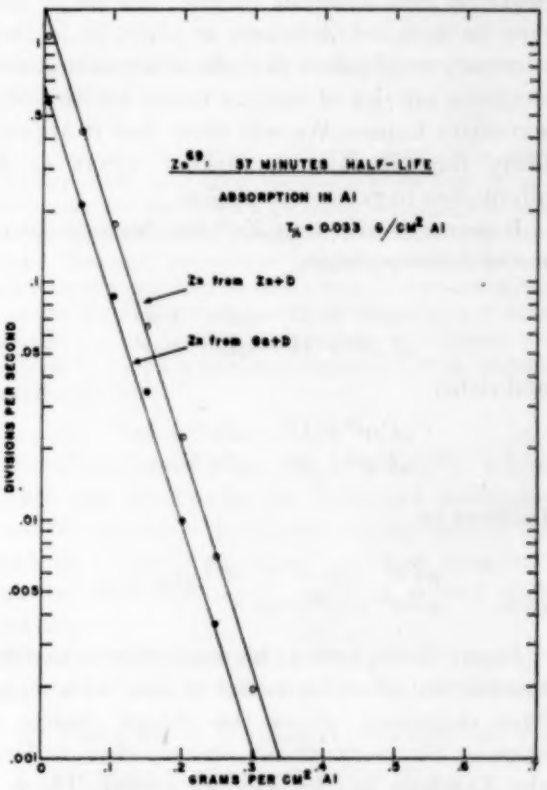

FIG. 4. Absorption curves of 57-minute period of Zn^{69}.

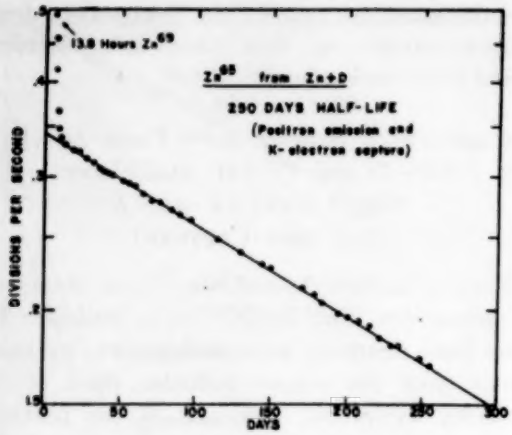

FIG. 5. Decay curve of Zn^{65}.

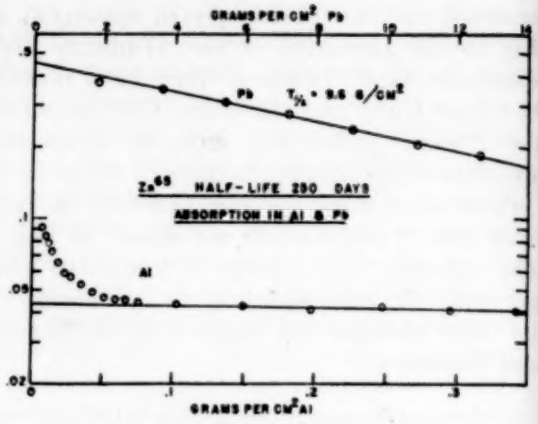

FIG. 6. Absorption curves of Zn^{65}.

This activity could be ascribed to either Zn^{65} or Zn^{63}, through the Cu(p, n)Zn reaction.

We have briefly announced[16] that the deuteron bombardment of zinc gives rise to a chemically identified zinc isotope with half-life of seven months, from which both positrons and electrons are observed. Since Zn^{63} cannot be produced by deuteron bombardment of zinc, the decay can now be assigned definitely to Zn^{65}; it is then necessary to postulate that the observed negative electrons are not of nuclear origin but are of a secondary nature. We will show that it appears likely that K electron capture occurs as an alternative to positron emission.

It seems certain that Zn^{65} has been produced in the following ways:

$$_{30}Zn^{64}+{}_1D^2\rightarrow{}_{30}Zn^{65}+{}_1H^1,$$
$$_{29}Cu^{65}+{}_1H^1\rightarrow{}_{30}Zn^{65}+{}_0n^1,$$

and either

$$_{29}Cu^{65}+{}_1D^2\rightarrow{}_{30}Zn^{65}+2{}_0n^1$$

or

$$_{29}Cu^{63}+{}_1D^2\rightarrow{}_{30}Zn^{65}+\gamma,$$

followed by

$$\left.\begin{aligned}&{}_{30}Zn^{65}\rightarrow{}_{29}Cu^{65}+{}_{+1}e^0\\ \text{and}\quad&{}_{30}Zn^{65}+{}_{-1}e^0\rightarrow{}_{29}Cu^{65}\end{aligned}\right\}\ 250\text{ days.}$$

Figure 5, displaying the decay of zinc precipitated from a bombardment of zinc with eight-Mev deuterons, shows the abrupt change of slope as the predominant activity changes from the 13.8-hour to the 250-day period. There is no trace of the 30-day decay quoted by Thornton.

Figure 6 exhibits the absorption curves of the 250-day activity. When beta-particles and gamma-rays are present in equal numbers, the ionization due to the particles is usually 30 to 70 times as much as that due to the gamma-rays. In this case, however, the gamma-ray causes more ionization than does the soft component. The presence of such a relatively small number of particles suggests at once that most of the transformations of Zn^{65} to Cu^{65} must occur as the result of the capture by Zn^{65} of one of its K electrons. The gamma-rays are emitted by the nucleus of Cu^{65} and are only slightly internally converted. The Cu $K\alpha$ x-ray line should also be present, emitted when the vacancy in the K shell is filled.

In one experiment, all of the particles were removed by a magnetic field between the specimen and the electroscope, and an absorption curve in aluminum was taken; this showed the presence of x-rays with approximately the absorption coefficient appropriate to the Cu $K\alpha$ line. A precise demonstration that the radiation actually is Cu $K\alpha$ would consist in showing that the absorption shows a discontinuity in the neighboring elements cobalt and nickel: Cu $K\alpha$ is strongly absorbed in cobalt and only weakly in nickel. This experiment was not attempted because sufficiently thin foils of cobalt were not available.

Alvarez[26] has also made x-ray absorption measurements on this activity. He found that the radiation could not be Zn $K\alpha$ since there

[26] L. W. Alvarez, Phys. Rev. **54**, 486 (1938).

was no large difference in the absorption in nickel and copper. The magnitude of his experimentally determined absorption coefficients showed that the x-rays were from an element in this region but of atomic number less than that of zinc; since they could not reasonably be from nickel, they must be copper $K\alpha$ radiation.

The soft component in Fig. 6 consists of x-rays and secondary electrons as well as positrons; for this reason it is not possible to give a value for the upper energy limit for the positrons from these data. Barnes and Valley, from cloud-chamber measurements, give a range of 0.20 gram per cm² Al, corresponding to an energy of about 0.7 Mev.

The absorption curve in lead shows the gamma-ray to be reduced to half-value by 9.6 grams per cm² Pb, which indicates an energy of 1.0 Mev. The fact that the 0.5-Mev annihilation radiation is present to an inappreciable amount lends confirmation to the conclusion that most of the Zn^{65} atoms decay by K electron capture rather than by positron emission.

In an earlier paper[21] one of us reported an activity of 130 days half-life in deuteron-activated copper, after following the decay for three months. Continued observations for two years have shown the period to lengthen out to 222 days, so that the activity is doubtless that of Zn^{65}, formed in the same manner as when reported by Perrier *et al.*, but contaminated with some shorter lived impurity.

This research has been made possible by the generous support of the Research Corporation. We wish also to thank the W.P.A. for valuable assistance.

MARCH 1, 1939 PHYSICAL REVIEW VOLUME 55

The Emission of Secondary Electrons Under High Energy Positive Ion Bombardment

A. G. Hill, W. W. Buechner, J. S. Clark and J. B. Fisk*
George Eastman Research Laboratory of Physics, Massachusetts Institute of Technology, Cambridge, Massachusetts

(Received January 6, 1939)

The yield of secondary electrons from metallic surfaces produced by high energy positive ions has been measured for the energy range 43 to 426 kv. Cold targets of Mo, Pb, Al and Cu were bombarded by protons, H_2^+ ions and He^+ ions. For protons the yield decreased from approximately 4 at low energies to approximately 2 at high energies. For H_2^+ ions the yields were more nearly constant with energy and about equal to 6. No great dependence of the yield on the kind of metal used was detected. The yield of secondaries from Mo under He^+ bombardment was approximately 13 and varied very slowly with the energy. The great majority of the secondaries had energies less than 30 volts in all cases. The electrostatic generator and associated high voltage apparatus is of a type which has been described before. However, several new features in the design and operation are described in detail here. The proton source is of the low voltage, capillary type and delivers 50 μa of focused ions of which approximately 50 percent are protons. This arc has been in operation for a year without replacement.

Introduction

THE emission of secondary electrons from metallic surfaces bombarded by positive ions has been studied in detail by several investigators in the range below 2000 volts energy. Representative examples are given by the work of Oliphant and Moon[1] in which molybdenum was bombarded by singly charged helium ions, and the work of Healea and Chaffee,[2] in which nickel was bombarded by hydrogen molecular ions. In the region of higher energies there is the work of Linford,[3] who used mercury ions, and the recently announced work of Allen,[4] with protons.

It is the purpose of the present work to investigate the yield of secondary electrons from several

* Society of Fellows, Harvard University; now at University of North Carolina, Chapel Hill.

[1] M. L. E. Oliphant and P. B. Moon, Proc. Roy. Soc. **A127**, 373 (1930).

[2] M. Healea and E. L. Chaffee, Phys. Rev. **49**, 925 (1936).

[3] L. H. Linford, Phys. Rev. **47**, 279 (1935).

[4] J. S. Allen, Bull. Am. Phys. Soc. **13**, No. 5, Abs. No. 17 (1938).

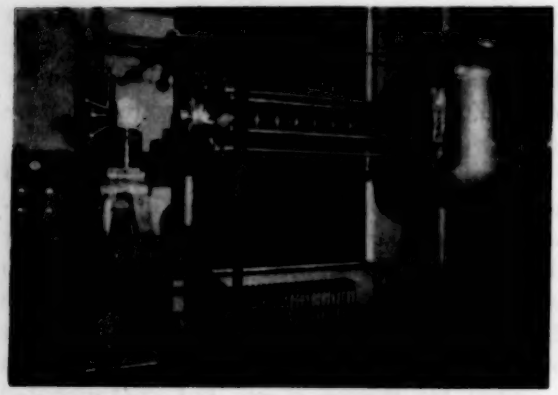

FIG. 1. Assembly.

metals when protons, hydrogen molecular ions, and singly charged helium ions are used as the primary particles at energies up to 426 kilovolts. Since the production of secondaries is an important factor to be considered in the design of high voltage discharge tubes, it was decided to study first the yield of secondaries at various primary energies under reasonably good vacuum conditions, such as obtain in the usual high voltage discharge tube, and leave for the future, work on thoroughly outgassed targets.

The electrostatic generator and associated equipment used in the present work is similar in construction to that which has been described in detail elsewhere.[5] However, several new features have been incorporated in the design, and these will be described in some detail.

THE HIGH VOLTAGE APPARATUS

The complete assembly is shown in the photograph, Fig. 1. The belt generator is external to the high voltage body and is of the type described by Bramhall.[6] The discharge tube is very similar to the tube described by Van Atta, Van de Graaff and Van Atta[7] and consists of eleven porcelain sections $10\frac{1}{2}$-in. inside diameter by 5 in. long, which contain the steel focusing electrodes. A schematic drawing of the tube is shown in Fig. 2. The power in the high voltage body is supplied by a belt-driven 110-volt 7-amp. alternator which is compact and allows a 50 percent capacity over the usual load requirements. The high voltage is regulated by means of a set of grounded corona points fastened to an adjustable lever arm shown at the top of the photograph.

The tube is evacuated by a steel mercury diffusion pump with a dry ice trap designed to hold 20 lb. of dry ice, which is sufficient for 24 hours operation. The net pumping speed for air at the outlet from the high voltage tube is 75 liters per second. This pump is backed by a glass diffusion pump of the design described by Copley, Simpson, Tenney, and Phipps,[8] which in turn is backed by a Cenco Hyvac. The tube is provided with a separate outlet for pumping the tube down to a rough vacuum by means of a Cenco Hypervac. To avoid the necessity of keeping dry ice on the traps whenever the pumps are not in use, a simple sylphon sealed valve is provided on the high vacuum side of the trap to prevent mercury from entering the high voltage tube. This pumping system has proved itself extremely reliable in operation and does away with the uncertainty regarding tube condition and surface contaminations sometimes attendant upon the use of oil pumps in high voltage work of this kind.

The tube vacuum is measured by a McLeod gauge, and is approximately 1×10^{-6} mm when the ion source is not in use. With the source turned on, the pressure in the tube rises to about 10^{-4} mm of Hg. All joints in the vacuum system are provided with guard rings wherever possible to enable rapid and reliable checking of the lead wires used as vacuum seals. It has been our experience that in a system having a large number of joints, including many which must be changed frequently, it is very desirable to be able to determine quickly and definitely which joint, if any, may be limiting the pressure.

The belt generator terminates in a two-foot sphere supported on a one-foot diameter Textolite column. Unless this column is of the proper conductivity, this type of assembly is characterized by a very high potential gradient at the joint between sphere and column, which gives rise to large corona losses. To reduce this gradient and hence eliminate these losses the following procedure was used very successfully. Four hundred I.

[5] L. C. Van Atta, D. L. Northrup, C. M. Van Atta and R. J. Van de Graaff, Phys. Rev. **49**, 761 (1936).
[6] E. H. Bramhall, Rev. Sci. Inst. **5**, 18 (1934).
[7] C. M. Van Atta, R. J. Van de Graaff, and L. C. Van Atta, Phys. Rev. **51**, 1013(A) (1937).
[8] M. J. Copley, O. C. Simpson, H. M. Tenney and T. E. Phipps, Rev. Sci. Inst. **6**, 265 (1935).

R. C. resistors of 20 meghoms each were soldered together and wrapped in a helix around the column from sphere to ground, roughly 27 turns in all. To space the adjacent turns, two strands of ½-in. cotton rope, thoroughly dried and soaked in boiling beeswax, were wrapped concurrently with the resistance wrapping. The whole was then covered with a plastic mixture of beeswax and Venice turpentine to protect the resistors from corona currents. This method of equalizing the gradient raised the available voltage by approximately 30 percent. Furthermore, when calibrated in terms of a standard high voltage resistance this provided a means of measuring the voltage quickly and accurately. The current through this resistor is about 60 μa at 450 kv.

Up to the present time the maximum operating voltage has been 450 kv. This voltage is obtained with approximately 350 μa of charging current carried by the belt. Under normal conditions there are no visible corona losses to the walls of the room. The maximum voltage is evidently limited by leakage currents along the insulating columns, and can be raised by increasing the charging current. It has been noticed that this current can be increased by 10 to 20 percent by saturating the air in the belt compartment of the generator with carbon tetrachloride.

The room itself is somewhat small for this installation, being 19 ft. long by 13 ft. wide by 16 ft. high, with a minimum distance of 3 ft. from the high voltage body to the walls. When the charging current is raised much in excess of 400 μa corona currents appear, and if the voltage is to be raised still further the insulating properties of the air must be increased. This has been accomplished by saturating the air around the high voltage body with carbon tetrachloride as was done by Joliot, Feldenkrais and Lazard.[9] While this method has not been pushed to its limit, preliminary trials suggest that the limiting voltage obtainable in the future will be well over 500 kv. In order to screen the control part of the room from the carbon tetrachloride vapor, a rubberized canvas partition has been installed coincident with the iron framework shown in the photograph.

In an apparatus of this sort, where both the space and power available at high voltage are limited, the problem of a suitable ion source is particularly important. The source should give as high an ion purity as possible, should be small, reliable, and easy to start and operate, and should be as efficient in power consumption as possible. In addition, it should deliver the ions in a state which makes for ease of focusing, since auxiliary power supplies for probe and accelerating electrodes are necessarily bulky and power consuming. The type chosen for use in the present installation was the Pyrex capillary source described by Lamar, Buechner, and Compton,[10] and was constructed as shown in Fig. 3.

[9] F. Joliot, M. Feldenkrais, and A. Lazard, Comptes rendus **202**, 291 (1936).

[10] E. S. Lamar, W. W. Buechner, and K. T. Compton, Phys. Rev. **51**, 936 (1937).

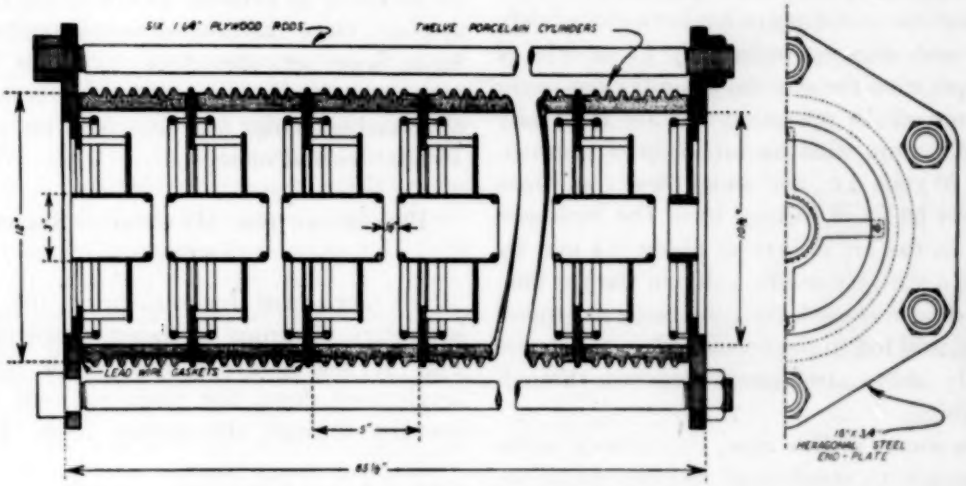

FIG. 2. Cross section of high voltage discharge tube.

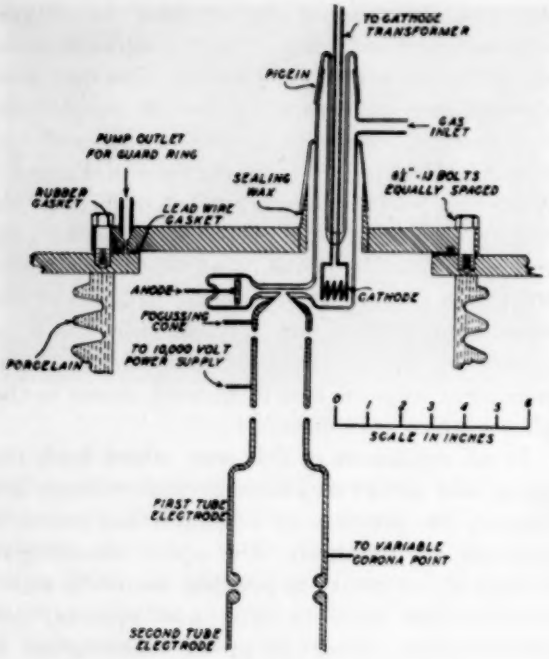

FIG. 3. Schematic diagram of ion source.

The capillary was constructed of heavy wall Pyrex capillary with an inside diameter of 3.5 mm having an outlet hole 0.5 mm in diameter in the center. This hole was beveled so that the hole itself had "zero thickness." Onto this capillary were blown chambers for the anode and cathode and the whole assembly was supported on a single glass grind, as shown. To facilitate replacement of cathodes the cathode leads were brought out on a grind sealed with Picein.

The source so constructed has been exceedingly reliable, and after approximately 12 months of steady operation the original assembly has never been removed. In operation the arc is usually run at 0.2 amp. with an arc drop of approximately 120 volts d.c., and under these conditions will deliver 60 μa of focused ions. The hydrogen pressure in the arc is kept at about 0.1 mm by means of a variable needle valve in the gas line. Tank hydrogen is used, the tank being at ground potential, and fed to the needle valve and source at slightly above atmospheric pressure through Pyrex tubing.

With a source of this type, the cathode is the main obstacle to steady and reliable operation. After some experimentation, we found that commercial uncoated ribbon as used in 866 tubes[11] wound into a helix and then coated with R-500 solution, were, when used at 2.5 v and 5 amp. very reliable and trouble free. (The R-500 solution is a barium carbonate-strontium carbonate suspension made by the Baker Chemical Company.) Cathodes of this type have useful lives of over 500 hours and, when they fail, a cleaning with HNO_3 and recoating is usually sufficient to restore emission properties.

As pointed out by Lamar, Samson and Compton,[12] there are numerous advantages to allowing the ions to drift out of the arc into a region of relatively high vacuum before applying a focusing voltage. This is particularly true with a nonmetallic source. In the present installation the first few high voltage electrodes were constructed as in Fig. 3. To provide a focusing field around the source outlet, a steel cone was placed as shown. The first cylinder was connected to a 10,000-v power supply Variac controlled in the high voltage body and the second cylinder was held at some definite unmeasured potential by means of an external corona point. The adjustment of the potential on the first two cylinders could be made from the ground end of the apparatus, thus enabling the operator to focus the beam to any desired size, without changing the tube voltage. With this arrangement the spot could be varied in diameter from 1 mm to about 2.5 cm without appreciable change in ion current. The spot size was determined by inserting a quartz plate into the line of the beam, by means of an external switch acting through a sylphon. Once the desired voltage and spot size have been set the three variables, voltage, current and spot size, remain very constant; no appreciable change was detected over periods of 15 minutes and more.

PROCEDURE FOR MEASURING SECONDARY EMISSION

The apparatus for measuring the yield of secondary electrons is shown schematically in Fig. 4. The positive ions which have been accelerated down the main vacuum tube are brought through the narrow tube, A, into a

[11] Obtained through the courtesy of Raytheon.
[12] E. S. Lamar, E. W. Samson and K. T. Compton, Phys. Rev. **48**, 886 (1935).

magnetic field chamber, B, for analysis. The ions of the desired mass are selected and passed through the tube, C, into the collector chamber. In this chamber are situated the target, P, set at 90° to the positive ion beam, a collecting cylinder, S, and an auxiliary collecting plate, D, of circular cross section with a hole through the center slightly larger than the diameter of the tube, C.

The magnet used was similar in design to the Cenco 79650 with 8-cm pole pieces producing a fairly constant field up to 7500 gauss across a 1.6-cm gap. The ion stream down the main vacuum tube was analyzed by means of this magnet, and under normal operating conditions roughly 50 percent of the total current was due to protons.

With the target at ground potential practically all the secondaries will be collected by the cylinder with a potential of +45 volts or above, as can be seen in Fig. 6. In measuring the yield of secondaries the following procedure was used. With the collector, S, at −90 volts the current to the target was measured. Under this condition all secondary electrons were returned to the target and a true positive ion current, I_p was measured. Then the collector potential was changed to +90 volts and the secondary electron current, I_s, to the collector was determined. As a check the current to the target, with +90 volts on the collector was then determined and this, as it should, equalled the sum of the positive ion current to the target and the secondary negative current leaving the target, I_p+I_s.

The purpose of the auxiliary collector, D, is to detect the presence of any secondary negative current from the tube, C, or any secondary currents from the target of sufficient energy to escape the collector. In all cases the currents to this auxiliary collector were much less than one percent of the positive ion current or the secondary currents. With a negative potential of 90 volts on the collector a minute positive current to the collector was noticed, but was sufficiently small to be neglected, i.e., about 0.1 percent of the target current. These positive currents may be reflected positive ions from the target or photoelectrons caused by soft x-rays striking the collector.

On installing a new target, pumping down the tube and beginning measurements.it was found that the yield initially for any voltage was relatively high. After about two hours under high vacuum followed by bombardment for half an hour at 400 kv, the yields dropped as much as 50 percent to steady values which thereafter were quite reproducible. Evidently the preliminary bombardment serves to free the surface of some impurities the presence of which makes the initial readings unreliable. The results quoted below are actually average values of a large number of readings. The spread in values is roughly five percent of the average, providing the procedure mentioned above is followed.

Since the heating or degassing should be higher at higher energies we tried to minimize any cumulative heating effect by varying the voltage at random. This produced no noticeable change in the results. The readings for both H_2^+ ions and protons were taken concurrentiy, that is, with the tube voltage fixed the magnetic field current was changed to bring in the desired particle. The positive ion currents used were usually about 5 μa, with the focusing adjusted so that the beam was spread over a square cm area.

The targets were prepared by acid cleansing followed by polishing with emery, and were then washed in alcohol and distilled water. Several molybdenum targets were prepared in different ways, but in no case did this affect the results appreciably.

No especial effort was made to adapt the proton source for use with helium. Under the same conditions already described for protons the arc behaved very satisfactorily as a He^+ ion source giving currents of the same order of magnitude as for hydrogen. Commercial helium was used, which we attempted to purify by means of a misch-metal arc plus hot copper oxide to

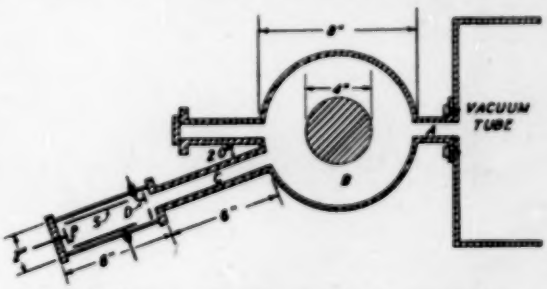

FIG. 4. Cross section of apparatus for measuring secondary electrons.

remove the hydrogen. Evidently, not all the active components were removed since the arc filaments became completely worthless after about five hours' use. On removal the filaments were found coated with a hard greenish compound, and no recoating restored the emitting properties. This deterioration of the filament also made for unsteadiness in the He^+ currents, which reduced the reliability of these measurements. The magnetic field was not strong enough at the highest energies used to make possible an adequate mass-spectrographic analysis of the He^+ beam. Protons and H_2^+ ions were present in small amounts. These ion groups decreased with time of use of the arc and must in part have been due to hydrogen left on the walls of the arc system. Since the magnetic field was insufficient to bend the helium particles through 20° for all energies, the measurements with helium were generally taken with the target directly in line with the tube, which has the disadvantage of including all ions of different mass. However to check the yields obtained with the unanalyzed beam, measurements were made at the low energies, 107 kv and below, with the helium beam bent through 20°. These readings checked within 10 percent of the readings made without magnetic analysis indicating that the effect of ion impurities in the helium was small.

Results

The yield of secondaries per primary for Mo, Cu, Al and Pb bombarded by protons, hydrogen molecular ions and He^+ ions over the range from 43 to 426 kv is summarized in Table I. For molybdenum, which was studied the most thoroughly, the results are plotted in Fig. 5.

Table I. *Yield of secondary electrons per primary particle from several targets at various energies.*

Metal	Energy (kv) 43	78	107	142	213	284	355	426
				Protons				
Mo		4.10	3.77	3.27	2.76	2.35	2.18	2.01
Cu		3.88	3.61	3.41	2.90	2.52	2.44	2.21
Al		4.19	3.82	3.51	3.01	2.68	2.19	2.17
Pb		4.23	3.87	3.56	3.12	2.89	2.70	2.50
				H_2^+ Ions				
Mo		6.31	6.59	6.40	6.19	5.56	5.45	
Cu		6.68	6.64	6.45	6.26	6.30	5.71	5.60
Al		6.08	6.30	6.23	6.43	6.29	5.98	5.46
Pb		8.24	7.74	7.58	7.46	7.34	6.99	6.61
				He^+ Ions				
Mo	11.1	12.8	13.3	13.9	14.1	14.3	14.3	14.1

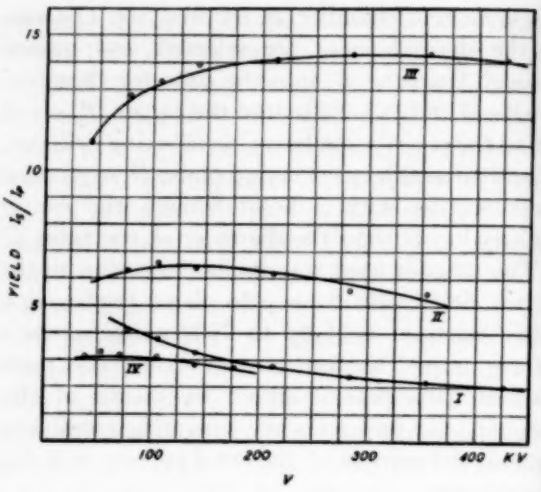

Fig. 5. Yield of secondaries per primary for molybdenum. I. protons; II. H_2^+; III. He^+; IV. yield/2 *vs.* $V/2$ for H_2^+.

For protons these results show a relatively rapid decrease in yield with increasing energy. This characteristic might be explained in a qualitative way by reference to the theory of stopping power of matter for high speed ions. As is well known the rate of energy loss increases with decreasing energy, hence more energy is lost near the surface by the low speed ions, and hence more electrons presumably can escape from the metal. However, this energy variation is not nearly so pronounced when H_2^+ and He^+ ions are used for the bombarding particles; and therefore it must be due to some property of the target or the bombarding protons. For both protons and H_2^+ molecules the yields show very little dependence on the type of metal used, which may indicate that the presence of foreign atoms on the surface is the controlling factor in our measurements.

The yield of secondary electrons when H_2^+ molecules are used as the bombarding particles shows much less energy dependence than the proton curves show. The yield is more nearly constant over the energy range and the average value is roughly twice that for protons. From a naive point of view one might expect the H_2^+ yield to be equal to that of two protons each of one-half the energy of the molecule, V, plus one

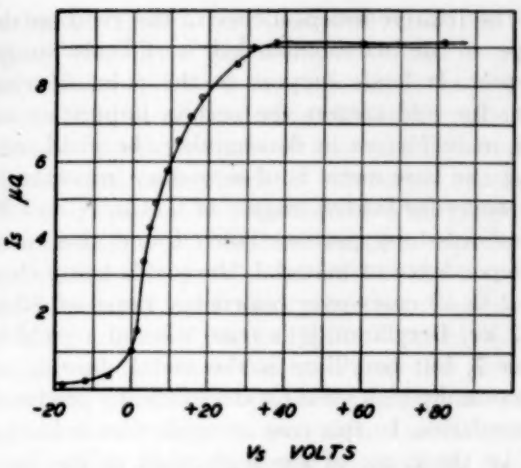

FIG. 6. Secondary current as a function of collector potential.

electron of energy $V/3680$, since the electron binding energy is small compared to the kinetic energy of the molecule. If we plot one-half the yield against one-half the energy (curve IV of Fig. 5) we should expect from this point of view that the difference between this curve and the proton curve would then be half the electronic yield at energy $V/1840$, where V is now the proton energy. This difference is seen to be negative, and this point of view of rather questionable validity.

The high yields obtained with helium are very interesting, and for the three particles used, indicate an average yield almost proportional to the mass of the bombarding particle. Here again it is instructive to plot $\frac{1}{4}$ the yield against $\frac{1}{4}$ the energy to compare with the corresponding H_2^+ curve. It is hoped to continue these experiments with heavier ions, possibly argon and nitrogen in the near future to investigate how much further such a relation holds. In this connection the work of Linford using Hg ions of between 0.7 and 2.3 Mev energy is very interesting. Linford found yields from various targets varying from 7 to 20, depending on the condition of the target. The yield curve for He^+ indicates a maximum in the neighborhood of 300 kv. For H_2^+ particles on Mo and Al there is some indication of a maximum around 100 kv, but no maxima were found for protons. Since a maximum must exist between zero and 78 kv (the lowest voltage for which protons could be focused in our apparatus), we see that the voltage at the maximum rises with the mass of the bombarding particle.

It is interesting here to note the results of Healea and Chaffee using H_2^+ ions. At 1600 volts they obtained a yield of 0.22 electron per primary ion for a heated nickel target, and 0.80 electron per primary for a cold target. Similarly, Oliphant and Moon, using He^+ ions at 1000 volts obtained a yield of 0.7 for heated and 1.2 for cold molybdenum targets. Below these voltages the yields of secondary electrons appear to increase linearly with the energy of the bombarding ion.

In order to get some idea of the energy of the secondaries the current to the collector (for a fixed positive ion voltage) was measured as a function of the voltage on the collector. The results of these measurements are shown in Fig. 6 for 213-kv protons on Mo. This indicates that the majority of secondaries have energies below 30 volts. Similar curves for other proton energies are identical with the one shown in the figure, and when H_2^+ molecules are used the figure is changed very little. No such curve was taken using He^+ particles as the arc was somewhat unsteady with helium and precluded any long measurements where both the voltage and positive ion current must be kept constant. However, the maximum energy of the secondaries was not far different from that observed for the protons and hydrogen molecules.

The question of the effect of surface impurities and their elimination is a very important one. In this type of apparatus there is necessarily present about 10^{-4} mm pressure of the gas of the bombarding particles. An ideal method of eliminating this gas, and any absorbed impurities, would be to enclose the target in its own vacuum chamber where it could be thoroughly cleaned up. This would require using a window between the two parts of the apparatus which would be rugged and still not slow down the particles to any great extent. For an apparatus limited to 450 kv this would necessitate a window of thickness equivalent to 1 mm of air for protons assuming a 50-kv loss. Since this is not feasible perhaps the best method would be to use heated targets with differential pumping as has been done by Oliphant and by Healea and Chaffee. An objection to this could be raised

in that there might exist a temperature effect to obscure the effect of impurities. This is unlikely since the temperature effect for electronically produced secondaries is small. While the quantitative interpretation of results for cold targets is difficult, nevertheless, the conditions under which such measurements are made make the results immediately applicable in the understanding of some high energy phenomena.

In the region below 300 kv energy, our measurements of the yield for copper are roughly 1.5 to 2 times higher than those obtained by Allen for heated targets. For cold targets Allen found the yield increased by about 50 percent. It is probable then that at least at low energies the yield is greatly influenced by gas molecules absorbed on the surface. As the energy is raised our yields begin to approach the yields found by Allen, although his maximum energy was less than ours, and the results are not strictly comparable. This decrease in yield with increasing energy may be due to the increased heating effect at the higher energies. In this connection we have already pointed out that our results were reproducible only after a bombardment of several hours at high energy, which evidently serves to clean up the surface until a stable point is reached.

The relative independence of the yield on the type of surface bombarded is difficult to interpret. It lends support to the point of view that for cold targets the surface impurities are the main factors in determining the yield, and that the base metal is of secondary importance. However for heated targets of C, Cu, N and Pt bombarded by protons Allen found this same independence of material, the yields being close to 2 in all cases over his energy range of 72 to 212 kv. Beryllium, it is true, showed a yield of over 7, but beryllium is the metal showing an abnormally high yield for electronically produced secondaries. In this case an oxide film is known to be the cause of the high yield as has been shown by Schneider,[13] and it is possible that this oxide film is causing the high yield found by Allen, even though the surfaces were heated during the bombardment.

In conclusion, the authors wish to express their thanks to Professor R. J. Van de Graaff and Professor E. S. Lamar for much helpful advice throughout the course of this work. We also wish to gratefully acknowledge a grant of the Research Corporation for aid in construction of the high voltage apparatus.

[13] E. G. Schneider, Phys. Rev. **54**, 185 (1938).

MARCH 1, 1939 PHYSICAL REVIEW VOLUME 55

A New Infra-red Absorption Band of Liquid Water at 2.52μ

J. R. COLLINS
Cornell University, Ithaca, New York

(Received January 17, 1939)

The absorption of liquid water in the spectral region from 2.00 to 2.65μ was measured by means of a thermopile and glass prism spectrometer with a slit width of 100 angstroms in a search for a weak absorption band predicted by Ellis as a combination band occurring in liquid water but not in water vapor. A band was found with a peak at 2.52μ and with a maximum absorption coefficient of about 34. This is the fifth absorption band to be found in the spectrum of liquid water that has no counterpart in the spectrum of water vapor.

THE description of the liquid state of water by Bernal and Fowler[1] as a quasi-crystalline state and the elaboration of this idea by Cross, Burnham and Leighton[2] lends weight to the suggestion of Ellis[3] that certain absorption bands

[1] J. D. Bernal and R. H. Fowler, J. Chem. Phys. **1**, 515 (1933).

[2] P. C. Cross, J. Burnham and P. A. Leighton, J. Am. Chem. Soc. **59**, 1134 (1937).

[3] J. W. Ellis, Phys. Rev. **38**, 693 (1931).

occurring in the near infra-red spectrum of liquid water and which do not occur in the spectrum of water vapor are bands arising from a combination of fundamental vibration states common to the molecule in both the liquid and vapor state and states of hindered rotation occurring only in the liquid state. The existence of such states of hindered rotation has been verified experimentally by Cartwright[4] who found two infra-red absorption bands of considerable intensity due to liquid water at wave-lengths of 20μ and 60μ and also by Cross, Burnham and Leighton,[3] who found Raman frequencies corresponding to those wave-lengths.

The two absorption bands occurring in liquid water at wave-lengths 4.70μ and 1.79μ were ascribed by Ellis[3] as due to (a) a combination of the 6.10μ fundamental vibration band and the 20μ hindered rotation band and (b) a combination of the 6.10μ band, the 3.00μ fundamental vibration band and the 20μ band, respectively. It is to be expected that a band would occur at about 2.50μ which would be a combination of the 3.00μ band and the 20μ band. Ellis[3] searched for this band with a recording spectrometer but found no clear cut evidence for its existence. If one examines the curves of Aschkinass[5] and Dreisch[6] who measured the absorption of liquid water by means of spectrometers with rather wide slits, there appears to be some indication of a weak absorption band at the short wave-length foot of the strong band with peak at 3.00μ.

Accordingly, it seemed worth while to examine the spectral region from 2.00μ to 2.60μ with a greater resolving power and in greater detail than these investigators had used. A mirror spectrometer with a glass prism and a choice of slit width such that 100 angstroms were included in it at 2.50μ was used with a linear thermopile and galvanometer. At the long wave-length end of the spectral range a Moll thermorelay was used to magnify the galvanometer deflections. The wave-length calibration of the spectrometer was obtained by means of the emission lines of mercury vapor, the absorption bands of water vapor as given by Hettner[7] and Sleator.[8] The

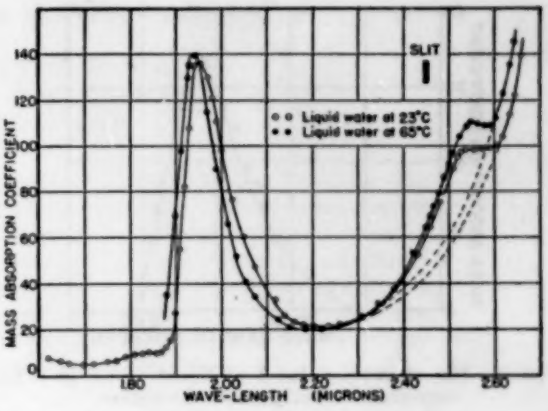

FIG. 1. The absorption spectrum of liquid water at temperatures of 23°C and 65°C.

results of Sleator are of particular value, since he gives the details of the absorption of water vapor from 2.45μ to longer wave-lengths as measured by a grating spectrometer with a slit width of the same magnitude as that used in the present work.

Fused quartz windows as well as thin glass windows were used for the ends of the absorption cells and a range of thickness of the liquid water from 0.0060 cm to 0.020 cm was used. Good agreement in the values of the absorption coefficients calculated for the various thicknesses was obtained for wave-lengths less than about 2.55μ. For wave-lengths longer than this there were progressive deviations as the thickness of the absorbing layer was increased. These deviations are undoubtedly due to stray radiation of shorter wave-length and the values of the absorption coefficients for wave-lengths greater than 2.55μ are probably somewhat too small.

The results in Fig. 1 are the average results of ten runs with various thicknesses, most of which were in the neighborhood of 0.0060 cm. The absorption coefficient is plotted for a sufficiently large range of wave-lengths to include the absorption band with peak at 1.95μ. As would be expected, the maximum value of the absorption coefficient in this 1.95μ band is somewhat greater than has been reported before when measured with a greater slit width.[5, 9] At about 2.30μ the strong absorption band with peak at 3.00μ begins and there appears a very definite indication of an absorption band at the

[4] C. H. Cartwright, Phys. Rev. **49**, 470 (1936).
[5] E. Aschkinass, Ann. d. Physik **55**, 401 (1895).
[6] T. Dreisch, Zeits. f. Physik **30**, 200 (1924).
[7] G. Hettner, Ann. d. Physik **55**, 476 (1918).
[8] W. W. Sleator, Astrophys. J. **48**, 125 (1918).
[9] J. R. Collins, Phys. Rev. **26**, 771 (1925).

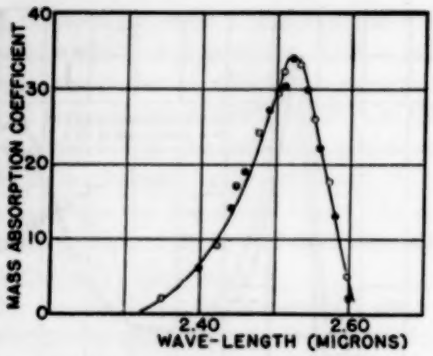

FIG. 2. The absorption band of liquid water at 2.52μ corrected for background absorption.

foot of this strong band. The effect of temperature on the band was obtained as additional evidence for the classification of the band. Note that the resolution seems to be better at the higher temperature than at lower temperature. The effect of temperature on the strong fundamental band at 3μ is to shift the band toward shorter wave-lengths, an effect first shown by Ganz.[10]

In order to have some idea as to the intensity of the new absorption band and to find where the peak of absorption lies, an attempt was made to estimate the background of absorption due to the main band. The dotted lines in Fig. 1 were drawn and the differences between them and the absorption coefficient as determined experimentally taken as the absorption due to the new band. The results are shown in Fig. 2. Nearly the same results were obtained by different persons who made an independent estimate of the background. There is not enough difference in the results for the two different temperatures to warrant any statement as to a shift in position or intensity as a result of a change of temperature. However, there is a difference in the experimentally measured results here as contrasted with the results at the absorption band located at 1.79μ. In the present case the band is as distinct or more so at higher temperatures as at lower temperatures while the reverse was true at the 1.79μ band. This result is to be expected if the classification by Ellis[3] is correct. The band at 2.52μ is a combination band including the 3.00μ band and the 20μ band. Since Ganz[10] has shown that the 3.00μ band shifts toward shorter wave-lengths with rise in temperature, the 2.52μ band should also shift with increase in temperature and the masking effect of the strong 3.00μ band should therefore not be greater than at lower temperatures. The 1.79μ band, on the other hand, is a combination band including the 6.10μ band as well as the 3.00μ band. Ganz[10] has shown that the 6.10μ band shifts toward longer wave-lengths as the temperature rises so that the band at 1.79μ will not shift as much as the 2.52μ band with rise in temperature and the masking effect of the 1.95μ band, which shifts toward the 1.79μ band with rise in temperature, will be greater at the higher temperatures. Ganz[10] has also shown that the 4.70μ band shifts toward longer wave-lengths as the temperature rises which fact is in accordance with Ellis' classification.

Not so much can be said concerning the intensities of the three bands. The absorption coefficients at the peaks of the three bands at 4.70μ, 2.52μ and 1.79μ when corrected for background absorption are 320, 34 and 1.8, respectively, at room temperature. The band at 1.79μ is expected to be much weaker than the other two since it is a more complicated combination of the fundamental states. This expectation is borne out by the experimental results.

[10] E. Ganz, Ann. d. Physik **28**, 445 (1937).

The Energy Distribution in Field Emission*

JOSEPH E. HENDERSON AND R. K. DAHLSTROM**
University of Washington, Seattle, Washington

(Received September 16, 1938)

The energy distribution for field-current electrons from tungsten has been obtained. The distribution was obtained experimentally by the method of retarding potentials. It was possible to apply this method even at the high potentials necessary for field-current emission, since in this experiment the accelerating potential which liberated the electrons also served to decelerate them. This distribution exhibits three major features: (1) Only a minute portion of the electrons reach a copper collector unless the potential of the collector is positive by at least 4.5 volts with respect to the emitter; (2) the greatest number of electrons have energies very close to the maximum energy obtained; (3) the range of energies is at least 10 volts.

INTRODUCTION

THE emission of electrons from metals subjected to high surface fields was first discovered in a study by R. W. Wood of the radiation produced by discharges across small gaps.[1] The conclusion that the carriers of charge actually came from the metal itself was strengthened by later work on short spark discharges.[2–6] Some investigators supported the theory that field emission originated in the residual gas molecules between the electrodes.[7] It was not until the development of high vacuum technique that the laws governing field currents were formulated and its emission nature established.

Experiments by the General Electric Company of London[8] and by Millikan and his co-workers[9–11] established the first empirical field-current equation,

$$i = Ce^{-b/F}, \qquad (1)$$

where i is the current, F the strength of the surface field computed geometrically, and C and b constants for the particular surface under investigation. The values of C and b are subject to change by any process which might change the surface; such as heating, positive ion bombardment, etc. The observed variations in b led to the conclusion that the emission was from small localized areas or "points" where the field computed from the geometry of the apparatus is greatly magnified.

Classical methods alone have produced no satisfactory theory of field-current emission, but wave-mechanical methods give a justification for the empirical formula based on assumptions concerning the changes of the surface potential barrier with an accelerating field.[12–17] In this work of Oppenheimer, Fowler and Nordheim, Houston, and others the electrons within the metal are assumed to be incident upon a potential barrier at the surface of the metal. With zero accelerating field the barrier is infinitely thick; the electrons cannot penetrate the barrier and escape but must have enough energy to surmount the barrier. With an accelerating field the barrier becomes thinner and there is a finite probability of an electron escaping by tunneling the barrier. Field emission occurs when an appreciable

* A preliminary report of this work was presented at the Pullman, Washington Meeting of the American Physical Society, June, 1932.

** Now at the Eastern Washington College of Education, Cheney, Washington.

[1] R. W. Wood, Phys. Rev. **5**, 1 (1897).
[2] R. F. Earhart, Phil. Mag. **1**, 147 (1901); Phil. Mag., **16**, 147 (1908).
[3] C. Kinsley, Phil. Mag. **9**, 692 (1905).
[4] G. M. Hobbs, Phil. Mag. **10**, 617 (1905).
[5] G. Hoffman, Physik. Zeits. **11**, 961 (1910).
[6] J. E. Lilienfeld, Akad. d. Wiss., Leipsiz, Ber. **62**, 31 (1920); Verh. d. Deutsch Phys. Ges. p. 11 (1921); Physik. Zeits. **20**, 280 (1919); **23**, 506 (1922).
[7] C. del Rosario, J. Frank. Inst. **203**, 243 (1927).
[8] Research Staff General Electric Company, London, Phil. Mag. **1**, 609 (1926).
[9] R. A. Millikan and C. F. Eyring, Phys. Rev. **27**, 51 (1926).
[10] C. F. Eyring, S. S. Mackeown and R. A. Millikan, Phys. Rev. **31**, 900 (1928).
[11] R. A. Millikan and C. C. Lauritsen, Proc. Nat. Acad. Sci. **14**, 45 (1928).
[12] R. H. Fowler and L. Nordheim, Proc. Roy. Soc. **A119**, 173 (1928).
[13] J. R. Oppenheimer, Phys. Rev. **31**, 66 (1928); Proc. Nat. Acad. Sci. **14**, 363 (1928).
[14] C. Eckart, Phys. Rev. **35**, 1303 (1930).
[15] W. V. Houston, Phys. Rev. **33**, 361 (1929); Zeits. f. Physik **47**, 33 (1928).
[16] L. Nordheim, Physik. Zeits. **30**, 177 (1929).
[17] T. E. Stern, B. S. Gossling and R. H. Fowler, Proc. Roy. Soc. **A124**, 699 (1929).

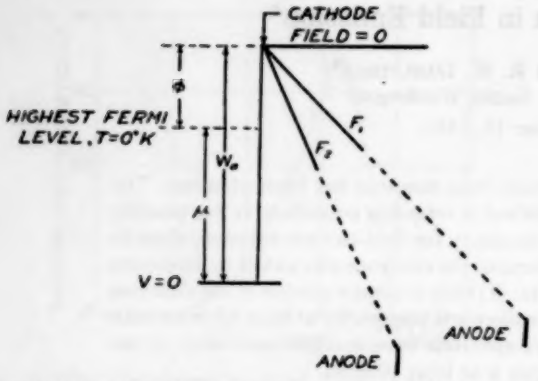

FIG. 1. Schematic potential barrier at the surface of a metal for field = 0; F_1; F_2; $(F_2 > F_1)$.

number escape and requires an accelerating field at the surface of the emitter which computed from the geometry of the electrodes is of the order of magnitude of 10^6 volts/cm. Because of surface irregularities the actual field where the emission occurs may be many times this value, possibly between 10^7 and 10^8 volts/cm.

Figure 1 shows the type of barrier postulated and the change in the nature of the barrier with accelerating field. The computation of the transmission coefficient for such a barrier with changing accelerating field gives rise to an equation for field currents which has the same form as the empirical Eq. (1) above. The evaluation of the actual current density necessitates the assumption of the number of electrons incident upon the barrier per second and their distribution in energy. Fowler and Nordheim, assuming a Fermi-Dirac energy distribution arrive at the following equation for the current density:

$$I = 6.2\times10^{-6}\mu^{\frac{1}{2}}F^{2}(\phi+\mu)^{-\frac{1}{2}}\phi^{-1} \times\exp\left[-6.9\times10^{7}\phi^{\frac{3}{2}}/F\right]. \quad (2)$$

Here μ is the usual parameter of electron distribution in the Fermi-Dirac statistics, ϕ the thermionic work function, and F the accelerating field in volts per cm. Although the equation is of the same algebraic form as that found experimentally its quantitative confirmation is difficult because of two facts. The actual value of F is indeterminable since the current is known to arise from small isolated regions where the field may be much higher than that given by geometrical considerations, and furthermore the areas involved in the emission are unknown.

General confirmation of the idea of transmission through potential barriers has been demonstrated by Henderson and Badgley[18] who showed that electrons emitted from platinum are not received by a copper collector unless the copper is higher in potential than the platinum by at least an amount equal to the work function of copper. The method used by Henderson and Badgley likewise permits the determination of the energy distribution of the emitted electrons. The present paper is concerned with this determination.

THEORY OF THE METHOD

The schematic diagram of the apparatus shown in Fig. 2 illustrates the method used. A fine wire F is stretched coaxially with the two hollow cylinders C_1 and C_2. Cylinder C_1 is perforated and functions as a grid. The potential V_1 produces field emission from the filament to C_1 where a portion of the electrons penetrate into the region between C_1 and C_2. C_2 is connected to the filament F through a small potential V_2, which tends to accelerate the electrons. Electrons passing through C_1 to C_2 are thus decelerated by a potential $V_1 - V_2$ where V_1 is the same potential that liberated them. They will reach C_2 and be collected provided V_2 is at least equal to the height of the potential barrier at the surface of the collector as the electron must pass over, but not through, this barrier to enter the copper (see Fig. 11). It was

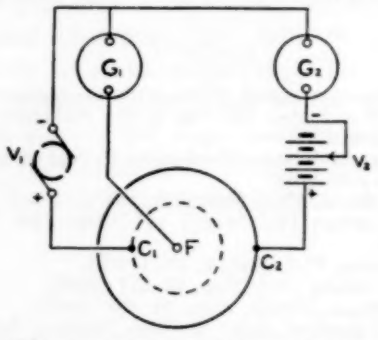

FIG. 2. Schematic diagram of apparatus. Electrons are emitted from the fine wire F by the action of the intense electrical field produced by the potential V_1 between F and C_1. Electrons passing through the grid C_1 only reach C_2 provided V_2 is at least equal to the work function of the copper collector C_2.

[18] R. E. Badgley, Thesis, University of Washington (1931); J. E. Henderson and R. E. Badgley, Phys. Rev. **38**, 590(A) (1931).

the minimum value of V_2 which permitted electrons to arrive at C_2 that was measured by Henderson and Badgley and found to agree approximately with the thermionic and photoelectric work functions of the metal used as collector.

If a distribution in energy exists for the emitted electrons, the current to C_2 will vary when V_2 is changed since different groups of electrons which have penetrated the potential barrier of the emitter will then be collected. Analysis of the current to C_2 as a function of V_2 will yield this distribution. By plotting the current against V_2 a curve is obtained, the slope of which represents the relative number of the emitted electrons which had been associated with the various energy levels of the emitter. This slope plotted against corresponding values of V_2 gives the distribution in energy among the emitted electrons.

The essential feature which makes the method experimentally feasible is the use of the large accelerating potential V_1 as a part of the decelerating potential $V_1 - V_2$. Consequently the resultant potential between the filament and collector is independent of V_1 and the distribution in energy of the emitted electrons is obtained by varying only the small potentials V_2 which can be accurately measured. In practice C_2 is made up of two cylinders usually connected together. Disconnected, however, there are two grids between the filament and the plate; and the second grid may be used in determining the effects of secondary electron emission.

Apparatus and Procedure

Figure 3 shows a cross section of the apparatus. The cylinders are mounted coaxially with the fine wire from which the electrons are emitted. They are made of one-mm copper and are supported by two 50-mil tungsten rods which also serve as electrical connections. The two inner cylinders, of inside diameters 1.2 and 2.4 cm, respectively, are seven cm long. The central four centimeters of this length are perforated by 60 holes of one-mm diameter per cm². The outer cylinder is eight cm long and has a diameter of 3.6 cm. It is unperforated; the central two cm is two mm thick and the rest one mm, to insure good heat conduction during outgassing. The

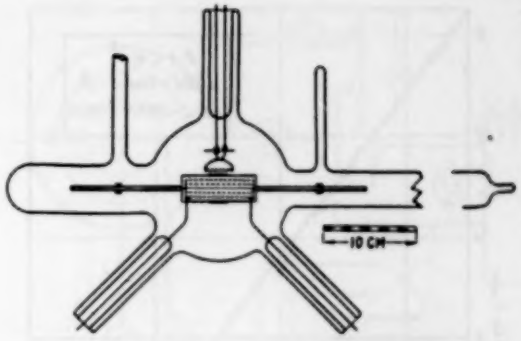

FIG. 3. Sectional diagram of the apparatus.

apparatus was outgassed by electron bombardment from an auxiliary filament mounted about three mm from the thick portion of the outer cylinder. The inner cylinders were heated by radiation from the outer one. The copper disk mounted directly behind the auxiliary filament protects the lead-in wires from ion bombardment.

The filament is mounted between two copper rods centered with respect to the cylinders. In mounting the filament the assembly is first fastened firmly to a slender steel rod which is then inserted in the tube. The steel rod is removed after the copper rods have been fastened securely to the filament supports. The filament itself is of tungsten 0.0013 cm in diameter and 7.5 cm long.

The apparatus was mounted within a Pyrex glass envelope constructed from a two-liter flask. The whole was evacuated by a two-stage mercury diffusion pump used with liquid air. The vacuum was measured by an ionization gauge calibrated against mercury vapor at room temperature. During operation the tube is evacuated to a pressure of approximately 2×10^{-8} mm Hg. This order of vacuum is essential to work of this character if reproducible results are to be obtained. It was only attained after repeated bakings of the apparatus as a whole at about 500°C. After each baking the copper parts were maintained at a bright cherry red for several hours by electron bombardment. Under these vacuum conditions it is possible to maintain the emission current constant to within one percent for several hours at a time. Inconstancy of emission at higher pressures is probably due to bombardment of the surface by positive ions. In particular this would be true if the emission

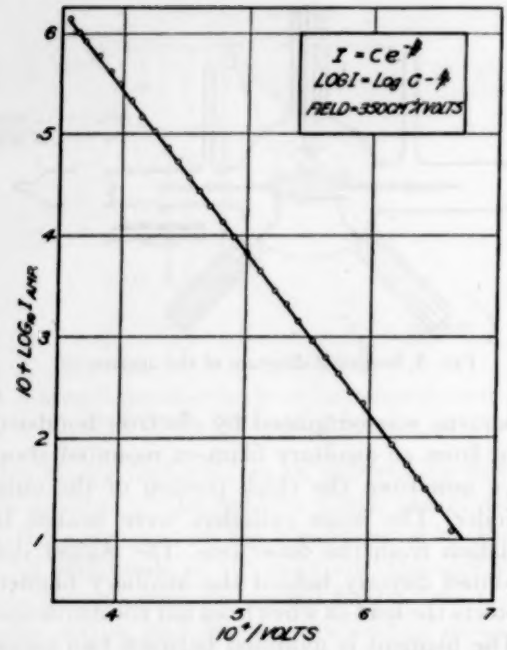

FIG. 4. Showing the straight line relationship between logarithm of the currents and $1/F$ in field current emission. F is the field as computed from the geometry of the apparatus.

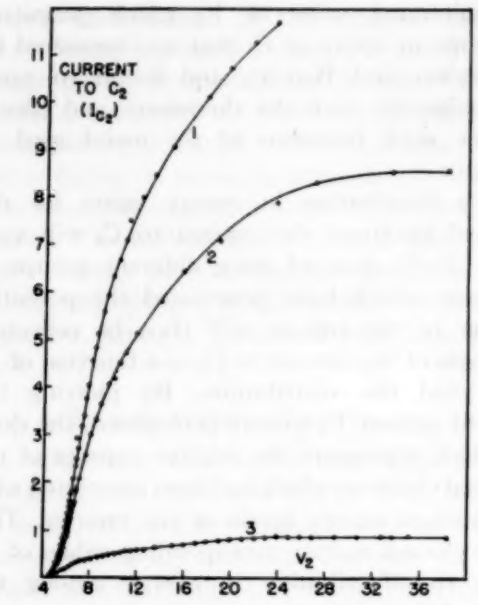

FIG. 5. The current to C_2 as a function of V_2. V_2 is the difference in potential between C_2 and the filament. Curves 1, 2, 3 are for field emission I_1, respectively equal to 9.6×10^{-4} ampere, 7.2×10^{-5} ampere and 7.2×10^{-7} ampere.

occurs from small regions so that the damage caused by one positive ion would represent a large portion of the emitting area.

The dimensions of the apparatus are such that there is a potential gradient of approximately $350V_1$ volts per cm at the surface of the filament. This field is given by the equation

$$F = V/b \log (b/a),$$

where V is the potential difference between the cylindrical filament of radius b and the surrounding cylinder of radius a. The actual field at the small areas from which the emission comes is doubtless much larger than that computed from the geometry of the apparatus.

The high potential represented by V_1 in Fig. 2 was supplied by a 3000-volt d.c. generator driven by a d.c. motor operating on storage batteries. This furnished a very steady source of potential as soon as the generator was in thermal equilibrium. During the later stages of the work an especially constructed 9000-volt generator similarly driven was used. Voltages up to 3000 v were measured with a Model 1 Weston voltmeter with multiplier. Above this voltage a rotary voltmeter[19] was used, which was found to be a very simple and trustworthy instrument for these measurements. The emission current, which ranged from 10^{-10} to 10^{-4} ampere, was measured by a Leeds & Northrup type R galvanometer, G_1. The variable potential V_2, between C_2 and the filament, is supplied by a battery of storage cells connected across a potentiometer. A voltmeter which could be read to 0.01 volt was used to measure this voltage. The current I_2 between C_1 and C_2 was measured by a type H. S., Leeds & Northrup galvanometer, G_2, of sensitivity of 3.0×10^{-11} amp./mm.

RESULTS

In Fig. 4 is shown a typical curve illustrating the characteristics of the emission current I_1 between the filament and C_1. By plotting the logarithm of the current against the reciprocal of the field a straight line is obtained, which verifies the experimental relationship obtained earlier by Millikan and Lauritsen.[11] This linear relationship can be regarded as the test for field currents. Curves exhibiting breaks may be ob-

[19] P. Kirkpatrick and I. Miyake, Rev. Sci. Inst. **3**, 1 (1932).

tained when the filament conditions are subject to change. In the following work only those filaments which exhibited unchanging characteristics are considered.

The field currents obtained were steadier than reported by previous investigators. This is probably due to two causes. The first is the potential source. As the emission varies exponentially with the field this is extremely important. The d.c. motor generator operated on storage batteries was much superior to any rectified a.c. sources of potential that were tried. The second is the degree of evacuation of the tube which is equally as important as the potential source. The variations in current were less than one percent over a period of several hours when the vacuum was approximately 2×10^{-8} mm Hg. With vacuum of 10^{-7} mm Hg it was found impossible to obtain currents free from variations as great as 10 percent. Even with the best vacuum obtainable the existing currents are not always steady. The initial emission from a new filament generally exists at abnormally low values of the field (2 to 3×10^{5} volts/cm). These currents are ordinarily unsteady and only become steady after large emissions have been drawn from the filament. In the process of increasing the field to increase the emission the current sometimes decreases suddenly by a factor as great as 10. The smaller currents are then generally quite steady. If the emission is from a localized area this sudden decrease can be interpreted as a breakdown of such a point

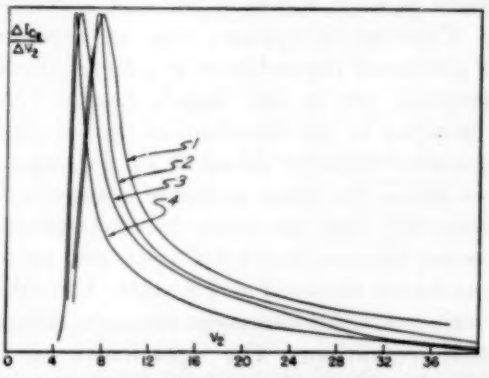

FIG. 6. Curves obtained from those in Fig. 5 by plotting the slope against V_2. Curve 4 is for a value of I_1 too small to be shown satisfactorily in Fig. 5. The slopes are arbitrarily adjusted to a common maximum. They are distribution curves representing the relative number of the emitted electrons which had been associated with the various energy levels of the emitter.

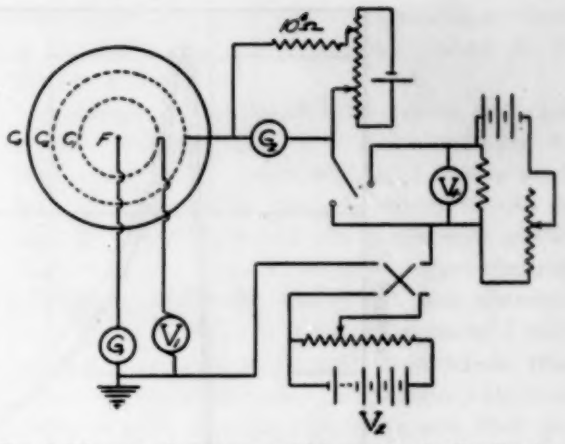

FIG. 7. Diagram of apparatus which permits the distribution curves to be obtained directly.

resulting in decreased field and smaller and more stable currents.

With each different point, or possibly distribution of points, the characteristics of curves of the type shown in Fig. 4 vary. This takes the form of a different slope of the curve. The variation may be interpreted as due to a change in b in the Eq. (1), or to a different proportionality between the applied potential and F or to a combination of these.

Figure 5 shows a typical group of curves obtained by plotting the current I_2, between C_1 and C_2, against the small potential V_2. It will be noted that independent of the magnitude of the current I_1, emitted by the filament, no electrons arrived at C_2 until V_2 reached a value of about 4.5 volts. This is very close to the accepted work function of copper. As V_2 was increased beyond 4.5 volts the current approached saturation and indicated that the probability of an electron penetrating the potential barrier decreases rapidly for electrons in the lower energy levels of the emitter.

The slope of these curves plotted against V_2 gives the energy distribution of the emitted electrons. The curves 1, 2 and 3, shown in Fig. 6, were obtained from the corresponding curves in Fig. 5 by mechanically measuring the slopes. They were arbitrarily adjusted to a common maximum. Curve 4 in Fig. 6 corresponds to a value for I_1 of 4.8×10^{-8} ampere, which is too small to be shown on Fig. 5. This mechanical differentiation proved to be a laborious and somewhat inaccurate method. A better and more

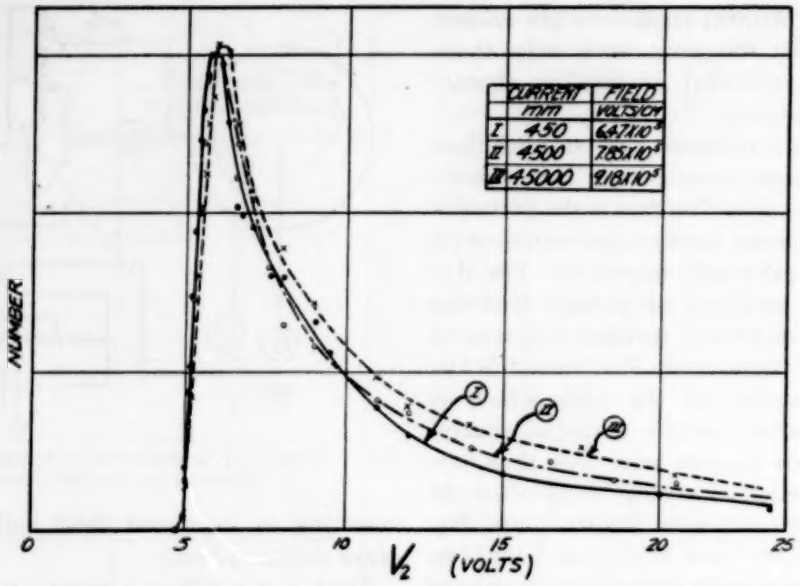

FIG. 8. Typical group of distribution curves obtained from the same filament for different values of the field. The curves are all adjusted to the same maximum.

accurate method of obtaining these distribution curves directly is illustrated in Fig. 7. Field currents were produced as before. The deflection of the galvanometer G_2 was then reduced to zero by adjustment of the auxiliary circuit connected to G_2. When the circuit is just balanced for a particular value of I_2 any change in I_2 will produce a corresponding deflection in G_2. The introduction into the circuit of V_4 which was kept constant and equal to 0.1 volt effectively increases V_2 by 0.1 volt and produces an accompanying increase in I_2. By plotting the deflection of G_2 against V_2 one obtains the distribution curves directly since this deflection represents the average change in I_2 over a 0.1-volt interval at V_2.

Figure 8 shows a typical set of distribution curves taken by this method for different magnitudes of the field. The curves rise sharply at 4.5 volts and rapidly reach a maximum after which they decrease more slowly. In this region the curves for larger emission currents are the higher. The range of this distribution which extends, in the curves shown, approximately 20 volts is of interest. The exact range is indeterminate since the curves in the region of large values of V_2 are not particularly significant. This is due to two causes to be discussed later, namely: (1) the existence of secondary electrons emitted at the last cylinder C_2; and (2) a distortion of the true distribution due to the geometry of the apparatus. Since tungsten was used as the emitter and copper as the collector the contact potential existing between them would be expected to be very small. Thermionic measurements showed it to be less than 0.2 volt.

Of more than 30 separate distribution curves obtained at room temperature all show a value of V_2 equal to 4.5 volts before an appreciable number of electrons are collected. There is no doubt but that the curves would extend below 4.5 volts as they approach the axis asymptotically. However, it appears that an extremely small portion of the electrons in a metal at room temperature are in the higher energy levels. The maxima in the distribution curves appear at somewhat different values of V_2. Twenty-four curves show the most probable energy to be between 5.5 and 6.0 volts. Seven showed a maximum between 6 and 6.5 volts, and on four the maximum occurred at 7.5 volts. The thirty-five curves studied represent fourteen different filament conditions. The appearance of the maximum at different values of V_2 is quite definite but the factors which determine its position are not. The variation in the position of the maximum is probably due to experimental conditions not controlled, though in general the

presence of the maximum at higher V_2 was associated with higher applied potentials.

Although the distribution curves indicate that field current electrons have a range of energy greater than thirty volts, secondary electron effects arising both at C_1 and C_2 distort the distribution in the region of lower energies (large V_2) and make that region unimportant except for purposes of comparison. The effect of the reflection at C_1 is negligible since electrons losing more than twenty volts energy would never reach C_2 with significant values of V_2. As twenty volts is less than two percent of the energy of the incident electrons, the number reflected with an energy loss smaller than this is insignificant.[20–22] Secondary electrons emitted at C_2 return to C_1 and cause an effective decrease in the electron current between C_1 and C_2. This slight decrease is shown on Fig. 5 for V_2 greater than 35 volts and it also produces the negative slope shown in Fig. 6.

If V_2 is fixed and C_2 used as a grid, the energy distribution may be determined by applying a retarding potential between C_2 and C_3 (Fig. 7) and analyzing this current as before except that it is a function of V_3, the potential between C_2 and C_3. Curve II of Fig. 9 is the result of such an analysis. In this case it is apparent from the figure that the secondary electrons emitted at C_2 go to C_3 and produce the increase for low energies or small V_3. The decrease from secondaries emitted at C_3 is also recognizable so there is no doubt that for the higher values of V_2 the curve is distorted.

A comparison of distribution curves obtained by the two different methods is shown in Fig. 10 where curve I was taken without C_3 being used. Since the secondary electron effects should be opposite for this curve the agreement shows that for V_2 less than ten volts secondary electron effects are negligible. Curve III was obtained with a new point and agrees with curve I only at higher energies. It is safe to conclude that these data are independent of secondary electron effects for V_2 less than 10 volts and that the energy of the field electrons extends over at least ten volts.

Curves I and II of Fig. 9 exhibit the effect of secondary electrons at different parts in the distribution curve. They show that the range of energies affected is only about six volts. This is further verification of the previous conclusion that the range of energies is at least 10 volts since that part of the curve is unaffected by secondary electrons and is therefore reliable.

Since the apparatus is cylindrical, if a general emission occurs electrons can escape through the ends of the cylinder and not be measured at all. Likewise velocity components along the axis of the cylinder would not be measured by the retarding potential gradient perpendicular to the filament. If the emission is from points

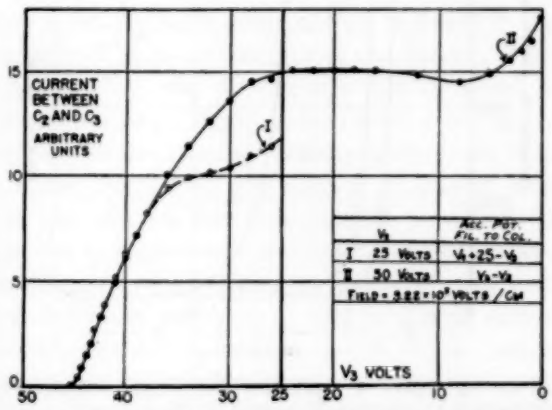

FIG. 9. Current voltage curves between C_2 and C_3 for constant values of V_2. V_3 is the retarding potential between C_2 and C_3. A range of energies extending over about 10 volts is free from secondary electron effects.

[20] P. B. Wagner, Phys. Rev. **35**, 98 (1930).
[21] A. Becker, Ann. d. Physik **78**, 228 (1925).
[22] K. H. Stehberger, Ann. d. Physik **86**, 825 (1928).

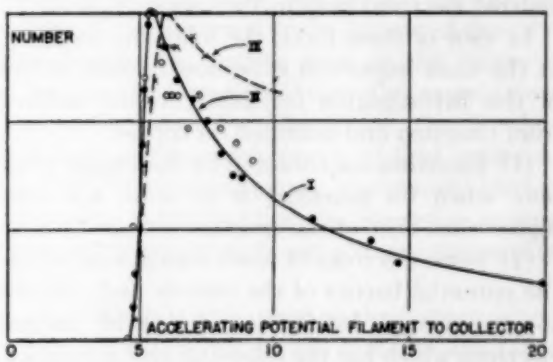

FIG. 10. Distribution curves I and II obtained by the two methods for the same "point." Note that they agree over the energy range investigated. Curve III was obtained with a new "point."

		Field $\frac{\text{volts}}{\text{cm}}$	I—mm	V_2 volts	V_3 volts	Acc. Pot. Fil. to Col.
I	●	$6.9 \cdot 10^5$	400	varied	0	V_3
II	○	$7.7 \cdot 10^5$	400	50.1	varied	$50 - V_3$
III	×	$9.2 \cdot 10^5$	4000	2.5	varied	$25 - V_3$

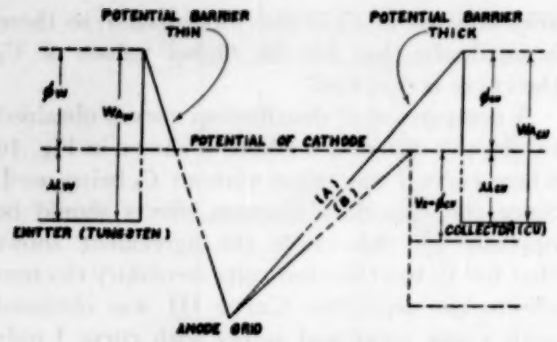

FIG. 11. Schematic representation of the surface potential barriers involved. The potential of the copper collector is lowered by an amount $V_2=\phi_{Cu}$ in order that electrons from the highest Fermi level ($T=0°K$) may surmount the barrier.

and in the form of definitely directed beams towards the grid, the energy distribution would be very close to that for total energies. The steep portions of the curve near small V_2 would be unaffected except for certain electrons with large velocity components along the filament. These higher energy electrons would be recorded as electrons of lower energy making the curve too high for large values of V_2. This is precisely the effect observed in some preliminary results on the total energy distribution reported by Dahlstrom, McKenzie and Henderson[23] where a point emitter at the center of a sphere was used. The results obtained from the cylindrical apparatus used in this experiment may be interpreted as measuring the total energy distribution of the emitted electrons only in the region of small V_2.

In view of these facts, the following are listed as the most important experimental conclusions of this investigation for field currents emitted from tungsten and collected on copper.

(1) Electrons are collected by the copper plate only when its potential is at least 4.5 volts higher than that of the emitter.

(2) Some electrons of lower energies penetrate the potential barrier of the emitter and give rise to an energy distribution for field current electrons which has the following characteristics: (a) A range of energies of at least 10 volts. (b) A most probable energy for the emitted electrons very close to the maximum observed energy. (c) A small variation of the position of this maximum depending upon filament conditions and upon the field strength.

DISCUSSION OF RESULTS

In Fig. 11 is shown schematically the potential barriers involved in this experiment. Because of the geometry of the apparatus the barrier at the surface of the tungsten emitter is thin compared to the barrier at the surface of the copper collector. Electrons which may tunnel through the barrier at the surface of the tungsten cannot enter the copper unless they pass over the barrier at its surface because of the thickness. It is immediately evident that the potential of the copper must be lowered by an amount equal to its work function in order that electrons may enter. This fact is demonstrated by the curves on Fig. 5 which shows clearly that no appreciable numbers of electrons reach the copper unless it is positive with respect to the tungsten by approximately 4.5 volts. This is close to the accepted value for the work functions of copper and tungsten. However, by using a platinum emitter and copper collector Henderson and Badgley[24] obtain, to within their experimental error, this same value which, because of the wide differences between the work functions of platinum and

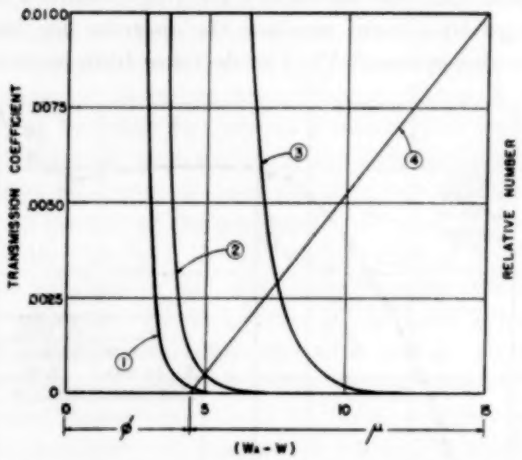

FIG. 12. Curve 4 represents the relative number of electrons with energies W normal to the surface in accord with the Fermi statistics. These are plotted as a function of (W_0-W). ϕ is assumed as 4.5 volts and μ, 10 volts. Curves 1, 2 and 3 are computed values of the transmission coefficient for fields of 7×10^7 volts/cm, 10^8 volts/cm, and 2.5×10^8 volts/cm, respectively.

[23] R. K. Dahlstrom, K. V. McKenzie and J. E. Henderson, Phys. Rev. **48**, 484(A) (1935).

[24] J. E. Henderson and R. E. Badgley, reference 18.

copper, demonstrates clearly that it is the work function of the collector rather than the emitter that determines the minimum value of V_2 that will permit the electrons to reach the collector. This verifies the general application of the idea of potential barriers to field emission.

As V_2 is increased beyond this minimum value, electrons which have tunneled through the barrier at energies below the highest Fermi level ($T=0°$) will be collected and will give rise to the distribution in energy observed. Eventually with further increase in V_2 a value will be obtained where either the lowest energy is reached or else electrons are unable to penetrate the barrier. The current to the collector will then attain a limiting or saturation value. That this is true is shown by Fig. 5. Increase of the applied field apparently increases the probability of transmission through the barrier as distribution curves taken at higher fields when no detectable change in the emitter has occurred are invariably above those taken at lower values in the region of large V_2.

A quantitative comparison of these results with the Fowler-Nordheim theory[12] is of interest. The transmission coefficient as obtained by them is:

$$D(W)=(4/W_a)W^{\frac{1}{2}} \times(W_a-W)^{\frac{1}{2}}\exp\left[-4K(W_a-W)^{\frac{3}{2}}/3F\right], \quad (W_a>W); \quad (3)$$

where W is the kinetic energy normal to the surface, W_a the total height of the barrier, F the applied field, and $K^2=8\pi^2m/h^2$ where h and m have their usual significance. Curve 4 in Fig. 12 represents the relative number of electrons with energies normal to the surface in accord with the distribution function at 0°K predicted by the Fermi statistics. The transmission coefficient for successively increasing values of the field are shown in curves 1, 2 and 3. These curves assume $\phi=4.5$ volts and $\mu=10$ volts, which values are reasonable in view of the nature of the emitter and the experimental results. The resultant curves for the distribution in normal energies of the emitted electrons are shown as curves 1, 2 and 3 in Fig. 13. For ease of comparison, these distributions are given with the ordinates adjusted to a common maximum. It is evident that these are of the same form as the typical experimental curves as given in Fig. 8. As has already been pointed out, the excess of slow electrons exhibited by the experimental curves can be accounted for by secondary emission, and because the cylindrical geometry of the apparatus does not permit the normal energy of the electrons to be measured directly. Nevertheless the general form of the curves is so nearly that predicted that the experiments give strong direct evidence for the Fowler-Nordheim-Sommerfeld theory of field emission. Certainly the experiments constitute further convincing evidence that the electrons leaving the metal come through and not over the surface barrier.

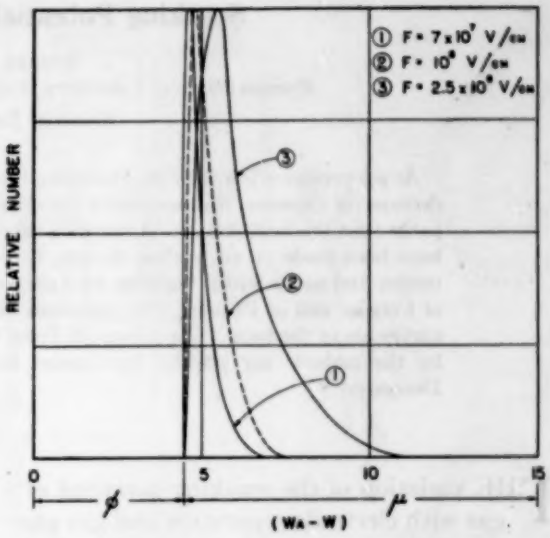

FIG. 13. Theoretical distribution of normal energies of electrons in field emission according to the Fowler-Nordheim-Sommerfeld theory. These are obtained from Fig. 12 by multiplying corresponding ordinates of curve 4 by those of curves 1, 2 and 3. The general form of these curves corresponds well with the typical experimental curves as given in Fig. 8. As in Fig. 8, the curves are adjusted to a common maximum ordinate.

The authors wish to express their appreciation to Mr. Frank Abbott for the material assistance given in the early part of this investigation. One of the authors, R. K. Dahlstrom, wishes to express his indebtedness to the University of Washington for the grant of the Lorretta Denny fellowship which greatly facilitated the progress of this work.

Sparking Potentials at Low Pressures

ROBERT B. QUINN
Ryerson Physical Laboratory, University of Chicago, Chicago, Illinois
(Received January 11, 1939)

At gas pressures less than the Paschen critical value the sparking potential rises rapidly with decrease in pressure. Measurements are difficult because of undesired discharges over longer paths than the intended one. A sparking tube has been constructed with which measurements have been made on air, carbon dioxide, hydrogen, and helium up to 24 kv with nickel electrodes, and on air with a stainless steel cathode. The results are compared with those of Carr, of Cerwin, and of Penning. The equations of the straight portions of the sparking potential curves are of the form $V=a+b \log pd$. From these equations the number of electrons released by the cathode per positive ion impact has been calculated by a method described by Dempster.

THE variation of the sparking potential of a gas with electrode separation and gas pressure was first extensively investigated by Paschen,[1] who announced the law that, with a uniform electric field, the sparking potential is a function of the product of distance d and pressure p. As the product diminishes the sparking potential decreases until, at a critical value, it becomes a minimum for a given gas. For still smaller values of the product, the sparking potential increases rapidly. For these smaller values measurements are difficult since any longer path permits a discharge at a lower voltage. Carr[2] made an investigation of the sparking potentials of a number of gases over a rather wide range of values of the product pd, but his highest voltage was only 1800. In his apparatus two flat electrodes were separated by an ebonite ring which covered the electrode edges and thus permitted the discharge only in a region of uniform field. Penning[3] found an anomalous behavior for helium: there were as many as three different values of the sparking potential for the same gas pressure. At a pressure of 0.84 mm between electrodes separated 2.6 cm, sparks occurred at 500, 1500, and 5000 volts.

In this laboratory Cerwin[4] has recently measured the sparking potentials of air between flat nickel electrodes separated 2–10 mm, using voltages which he believed to be as high as 80 kv. The results were in agreement with Paschen's law. The present problem began as an effort to obtain similar data for other gases, with the gas flowing continuously through the sparking chamber to minimize the concentration of possible impurities from the glass walls or the electrodes.

[1] E. T. Paschen, Ann. d. Physik **37**, 69 (1889).
[2] W. R. Carr, Phil. Trans. Roy. Soc. **A201**, 403 (1903).
[3] F. M. Penning, Proc. Roy. Acad. Amsterdam **34**, 1305 (1931).
[4] S. S. Cerwin, Phys. Rev. **46**, 1054 (1934).

APPARATUS

Figure 1 is a diagram of the apparatus. It was found very early that when the pressure was less than the critical value corresponding to the minimum sparking potential, a discharge would probably take place between the high potential electrode and the pump, reservoir, or gauge, and occasionally initiate the main spark. To prevent this, a pair of electrodes a was inserted in each of the connections to the sparking tube, the two electrodes being separated by a smaller distance than the main sparking distance, the one nearest the tube having no external connection and the other being grounded. Because of leakage over the glass it is not believed that the device was completely effective in preventing arc currents.

The first sparking tubes were patterned after those used by Cerwin.[4] It was practically impossible to make such tubes so that the discharge was confined to the space between the flat electrode surfaces when the pressure was less than the critical value; discharges could be seen terminating on the back surfaces of the electrodes. A second design of sparking tube used electrodes having flat faces but conical backs ground into glass seats and held snugly in place by springs. The angle of the cone was made large enough so that when the electrodes were

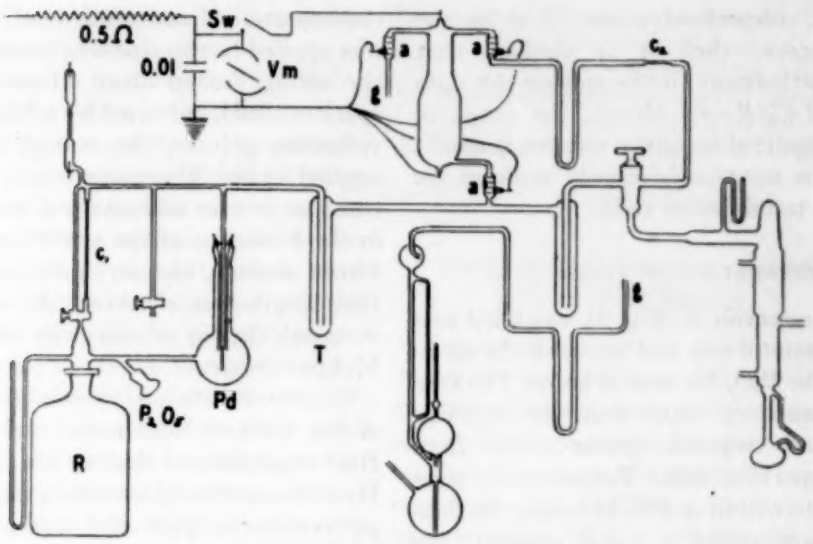

FIG. 1. Diagram of apparatus.

outgassed by induction heating the expansion did not crack the glass. Although there was no visible discharge to the backs of these electrodes, a discharge terminated at their edges. To prevent this, flat disk electrodes were enclosed, except for the central portion, in fired steatite. The glass supporting structure became sputtered, and the steatite enclosure broke.

Figure 2 shows the construction of a tube which provides one discharge path longer than any other, over which the electric field is not seriously distorted, and which is sufficiently removed from any dielectric that might become sputtered. The cathode is a spun cylindrical shell with a hemispherical end. The anode is a solid nickel cylinder with hemispherical ends. These latter were turned to fit fairly closely to a template and then polished with emery paper. The glass rings sealed in at the end of the cathode shell prevent a discharge from the edge of the shell to the anode up to the highest voltage used, which was about 24 kv. The first tube constructed had a stainless steel cathode, which rusted. When the tube was opened the pitted spots on the two electrodes resulting from the sparks were found distributed over a small area on each electrode centered approximately on its axis.

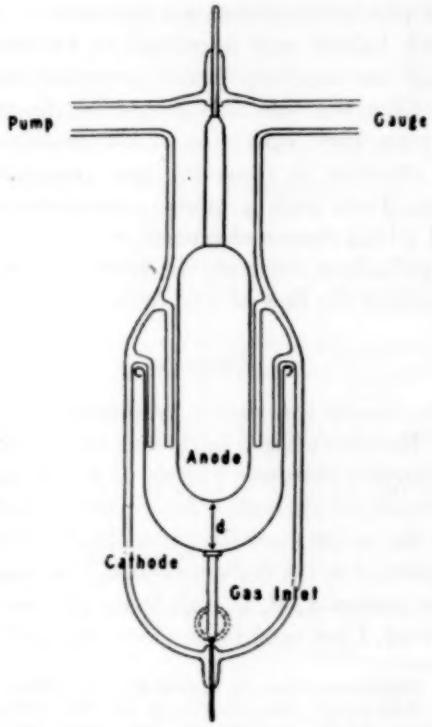

FIG. 2. Diagram of sparking tube.

The design of the tube was suggested by the nature of the electrostatic fields surrounding two opposing point charges. The equipotential surfaces are nonintersecting shells about each of the charges. If spherical conducting shells replace two surfaces, with a sufficient potential difference, and with a gas enclosed between them, a spark should take place along the line of greatest separation, where the field is approximately uniform. If R and r are the radii of the outer and

inner spheres, respectively, and if d is the sparking distance, then it is obvious that $d>(R-r)$. Furthermore, if the spheres are non-intersecting, $d<2(R-r)$. Hence, the range of values of d permitted for given spheres is small; and the field is most satisfactorily uniform for spheres of not too different radii.

Preparation of Gases

For air the reservoir R (Fig. 1) was filled to a pressure of about 10 cm, and left with the air in contact with the P_2O_5 for several hours. The trap T prevented mercury vapor from the reservoir manometer and stopcock grease vapor from entering the sparking tube. Temperatures were kept constant to within $\pm 1°C$. In taking the data the voltage was raised a small amount, the electrostatic voltmeter was read, and the voltage was applied to the sparking tube. Application of the voltage lasted about fifteen seconds. If no spark resulted, indicated by a "drop-back" of the voltmeter pointer, the voltage was raised and applied again. The voltage was not sufficiently constant to take advantage of any possible delay in the formation of the spark longer than about fifteen seconds, and no significant delay of even that length was observed. As soon as a spark occurred, the gas pressure was observed with the McLeod gauge.

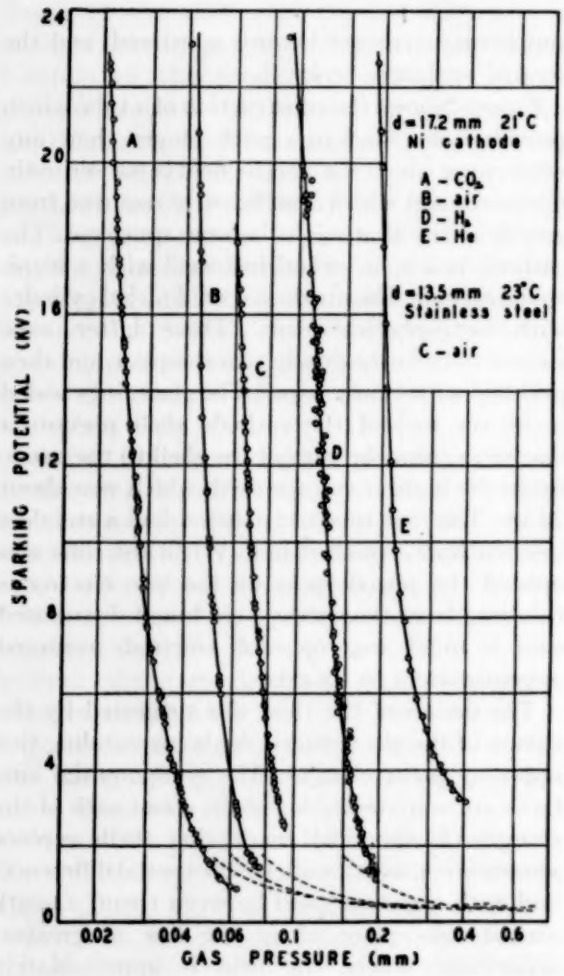

Fig. 3. Sparking potential as a function of gas pressure.

Carbon dioxide was chosen after consideration of the work of Buchmann[5] and of Klemperer.[6] Buchmann showed that air lies between CO_2 and H_2 in the number of secondary electrons produced per centimeter path at 1 mm pressure, over an extended velocity range of the primary electrons. Klemperer estimated the yield of electrons by the cathode per positive ion impact at the minimum sparking potential to be 0.66 percent for air, 0.09 percent for CO_2, and 0.74 percent for H_2. The carbon dioxide was obtained by evaporation of dry ice which had been pulverized and packed into a flask. Any air and a considerable volume of CO_2 were pumped off before the gas was admitted to the previously evacuated reservoir.

Tank helium was admitted to the reservoir through an auxiliary liquid air-cooled charcoal trap. Charcoal was also placed in the trap T. This trap, then, operating at low pressures, was very effective in removing any remaining impurity. Tests with a pocket spectroscope indicated a high degree of purity.

A palladium valve served both to purify and to regulate the flow of hydrogen.

Results

The results are shown graphically in Fig. 3. Since Paschen's law is fairly well established only one sparking distance, namely 17.2 mm, was used for the nickel cathode tube. Sparking potentials near the minima are computed from Carr's data and plotted as the broken curves. The transitions to the curves A, B, C, and D are not very good. However, Carr used brass electrodes and rubber

[5] E. Buchmann, Ann. d. Physik **87**, 523 (1928).
[6] O. Klemperer, Zeits. f. Physik **52**, 650 (1928). See I. Langmuir and K. T. Compton, Rev. Mod. Phys. **2**, 181 (1930).

insulation, with the consequence that the electrode system could not be outgassed.

It is apparent that the two curves B and C for air do not satisfy the relation that for a given sparking potential pd is a constant. The cathode was of stainless steel in one case and of nickel in the other. Anderson[7] has found for a 1-mm gap in high vacuum a breakdown voltage of 120 kv for stainless steel and of 96 kv for nickel. If a proportionate difference were supposed to hold for discharges in air at much lower voltages, pd for the stainless steel cathode at, say, 18 kv might be compared with that for the nickel cathode at 14.4 kv. These values agree approximately with those observed in the present experiments for $pd=0.80$. The observation at high pressures that the sparking potential is independent of electrode material probably does not hold for low pressures. The small temperature difference accounts for a very small part (0.005) of the discrepancy, since the cooler gas exerts less pressure for the same density. In general the sparking potential is of the same order of magnitude as the value obtained by Cerwin. At 20 kv pd (nickel cathode) $=0.75$, whereas Cerwin obtained about 0.82.

There is no indication of any anomaly in the behavior of helium at the pressures and sparking distance used.

The equations of the straight portions of the curves are, in terms of V_0 in kv, d in mm, and p_0 in mm at 0°C: For

(1) Air—stainless steel cathode, $d=13.5$ mm—
$V_0=1.72-128.45 \log p_0 d$ $\quad pd<0.95$
nickel cathode, $d=17.2$ mm—
$V_0=-2.5-121.5 \log p_0 d$ $\quad 9<V<14$
$V_0=-27.9-309.0 \log p_0 d$ $\quad 14.5<V<21$

(2) Carbon dioxide—nickel cathode, $d=17.2$ mm—
$V_0=-18.3-80.3 \log p_0 d$ $\quad 9<V<16$
$V_0=-38.9-129.1 \log p_0 d$ $\quad 16<V<23$

(3) Helium—nickel cathode, $d=17.2$ mm—
$V_0=107.8-179.4 \log p_0 d$ $\quad 11<V<23$

(4) Hydrogen—nickel cathode, $d=17.2$ mm—
$V_0=46.2-115.1 \log p_0 d$ $\quad 8<V<15.5$
$V_0=37.4-82.1 \log p_0 d$ $\quad 15.5<V<22$

TABLE I. *Cathode emission in sparks at low pressure.*

V (volts)	Air—Stainless Steel $s(V)$	Air—Stainless Steel $m(V)$	Air—Nickel $m(V)$	CO_2—Ni $s(V)$	CO_2—Ni $m(V)$	H_2—Ni $s(V)$	H_2—Ni $m(V)$
3000	2.70	3.99	4.34	4.10	4.88	0.43	10.39
4000	2.45	4.56	4.97	3.75	5.63	0.386	12.03
6000	2.00	5.98	6.54	3.04	7.74		
10000	1.35	10.13	11.17	2.05	14.13		
14000	0.92	16.94	18.80	1.4	25.27		
18000	0.65	27.24	30.43				

[7] H. W. Anderson, Elec. Eng. **54**, 1315 (1935).

Secondary Electrons from Positive Ion Impact

Dempster[8] has shown that the cathode emission of electrons under positive ion bombardment may be a primary factor in the mechanism of the spark discharge at low pressures, and that the number of such electrons may be calculated from equations for sparking potential curves with known values of the ionizing efficiency of the primary electrons in the gas. From Dempster's method and with Buchmann's[5] data for the number of ionizing collisions $s(V)$ in 1 cm at 1 mm pressure, the cathode emission $m(V)$ has been computed for the gas-electrode combinations, except helium-nickel, used in this experiment. If $V=a+b \log pd$, where V is in kv, d is in mm, and p is in mm of Hg, is the form of the equation of the straight portion of the sparking potential curve, then

$$s(V)m(V)=10 \exp\left[\frac{2.3026}{1000b}(V-1000a)\right] \times\left(1-\frac{2.3026}{1000b}V\right)$$

where V is in volts. Buchmann's values of $s(V)$ for CO_2 and H_2 are for voltages less than 5000 volts. However, $s(V)$ for CO_2 may probably be extrapolated. Table I gives the resulting values of $m(V)$, the number of electrons released by the cathode per positive ion impact.

The writer is indebted to Dr. A. J. Dempster, who suggested this problem, for helpful direction and criticisms. The successful construction of the tubes was made possible by the skill of Mr. C. C. Van Hespen.

[8] A. J. Dempster, Phys. Rev. **46**, 728 (1934).

Theoretical Evaluation of a Wide-Angle Interference Experiment

F. W. DOERMANN AND O. HALPERN
Department of Physics, New York University, New York, New York
(Received January 3, 1939)

Two previously published investigations of the wide-angle interference of multipole radiation and the theory of Lloyd's mirror are continued. The formulas are extended to cover the cases of total internal reflection and observation made through a single Nicol prism. The theoretical basis is thus obtained for the evaluation of a wide-angle interference experiment carried out by Selényi with light from a thin fluorescent layer. Comparison of this theory with his observations made with a Nicol prism shows that the source can be composed only of electric dipoles or magnetic quadrupoles. The possibility of the latter can be excluded either by general physical reasoning, or by comparison of our theory with his observations made at various angles of divergence without the Nicol prism. It may thus be said that the source of fluorescence light has been shown to consist of electric dipoles.

I. INTRODUCTION

IN a previous article,[1] in which the authors discussed the problem of the wide-angle interference of multipole radiation of various orders, it was shown that the contrast in the interference pattern must depend upon the wide-angle (2θ) of divergence of the original beams in a manner characteristic of the nature of the light source as well as of the experimental arrangement[2] employed to bring the two divergent beams to interference. The detailed analyses of the effects to be expected with various arrangements was restricted in this paper to those employing ideal mirrors and Nicol prisms. The limitation to the use of ideal mirrors was removed in a second article[3] in which, by the introduction of a complex interference parameter, the general theory was extended to cover polarization effects (phase changes) and was then applied in great detail to the evaluation of the effect for the Lloyd's mirror arrangement with nonideal reflecting surface.

About the same time, P. Selényi published[4] the results of a simultaneous and independent investigation in which he had very ingeniously overcome the experimental difficulty of obtaining a source sufficiently small and luminous to produce wide-angle interference of the type we described. He observed a variation in the visibility of the fringes with the angle 2θ and also, for $2\theta=90°$, with the setting of a Nicol prism through which both beams were passed.

It is our purpose to present here the results of a detailed theoretical evaluation of the Selényi experiment, and to show how the Selényi observations can be used for the purpose of drawing conclusions as to the nature of the source.

II. GENERAL THEORY

Although we must, of course, refer to the original paper[4] for all experimental details, we reproduce in Fig. 1 a schematic diagram of the Selényi interference arrangement. The source is a film S (of thickness small in comparison with the wave-length) of a fluorescing solution held between a prism P and a thin mica plate M. The refractive indices of S, P and M are very approximately the same ($n\approx 1.5$) so that the ray I from an elementary point source at O is reflected only

[1] O. Halpern and F. W. Doermann, Phys. Rev. **52**, 937 (1937).

[2] Our attention has been called to a paper [Physik. Zeits. Sowjetunion **3**, 103 (1932)], published some six years ago, in which S. I. Wawilow and E. M. Brumberg discussed the wide-angle interference of dipole radiation. In a more recent paper [C. R. Acad. Sci. URSS **17**, 463 (1937)], published subsequently to our paper (reference 1), Mr. Wawilow speaks of our "repetition" of his earlier theoretical results. As one of the chief points made in our paper was the specific dependence of the effect upon the experimental arrangement, and as the 1932 dipole formula of Wawilow and Brumberg was obtained by a method (unintelligible to us) that ignored the effect of the apparatus upon the light vectors and so gave a result independent of the arrangement, we must regard its purely formal agreement with but one of our formulas as entirely fortuitous. This means also that we must disclaim the interpretability of their experiments of the Young type (slits) by that part of our theory for which specific formulas have been developed—formulas which apply to experiments of the Fresnel type (mirrors and prisms) only. Furthermore, Mr. Wawilow did not proclaim the main thesis of our paper (reference 1)—namely, that well-defined interference experiments can be employed to distinguish between various types of sources—until after its appearance.

[3] F. W. Doermann, Phys. Rev. **53**, 420 (1938).

[4] P. Selényi, Zeits. f. Physik **108**, 401 (1938).

at the outer surface of M, and there totally for appropriate angles ($O<\theta<48°$). The interfering beams B, B' are either the reflected beam R and the parallel direct beam $R'\equiv I'$, or these same beams after they have passed through one and the same Nicol prism N.

From the geometry of the figure it is clear that the Selényi arrangement is that of a Lloyd's mirror; our formulas,[3] however, do not cover the case of total internal reflection, nor of the insertion of a Nicol prism. As we have already given detailed instructions for setting up formulas for more complicated arrangements, we need set down here merely the results of adapting them to apply to the Selényi experiment.

The employment of the single Nicol prism with the Lloyd's mirror arrangement requires the formula[5]

$$Q^*=\frac{4\alpha[(1+\cos\chi)\rho_\perp D_1{}^P+(1-\cos\chi)\rho_{||}D_2{}^P]}{(1+\cos\chi)|\rho_\perp|^2+(1-\cos\chi)|\rho_{||}|^2+2\alpha^2} \quad (1)$$

for the complex interference parameter Q, of which the magnitude $|Q|$ is a measure[6] of the contrast in the fringes and assumes the values 1 and 0 for perfectly black minima and the total absence of fringes, respectively. We are primarily interested in the dependence of Q upon the angle 2θ of divergence of the original beams: on the right side of (1) the complex reflection coefficients $\rho_\perp$, $\rho_{||}$ are functions[7] of θ as are also the quantities

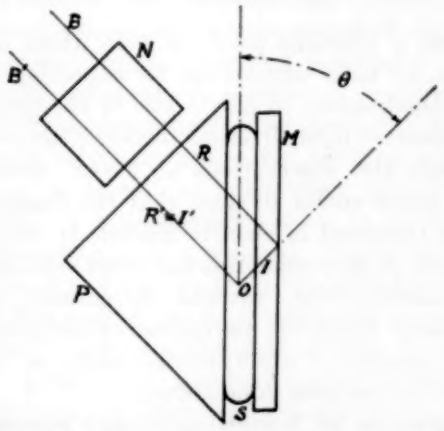

FIG. 1. Schematic diagram of the Selényi apparatus.

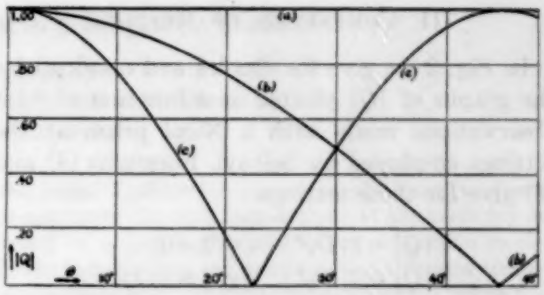

FIG. 2. $|Q|$ plotted as a function of θ for given settings of the Nicol prism: (a) electric dipole for $\chi/2=0$, magnetic dipole for $\chi/2=\pi/2$; (b) magnetic dipole and electric quadrupole for $\chi/2=0$, electric dipole and magnetic quadrupole for $\chi/2=\pi/2$; (c) magnetic quadrupole for $\chi/2=0$, electric quadrupole for $\chi/2=\pi/2$.

$D_1{}^P$, $D_2{}^P$ which for $P=E$ (electric 2^l pole) and $P=M$ (magnetic 2^l pole) assume the forms[8] $D_1{}^E=D_2{}^M=D_1(\theta, l)$, $D_2{}^E=D_1{}^M=D_2(\theta, l)$. The angle χ takes into account the setting of the Nicol prism; $\chi/2$ is the angle between the plane of incidence (the plane of the figure) and the plane containing the ray and its magnetic light vector after it has passed through the Nicol prism. The factor α takes into account the diminution in intensities of the two beams produced by nonpolarizing absorption effects: if this effect is the same for both beams, $\alpha=1$.

The well-known values of the coefficients of total internal reflection may be written in the explicit form

$$\rho_\perp=(n^2\sin^2\theta-d^2+i2nd\sin\theta)/(n^2-1),$$
$$\rho_{||}=(\sin^2\theta-n^2d^2+i2nd\sin\theta)/(\sin^2\theta+n^2d^2), \quad (2)$$
$$d\equiv(n^2\cos^2\theta-1)^{\frac{1}{2}},$$

where $n>1$ is the refractive index. These have the important property that

$$|\rho_\perp|=|\rho_{||}|=1. \quad (3)$$

We may with reasonableness assume $\alpha\approx1$ for the Selényi experiment; if we substitute this value into (1) and make use of (3), we thereby obtain:

$$Q^*=(1+\cos\chi)\rho_\perp D_1{}^P+(1-\cos\chi)\rho_{||}D_2{}^P. \quad (4)$$

The corresponding formula for the case in which no Nicol prism is employed is

$$Q^*=\rho_\perp D_1{}^P+\rho_{||}D_2{}^P. \quad (5)$$

[3] This replaces formula (10) of reference 3.

[5] The intensity in the fringe pattern is proportional to $1+|Q|\cos\delta$, where δ is, to within an additive constant, the phase difference between the interfering beams. See reference 2, Section II.

[7] θ is the complement of the angle of incidence; see Fig. 1.

[8] For the explicit form of D_1, D_2 for $l=1, 2, 3$ see Table I of reference 1. Instructions are given in the Appendix to reference 1 for obtaining the explicit form for higher values of l.

III. Comparison of Results

In Fig. 2 we give for dipoles and quadrupoles the graphs of $|Q|$ plotted as a function of θ for observations made with a Nicol prism at the settings employed by Selényi. Formulas (4) and (3) give for these settings

$$\begin{aligned} |Q| &= 2|D_1^P| \quad (\chi/2=0) \\ |Q| &= 2|D_2^P| \quad (\chi/2=\pi/2). \end{aligned} \tag{6}$$

From this it is apparent that at most four curves are required to cover the eight cases; as a matter of fact[8] $D_1(\theta)_{l=2} \equiv D_2(\theta)_{l=1}$ so that three curves suffice. The extreme simplicity of these curves is a direct result of the fact that *at these settings* of the Nicol prism, $|Q|$ does not depend upon the coefficients of reflection.

Selényi's observations were made for $\theta=45°$: the fringes had nearly black minima ($|Q| \approx 1$) for $\chi/2=0$, and were nearly invisible ($|Q| \approx 0$) for $\chi/2=\pi/2$. The values of $|Q|$ for $\theta=45°$ are especially shown in Table I. A glance at this table shows that the angle θ is unfortunately chosen for distinguishing between multipoles of different orders and types. Thus, in particular, both the Selényi observations are compatible with a source consisting either of electric dipoles or of magnetic quadrupoles. (Such an experiment could also not distinguish between magnetic dipoles and electric quadrupoles.) To draw conclusions as to the source from interference observations alone, it is therefore necessary to consider observations made at other angles.

In Fig. 3 we give for dipoles and quadrupoles the graphs of $|Q|$ plotted as a function of θ for observations made *without* a Nicol prism. Since, according to (5):

$$|Q|^2=(D_1^P)^2+(D_2^P)^2+(\rho_\perp\rho_{||}{}^*+\rho_\perp{}^*\rho_{||})D_1^P D_2^P, \tag{7}$$

we see that $|Q|$ is a symmetrical function of D_1 and D_2 so that the curves for electric and magnetic multipoles of the same order will coincide. Selényi states that no absolutely black minima were observable without the Nicol prism, but that the minima became darker when the angle of incidence upon the reflecting surface was increased, that is to say, when θ was decreased. The explanation of this phenomenon as the effect of the finite thickness of the layer S (of which the influence becomes less as θ is decreased) is not compatible with the fact, just recorded, that nearly black minima were seen with a Nicol prism at $\theta=45°$. The explanation in terms of the curves in Fig. 3 is immediate, and (since the observations were made roughly in the interval $25°<\theta<50°$) shows that the source consisted of dipoles rather than of quadrupoles.

Table I. *Values of $|Q|$ for $\theta=45°$ with the Nicol prism set at $\chi/2=0$ and $\chi/2=\pi/2$.*

P, $\chi/2$	$l=1$	$l=2$	$l=3$
E, 0	1	0	$\frac{1}{4}$
E, $\pi/2$	0	1	0
M, 0	0	1	0
M, $\pi/2$	1	0	$\frac{1}{4}$

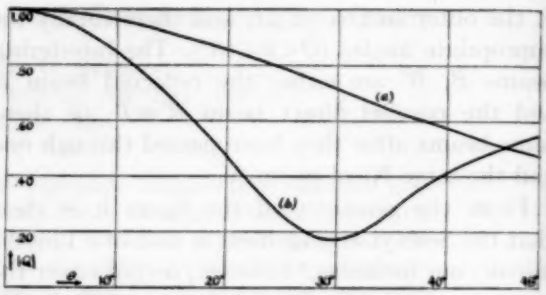

Fig. 3. $|Q|$ plotted as a function of θ for (a) electric and magnetic dipoles and (b) electric and magnetic quadrupoles.

IV. Conclusion

From a physical point of view there is, of course, no basis whatsoever for expecting magnetic quadrupoles to play a rôle in the emission of fluorescent light. It seems therefore justified to say that the observations at $\theta=45°$ with the Nicol prism suffice to show that the fluorescent source consisted of electric dipoles. If we wish, however, to determine this fact from interference experiments alone, without introducing other knowledge about the mechanism of emission, we must appeal to observations made at other angles, as has been done above.

It remains an interesting though experimentally perhaps more difficult problem to investigate whether other light sources, in which—as in the case of heat radiation—many atoms can be assumed to be cooperating in the process of emission, also consist of electric dipoles only.

On the Origin of the Earth's Magnetic Field

WALTER M. ELSASSER
California Institute of Technology, Pasadena, California
(Received October 25, 1938)

The terrestrial field is traced here to the existence of thermoelectric currents in the metallic interior of the earth. The currents owe their existence to inhomogeneities continually created by turbulent convective motions. In order to obtain a nonvanishing resultant angular momentum of the currents around the earth's axis, the current system must exhibit a particular asymmetry. The latter is shown to originate through the preponderant influence of the Coriolis force upon the convective motions. In Part I the well-known proof, based on potential theory, of the fact that the currents must flow inside and not outside the earth, is briefly reproduced. In Part II an analysis of the formal expression for the current density is given. By means of a development in spherical harmonics the conditions for a nonvanishing current momentum can be formulated. It appears that temperature fluctuations in an otherwise homogeneous medium always yield a zero momentum, therefore the existence of inhomogeneities in the material is also required. In Part III it is pointed out that geophysicists have previously obtained evidence of the existence of a metallic core of the earth in which the viscosity is extremely low as compared to the viscosity of the rocks. Radioactive impurities which are very small compared to the total radioactivity of the earth are sufficient to maintain thermally driven convective motions in the metallic core. An estimate of the various terms in the hydrodynamic equations shows that the Coriolis force is much larger than all other dynamical effects. In Part IV we discuss the effect of the Coriolis force in producing that particular asymmetry which leads to a resultant angular momentum of the currents. It is shown that the inhomogeneities in material required according to the analysis of Part II can be accounted for by phase transformations of the material induced by the pressure changes which are connected with the vertical component of the motions. In Part V an attempt is made to estimate numerically the current density, basing the estimate on some general results of the theory of conductivity. For temperature variations of the order of 10° the calculated value of the current is in satisfactory agreement with the observed magnitude of the earth's magnetic moment. At the end, the bearing of these ideas upon the magnetism of sunspots is briefly discussed.

SINCE the earth's magnetic moment is roughly parallel to the rotational axis, it has often been presumed that the terrestrial field is physically related to the earth's rotation. The direct influences of the rotation upon atomic and electronic motions, however, are much too small to account for the observed magnitude of the magnetic moment. A number of writers have proposed modifications of the fundamental equations of electrodynamics for rotating systems, often in connection with relativistic field theories. Theories of this type are unable to account for the deviation of the magnetic dipole axis from the rotational axis, for the quadrupole and higher momenta and for the large secular fluctuations of the field. They are therefore obliged to assume that a primary and symmetric field is modified by the magnetic properties of the substances constituting the earth. Since the mentioned irregularities are by no means very small, but are roughly of the order of a tenth of the total field, these theories do not afford a solution of the physical problem. It is well known that the hypothesis of a permanent magnetization of the earth (resembling a steel magnet) has long been abandoned, since it proved impossible to find any reasonable physical basis for such an assumption. The same arguments which have been put forward against the hypothesis of a permanent magnetization may also be raised against any of the mentioned theories.

Since the action of the earth's rotation upon atomic motions is very small, any influence of the rotation upon the generation of a magnetic field must be of an indirect nature. In the theory proposed here it is assumed that the magnetic field is a rather accidental consequence of fluid motions which take place in the interior of the earth. Since the central part of the earth is most probably metallic, temperature variations produced by the convection give rise to thermoelectric currents. It might at first sight seem rather surprising that such a current system can yield a steady mean transport of electricity encircling the earth's axis. We shall see that the Coriolis force is so preponderant in the dynamics of the motions that it brings about a strong east-westerly asymmetry of the latter. If we write

down the conditions of a nonvanishing current momentum, it appears that, in the language of perturbation theory, the momentum is an effect of the second order with regard to the deviations from the state of rest. Among the quantities which determine the thermoelectric currents, namely, the temperature, the thermoelectric constant and the electric conductivity (which are all considered as space functions), at least two must at the same time exhibit an east-westerly asymmetry. We shall, in the course of this paper, discuss the simplest and apparently most satisfactory model of the earth's interior which meets these requirements. It will also be shown that the currents to be expected from rather conservative estimates are of a sufficient order of magnitude to produce the observed magnetic moment.

I

It is known that the electric currents which produce the earth's magnetic field must necessarily be located *in the interior* of the earth. The proof depends upon some simple facts of potential theory and may briefly be reproduced here.[1] Consider the *horizontal* component H_h of the magnetic field at the surface of the earth. H_h is the gradient of a potential U which can be represented as a series of spherical harmonics

$$U=\sum_{m,\ n=1}^{\infty} u_n^m Y_n^m(\vartheta, \varphi), \quad |m|\leqq n, \tag{1}$$

where the Y_n^m are a complete set of normalized spherical harmonics and the arbitrary constant u_0 has been made to vanish. If H_h is measured at all points of the earth's surface, the coefficients u_n^m and the Y_n^m are uniquely determined. Now consider a thin spherical shell just above the earth's surface. Assume that there are no appreciable electric currents within the shell, so that the potential U within the shell obeys Laplace's equation

$$\Delta U=0. \tag{2}$$

As is well known, (2) has two particular solutions which involve the spherical harmonic Y_n^m, namely,

$$r^{-n-1}Y_n^m \quad \text{and} \quad r^n Y_n^m.$$

If, therefore, we consider the coefficients u_n^m in (1) as functions of r, we may write

$$U=U_1+U_2$$

where

$$U_1=\sum_{n,\ m} p_n^m r^{-n-1} Y_n^m(\vartheta, \varphi),$$
$$U_2=\sum_{n,\ m} q_n^m r^n Y_n^m(\vartheta, \varphi). \tag{3}$$

On the other hand, let us consider the *vertical* component H_v of the earth's magnetic field and let us write

$$H_v=\sum_{m,\ n=1}^{\infty} v_n^m Y_n^m(\vartheta, \varphi), \quad |m|\leqq n. \tag{4}$$

The v_n^m can be obtained by direct determination of the vertical magnetic force at all points of the earth's surface. Now

$$H_v=\partial U/\partial r. \tag{5}$$

Therefore if a designates the radius of the earth, we have from (1) and (3):

$$u_n^m=p_n^m a^{-n-1}+q_n^m a^n$$

and from (4) and (5):

$$v_n^m=-(n+1)p_n^m a^{-n-2}+nq_n^m a^n.$$

If u_n^m and v_n^m are known from observation, these equations can be solved for p_n^m and q_n^m. It is therefore possible to determine the potentials U_1 and U_2 separately. U_1 is called the potential of the internal field and U_2 the potential of the external field. In potential theory one demonstrates that if the source regions of a field are all contained inside a sphere $r=a$, then $\Delta U=0$ everywhere outside the sphere and the development of U in a series of spherical harmonies for $r\geqq a$ contains only *negative* powers of r. If on the other hand all the source regions of a field are located outside a sphere of radius a', then $\Delta U=0$ for $r\leqq a'$ and the development valid for $r\leqq a'$ contains only *positive* powers of r. The reverse of these statements is also true. If $\Delta U=0$ is valid within a thin spherical shell contained between $r=a$ and $r=a'$ and if the components U_1 and U_2 as defined by (3) have been determined separately, then $\Delta U_1=0$ for $r\geqq a$ and $\Delta U_2=0$ for $r\leqq a'$. Therefore the source regions of U_1 are all located in the space inside the spherical shell and

[1] G. Angenheister and J. Bartels, *Handbuch der Experimentalphysik* (Leipzig, 1928), Vol. 25, Part I.

the source regions of U_2 are located in the space outside it.

Our actual knowledge of the earth's magnetic field permits the conclusion that the potential U_2 of the external field is extremely small; although its precise value is still somewhat uncertain, it can be stated that the external field does not amount to more than a few percent of the total field.[2] It follows therefore that almost the whole of the electric currents which generate the field must flow in the interior of the earth.

II

The currents must be produced by electromotive forces and we shall now discuss the nature of these forces. Two principal possibilities seem to present themselves, namely, galvanic forces and thermoelectric forces. Galvanic forces originate through the migration of ions which takes place along a gradient of concentration. The diffusion velocity of ions may be assumed considerably smaller under the extreme pressures and higher densities in the interior of the earth than it is in liquids under ordinary conditions. If reasonable values for the concentration gradients are assumed, it appears that the currents thus obtained are much smaller than those required to produce the earth's magnetic field.

The conditions are far more favorable for thermoelectric forces. The latter are produced by the migration of electrons and appear in metallic conductors. Now it is rather generally assumed by geophysicists that the inner parts of the earth are metallic and consist mainly of iron and nickel. From seismic observations we know the existence of a surface of discontinuity in the interior of the earth which is located at a depth of about 2900 km.[3, 4] A large and sudden change of the physical properties of the material takes place there as evidenced by the change in transmission of the earthquake waves. We shall later come back to this point; for the present we need only follow the assumption generally made by geophysicists, namely, that this surface of discontinuity represents the boundary between the nonmetallic and the metallic constituents of the earth, the metals being concentrated below the boundary. We shall refer specifically to the central part of the earth bounded by the surface of discontinuity as the earth's *core* and assume it to be a metallic conductor throughout.

If the core were in itself perfectly homogeneous, no flow of electricity within it could persist. The existence of inhomogeneities is required; in order to simplify the mathematical treatment we may for a moment assume that within the core all physical properties are continuous functions of the coordinates. This is of course not an essential restriction; if discontinuities appear, the formulae for continuous variables are easily adapted to this case. It is furthermore convenient to assume that the nonmetallic exterior part of the earth does not give rise to electromotive forces.

If the electric field is a static one, so that it derives from a potential, say $E=-\text{grad}\,\omega$, then the most general expression for the electric *current density* in a conductor with inhomogeneities both of material and of temperature is given by

$$I=-\sigma\,\text{grad}\,\omega-\text{grad}\,A-B\,\text{grad}\,T. \qquad (6)$$

Here σ is the conductivity, A and B are functions of the material (which reduce to constants whenever the material is homogeneous), and T is the temperature. All quantities on the right-hand side of (6) are functions of the variables r, ϑ, φ. The term $-\text{grad}\,A$ corresponds to the existence of Volta contact potentials, as is readily seen by dropping the last term on the right-hand side and putting $I=0$. It appears then that A/σ is just the Volta potential apart from an additive constant. The contact potentials do not, of course, give rise to stationary currents; under stationary conditions they are fully compensated by space and surface charges. The term $-B\,\text{grad}\,T$, finally, represents the thermoelectric current density. In the case of an aggregation of homogeneous conductors contacting each other, (6) gives the usual expression for the thermoelectric currents.[5]

Stationary flow is characterized by the condition

$$\text{div}\,I=0. \qquad (7)$$

[2] S. Chapman, *The Earth's Magnetism* (London, 1936).
[3] H. Jeffreys, *The Earth* (second edition, 1929), Chap. 7.
[4] B. Gutenberg, *Handbuch der Geophysik* (Berlin, 1933), Vol. 2.

[5] A direct and fairly elementary derivation of formula (6) from the theory of electronic conductivity is given in R. Becker, *Theorie der Elektrizität* (Leipzig, 1933), Vol. 2, p. 239.

In the absence of an external force, ω is the potential of the space and surface charges which must accumulate in order to permit stationary flow. Since all quantities except ω on the right-hand side of (6) are given, Eq. (7) is a differential equation for ω, from which ω can be determined under proper boundary conditions. We may omit here the discussion of the boundary conditions, since it is quite elementary and will not be needed in the following.

We proceed now to determine the angular momentum of the current system with respect to the earth's axis. If I is measured in electromagnetic units, this will at the same time be the component of the *magnetic* momentum parallel to the earth's axis. If I_φ designates the φ-component of the current density and $d\tau$ the volume element we have

$$M = \int I_\varphi \cdot r \sin \vartheta d\tau$$

or from (6)

$$M = -\int B(\partial T/\partial \varphi)d\tau - \int \sigma(\partial \omega/\partial \varphi)d\tau. \quad (8)$$

We write

$$M = M_1 + M_2 \quad (9)$$

with

$$M_1 = -\int B(\partial T/\partial \varphi)d\tau = \int T(\partial B/\partial \varphi)d\tau \quad (10)$$

where the latter equality results from a partial integration with respect to φ. An analogous equation is valid for M_2.

We shall now discuss the properties of M_1 as given by (10). The discussion of M_2 is perfectly analogous and need not be explicitly repeated. It appears from (10) that a nonvanishing momentum is only obtained if both B and T are dependent on the geographical longitude φ. Explicit formulae may be obtained by developing both B and T in series of spherical harmonies

$$B = \sum_n a_n(r)P_n(\cos\vartheta) + \sum_{n,m} (m \neq 0)[a_n^m(r) \sin m\varphi + b_n^m(r) \cos m\varphi]P_n^m(\cos\vartheta),$$

$$T = \sum_n s_n(r)P_n(\cos\vartheta) + \sum_{n,m} (m \neq 0)[s_n^m(r) \sin m\varphi + t_n^m(r) \cos m\varphi]P_n^m(\cos\vartheta),$$

where the P_n^m are normalized Legendre functions and where the second sum in each case contains only terms for which $m \neq 0$. Substituting in (10) we obtain

$$M_1 = \sum_{n,m} (m \neq 0) \frac{m}{2} \int (a_n^m t_n^m - b_n^m s_n^m) r^2 dr. \quad (11)$$

For the validity of this formula no restrictions about the continuity of the function B are required. Formula (11) shows that definite *phase relations* between the coefficients of the two series must exist; for instance, the momentum would vanish if both series would contain *sin* terms only or *cos* terms only. If φ is changed into $-\varphi$, the right-hand side of (11) changes sign, as it must be. The phase relations among the coefficients express the east-west asymmetry in the structure of the current system which obviously is necessary in order to produce a nonvanishing momentum around the earth's axis. It is remarkable that B and T enter *antisymmetrically* in the expressions (10) and (11) for the momentum; an exchange of the variables B and T changes the sign but not the absolute value of the momentum.

The same analysis as carried through here for the pair (B, T) may be applied to the pair (σ, ω) and gives formulae for M_2 which are analogous to (10) and (11).

III

It is obvious that the rather special conditions for the electric current system pointed out above cannot reasonably be explained by a permanent asymmetric structure of the earth's interior. There is furthermore the difficulty of accounting for steady sources of heat distributed without rotational symmetry. The assumption of fluid motions must therefore appear as a rather natural basis of the theory. Convective motions set up by temperature differences in the earth have been quantitatively studied by Pekeris.[6] His calculations refer to motions of the upper parts of the earth where the viscosity is extremely high and where correspondingly low values of the velocity obtain (of the order of one cm per year). There is ample evidence that the mechanical

[6] C. L. Pekeris, Monthly Not. Roy. Astr. Soc. Geophys. Suppl. 3, 343 (1935).

properties of the core are fundamentally different from those of the higher strata. At the core's boundary the velocity of sound changes from about 13 km/sec. above to 8 km/sec. below the boundary; it then rises slowly again within the core and reaches about 11 km/sec. at the center of the earth.[4, 5] There are many indications that the boundary is a rigorous discontinuity. Transversal waves are reflected at the boundary and seem never to be transmitted through the core, while longitudinal waves are transmitted with very little damping. Jeffreys[7] concludes from the total available evidence that the core behaves much more like a liquid than like a solid body. From the damping of longitudinal waves in the core he derives an upper limit for the viscosity which he finds to be about 2×10^{10} c.g.s. units. (The viscosity of the crust is of the order of 10^{22}.) Reviewing the whole topic Jeffreys[7] comes to the conclusion that "there seems to be no reason to deny that the earth's metallic core is truly fluid."

We proceed now to write down the equations of motion for a fluid with internal friction.[8] Let $\mathbf{v}$ be the velocity vector, $\mathbf{S}$ the vectorial angular momentum of the earth, ρ the density, μ viscosity, and p the pressure. Then

$$\dot{\mathbf{v}}+(\mathbf{v}\ \text{grad})\mathbf{v}+2\mathbf{S}\times\mathbf{v}-\mu\rho^{-1}\Delta\mathbf{v}=-\rho^{-1}\ \text{grad}\ p.$$

Before entering into a discussion of these equations we might try to obtain an approximate estimate of the prevailing velocities. This is a very difficult task. A rough idea may be gained by anticipating the fact that the secular changes in the earth's magnetic field must in our theory be produced by the irregularities of the fluid motion. Since the secular changes of the field are appreciable in the course of a few centuries, we may be inclined to think that during this time a particle travels a distance comparable to the core's radius, say about 10^8 cm. This leads to velocities of the order of 10^{-2} to 10^{-3} cm/sec. We need not repeat that this estimate is extremely uncertain.

For stationary flow we will have $\dot{\mathbf{v}}=0$. Furthermore it is readily seen that for any reasonable value of the velocity the term $(\mathbf{v}\ \text{grad})\mathbf{v}$ is small compared to the Coriolis term $2\mathbf{S}\times\mathbf{v}$. In a first approximation the equations of motion reduce therefore to

$$2\mathbf{S}\times\mathbf{v}-\mu\rho^{-1}\Delta\mathbf{v}=-\rho^{-1}\ \text{grad}\ p. \qquad (12)$$

The cause of the motions is to be found in the change in density which is connected with a change in temperature. We may assume that a small amount of radioactivity distributed throughout the core produces continually a certain amount of heat, while heat is carried away by conduction through the superimposed, solid layers. If the core were thoroughly mixed by convection, an adiabatic temperature gradient would be established vertically, i.e., the increase in temperature in the downward direction would be exactly equal to the adiabatic heating of the matter produced by the vertical increase in pressure. Now since heat is produced in the interior and is carried away from the top of the core, the temperature gradient (and also the density gradient) becomes larger than adiabatic. Such a stratification is mechanically unstable and vertical motions will set in, carrying heat upwards. If a particle is carried upwards by the motion, it cools adiabatically, and since the temperature gradient of the surrounding mass is steeper than the adiabatic one, the particle after lifting is warmer than the surrounding mass at its new level. In the same way a sinking particle becomes cooler than the surrounding mass at its level. These variations will slowly be equalized by thermal conduction. The convective heat transport therefore yields the temperature differences at a given level which appeared necessary in the analysis of the preceding section.

We cannot enter here into a detailed discussion of the dynamic properties of convective heat transport. The motion is usually highly unstable dynamically and tends to break up in a number of vortices, often of a cellular form.[9] In our case we may also assume that the motion consists essentially of a juxtaposition of numerous vortices of more or less irregular shape. It is rather difficult to form an idea of the mean size of an individual vortex. We may note, however, anticipating the results of the present theory, that the observed irregularities of the magnetic

[7] H. Jeffreys, Monthly Not. Roy. Astr. Soc. Geophys. Suppl. 1, 371, 416 (1926).
[8] H. Lamb, *Hydrodynamics* (sixth edition), Chap. 11.
[9] D. Brunt, *Physical and Dynamical Meteorology* (Cambridge, 1934), Chaps. 12, 13.

field and of its secular variation are so large that at least some of the vortices must be of a fairly good size as compared to the dimensions of the core.

If a vortex is very small, its motion will be damped out by friction before the Coriolis force has any appreciable effect on it. This may be seen by comparing the order of magnitude of the two terms on the left-hand side of (12). Let L designate the linear dimensions of a vortex, then we may write L^{-2} for the order of magnitude of the symbol Δ. Now approximately $S=10^{-4}$ sec.$^{-1}$. Further, take $\mu=2\times10^{10}$ and roughly $\rho=10$. Therefore the frictional term is larger or smaller than the Coriolis term according to whether the size of the vortex is smaller or larger than $L=3\times10^{6}$ cm. This is only about one percent of the core's radius and since the value of μ is an upper limit, this also represents an upper limit for the critical value of L, below which the vortex motion is aperiodically damped. These considerations show that for vortices of large size the Coriolis force is vastly predominant as compared to all other mechanical forces including friction.

If the frictional term on the left-hand side of (12) is left out, the equations of motion represent merely the equilibrium condition for steady flow.[10] It is readily seen that for velocities of the order of 10^{-2} cm/sec. the "dynamical" pressure differences which appear on the right-hand side of (12) are excessively small compared to the total pressure prevailing in the interior of the earth.

In order to make our picture complete, it is necessary to show that small amounts of radioactivity can actually set up convective motions. The kinetic energy transformed into heat by friction is per unit time[8]

$$W=\mu\int(\text{curl }\mathfrak{v})^2 d\tau,$$

which is of the order of magnitude

$$W=\mu v^2\cdot V\cdot L^{-2},$$

where V is the volume of the core. With $\mu=2\times10^{10}$, $v=10^{-2}$ and $L=3\times10^{7}$ cm, say, we obtain $W=10^{17}$ erg/sec. This is to be compared with the total radioactive heat output of the earth as measured by the loss of heat by conduction through the surface rocks. The latter figure is about 4×10^{20} erg/sec. It is seen that extremely small radioactive impurities are sufficient to maintain the convective motions; in view of the small heat development, the temperature gradient in the solid layers just above the core need only be a small fraction of the gradient near the earth's surface. Our theory is therefore in agreement with the well-established geophysical fact that the earth's radioactivity must be quite strongly concentrated in the uppermost layers of the crust.[11]

[10] D. Brunt, reference 9, Chap. 9.

IV

We have now to investigate the generation of thermoelectric currents as a consequence of the turbulent convective motions. In the first place it is necessary to account for the east-west asymmetry which is obviously required in order to obtain a nonvanishing current momentum. It is readily seen that the fluid motions are not symmetrical with respect to the east-west direction. The primary convective motions are vertical, but under the preponderant influence of the Coriolis force which is perpendicular to the velocity, the mean turbulent motions can be expected to take place in all directions. Let us pick out an individual vortex and introduce a system of coordinates whose origin is located within the vortex. Let the x axis be horizontal from west to east, the y axis horizontal from south the north, and the z axis going vertically upwards. If $\mathbf{S}$ is again the vectorial angular velocity of the earth, then $S_x=0$, $S_y=S\sin\vartheta$, where ϑ is the geographical latitude. We have therefore for the *vertical* component of the Coriolis force

$$C_z=2S\sin\vartheta\cdot v_x. \tag{13}$$

The vertical Coriolis force depends therefore only upon the east-westerly component of the fluid motion; the force is directed vertically upwards if the motion is from west to east and vertically downwards if the motion is from east to west. We may therefore expect that *in any vortex*, whatever its particular structure and shape, *there will be a mean upward motion in the eastern part and a mean downward motion in the*

[11] H. Jeffreys, reference 3, Chap. 8.

western part of the vortex. According to previous considerations this means that the eastern part of the vortex will be warmer and the western part of the vortex will be cooler than the surrounding material at the same level. The true turbulent motion will, of course, be extremely complex, but we might still expect that there remains a statistical correlation between the warm and cold areas so that in the east of an area with less than average temperature there will be in the mean an area with more than average temperature, and vice versa.

This condition, however, although it yields thermoelectric currents, is not enough to insure the existence of a magnetic moment of the earth, as has been demonstrated in Part II. If the material is homogeneous, the thermoelectric constant B is a true constant and the resultant angular momentum of the currents vanishes. The simplest way of accounting for a variation of B seems by the assumption that the material undergoes phase transformations caused by the changes in pressure. There are, of course, quite considerable pressure changes connected with any vertical displacement of a material particle and it seems that phase transitions due to pressure changes are a rather common occurrence at high pressures.[12]

While the pressure gradient is mainly vertical, there are small "dynamical" pressure gradients in horizontal direction which appear on the right-hand side of (12) and which cause the convective motions. The latter variations in pressure are, however, exceedingly small so that their effect upon a phase transformation appears negligible. Therefore the phases at a given depth are determined by the temperature alone. We shall then expect that if at a given level a phase transformation does actually occur, the constant B can assume two values, say B_1 for $T>T_0$ and B_2 for $T<T_0$, where T_0 is the transformation temperature at that level. Substituting these values in the first integral (10) we readily see that the resultant momentum vanishes. We come so to the conclusion that the hypothesis of phase transformations alone is not sufficient to insure the existence of a current momentum. If the phases are not determined at any moment by the temperature and depth alone, it means that the phases *are not in thermodynamical equilibrium*.

How can we now account for deviations from thermodynamical equilibrium in the interior of the earth? There seem to be two mechanisms which produce such deviations. First there may occur, in the phase transformations, a time lag comparable to the time which a particle needs to travel an appreciable vertical distance. The amount of lag will depend essentially upon the viscosity and it appears possible that the latter, although not large enough to prohibit slow fluid motions, is sufficient to retard phase changes which extend over large areas. Secondly, deviations from a thermodynamical equilibrium may arise in connection with chemical inhomogeneities. Almost certainly the earth's core possesses a very complex chemical constitution and in this case *heterogeneous* phases may form. We can for instance think of one phase as interspersed in another in form of macroscopic drops or blocks. If the phase differs slightly in density, vertical motions of the phases relative to each other must arise; i.e., there is a trend towards sedimentation. If the velocity of sedimentation is comparable to that of the thermal convection, the result will be a redistribution of the inhomogeneities over the core.

We have explained above in which way the asymmetry of the convective motions caused by the Coriolis force results in an asymmetry of the temperature distribution. In a perfectly analogous way the asymmetry of the motions combined with the mechanisms just outlined will tend to produce an asymmetric variation of the thermoelectric constant of the material. Now in the absence of a thermodynamical equilibrium there is no reason that the fluctuations of T and B should exhibit a strict parallelism, and in view of the asymmetry of the field of motion the conditions for a nonvanishing current momentum appear fulfilled. We must, of course, expect that the one-sided excess of the currents which yields the momentum is much smaller than the mean of the absolute value of the currents.

The same arguments which have been applied here to the pair B, T may be applied to the pair σ, ω in (8). Now it seems rather plausible that the percentage variation of the conductivity σ caused by a phase transformation will in general be less

[12] P. W. Bridgman, *The Physics of High Pressures* (London, 1931), Chap. 8.

than the percentage variation in the thermoelectric constant B. We may therefore be justified in neglecting the contribution to the momentum which comes from the second term on the right side of Eq. (8).

The preceding considerations are of course far from being a constructive theory of the thermoelectric currents. Such a theory would have to start with an integration of the equations of motion (12). In the present preliminary state of the theory we must confine ourselves to these qualitative indications of how a more rigorous theory would explain the existence of a current momentum.

V

We shall finally try to obtain a quantitative estimate of the thermoelectric currents. The connection between our thermoelectric constant B and the ordinary thermoelectric potentials is readily found. If we consider a circuit composed of two different materials with constants B_1 and B_2, respectively, the two connections being at different temperatures, we can determine the thermoelectric potential by a simple integration of (6). Suppose the circuit is interrupted somewhere so that $I=0$ and let us put $A=0$ in (6), in order to obtain the pure thermoelectric force; then

$$\sigma\Delta\omega=\Delta T(B_1-B_2).$$

As shown above, the main contribution to the earth's magnetic moment comes presumably from the term B grad T in (6). We may assume as order of magnitude of this current density $\Delta B\Delta T/L$, where L designates again the mean linear dimensions of a vortex, or

$$I\sim\sigma\Delta\omega\Delta T/L. \qquad (14)$$

We have now to estimate the various quantities which appear in (14). The two first factors on the right-hand side are connected with the properties of the material as a metallic conductor. We may take for σ the conductivity of iron. We have, of course, to take into account the influence of temperature and pressure. Very little is known about the temperature of the earth's core. Estimates vary between 2000° and 6000°. It is shown in the theory of metallic conductivity[13] that for high temperatures (higher than the critical temperature of Debye) the conductivity is inversely proportional to the absolute temperature T. On the other hand, the theory shows also that the thermoelectric forces increase proportional to the absolute temperature. Both results are in good agreement with the experiments in the restricted temperature range accessible to the latter. The product $\sigma\Delta\omega$ is therefore approximately independent of temperature and we may, in a very rough approximation, use its value at room temperature.

Next, we take into account the pressure effect. The pressure in the earth's core is of the order of several million atmospheres. Since the pressures measured by Bridgman go up to about 10^4 atmospheres, any extrapolation is extremely difficult. We can, however, obtain some information about the pressure dependence of the conductivity in a semi-theoretical way: The conductivity may be expressed as $\sigma=C\Theta^2/T$ where C is a constant which depends on the form of the electronic motions in the metal, and Θ is the critical temperature of Debye. There is good reason to believe that C, although it might change with pressure, does not alter its order of magnitude and we may therefore disregard the dependence of C on pressure. The Debye temperature can be expressed as[14]

$$\Theta=(h/k)(3n/4\pi)^{\frac{1}{3}}\cdot u,$$

where h and k are Planck's and Boltzmann's constants, respectively, n is the number of atoms per cm^3 and u is the velocity of longitudinal sound waves. Neglecting the small variation with the cube root of the density, we see that the Debye temperature is proportional to the velocity of sound. Now the mean velocity of longitudinal waves in the earth's core is of the order of 10 km/sec., which is about twice the value of the velocity of sound in iron under ordinary conditions. We may therefore assume a value for the conductivity of the earth's core which is about four times that of the ordinary conductivity of iron.

Still to be estimated is the influence of the pressure upon the thermoelectric forces. This is

[13] See for instance: H. Fröhlich, *Elektronentheorie der Metalle* (Berlin, 1936).

[14] A. Sommerfeld and H. Bethe, *Handbuch der Physik*, Vol. 24 (second edition), Part II, p. 502, 521.

extremely difficult, since the variation with pressure seems to be very complicated, both experimentally[15] and theoretically. The available data are scarcely adequate to permit an extrapolation to extremely high pressures. On the other hand, we may gather from the theory of electronic conduction that most probably there is no change in order of magnitude of the thermoelectric forces at high pressures. Since the elementary theory of conductivity gives the right order for the usually observed thermoelectric potentials, we may be justified in giving $\Delta\omega$ a value which is representative of the ordinary thermoelectric potentials, say 10^{-5} volt per degree.

One might object to the previous estimates on the basis that the earth's core is a liquid, rather than a solid body. It is known, on the other hand, that neither the thermoelectric forces nor the conductivity of a metal change their order of magnitude during the melting process. The change to be expected must be very much smaller under the extreme pressure in the earth's core than it is under ordinary pressures, and it appears quite negligible compared to some other uncertainties involved.

If we now take $\Delta T = 10°$ which seems a sufficiently low estimate and $L = 3\times10^{7}$ cm, we obtain by substitution of the numerical values in (14)

$$I = 1.5\times10^{-6} \text{ amp./cm}^2.$$

This has to be compared with the current which is required to produce the terrestrial field. The magnetic moment of the earth is $M = 8.2\times10^{25}$ electromagnetic units. If a solid sphere of radius R is completely filled with a current of homogeneous density I, so that the flow has everywhere the direction of the circles of latitude, the momentum produced is $M = (\pi^2/4)IR^4$. If for R we take the radius of the earth's core $R = 3.5\times10^{8}$ cm, the corresponding current density is found to be about $I = 2\times10^{-8}$ amp./cm^2. Since the current which actually contributes to the earth's magnetic momentum can only be a small excess of a current system with nearly random distribution, the thermoelectric currents must be much larger than the last mentioned value. The current estimated above is seventy-five times larger than the last one. A still somewhat larger value of the current might seem preferable, but in view of the extreme roughness of some of the estimates involved the numerical agreement appears rather satisfactory.

We might add here a few words about the magnetism of sunspots. It is well known that many sunspots are accompanied by magnetic fields which are often very strong and reach intensities of many thousand gauss. On the other hand, from the mechanical viewpoint a sunspot represents undoubtedly a vortex and we might therefore expect that the origin of its magnetic field is analogous to the one outlined above for the earth. At closer sight certain difficulties appear. It is readily seen by an inspection of formula (14) that the field which can be produced by thermoelectric forces is limited in intensity. The value assumed for the conductivity of the earth's core is rather high and it can scarcely be much higher for the sun. The order of magnitude of the thermoelectric forces is given. The temperature dependence of the two first factors in (14) cancels, as we saw above. We would therefore have to raise the order of magnitude of the other two factors in (14) by 10^4 which seems beyond the reach of possibility. We might on the other hand consider galvanic rather than thermoelectric forces, which would allow somewhat higher potentials. There is however a much more serious difficulty. For the building up of a magnetic field a finite time is required and, as is well known, the mean of this time for any circuit is equal to the inductance divided by the resistance of the circuit. For the earth, this leads to a period, roughly of the order of 10^8 years, required to build up the total magnetic field. The linear dimensions of the sunspots are comparable to those of the earth, but on account of the larger inductance of the sun we might expect the time to be even longer. On the other hand, sunspots have a lifetime of only a few months. This is a very serious contradiction and it appears that the thermoelectric mechanism as outlined above breaks down completely if applied to sunspots. We must rather look for a very low value of the conductivity and extremely high values of the electromotive forces. This at once suggests a location for the currents which

[15] P. W. Bridgman, reference 12, Chap. 10.

produce the sunspot magnetism, namely, in the upper layers of the sun's atmosphere. It can scarcely be doubted that extremely high electric space charges can develop there by the effect of variations in light pressure and ionization. It is known that the small *external* magnetic field of the earth is due to currents in the higher parts of the earth's atmosphere.[2] It seems probable, therefore, that the proportion of the external and internal field is the reverse for sunspots as it is for the earth and that the sunspot field is mainly of an external, atmospheric origin. This being stated, we may expect the *primary* causes of the field to be the same as assumed above, namely, differences in temperature and state of aggregation exhibiting a typical asymmetry due to the action of the Coriolis force. These differences need not be located only in the higher atmospheric layers where the electric currents flow, but may arise in the lower and denser layers of the photosphere. They may then be transmitted to a higher level by local variations in intensity and composition of the radiation which flows upwards from these layers.

MARCH 1, 1939 PHYSICAL REVIEW VOLUME 55

Thermal Vibrations and Atomic Structure of Zinc Crystals at 100° and 298°K

G. E. M. JAUNCEY AND E. M. McNATT
Wayman Crow Hall of Physics, Washington University, St. Louis, Missouri

(Received January 16, 1939)

The diffuse scattering of x-rays from single crystals of zinc has been investigated over a greater range of angles of scattering than in previous experiments. As a result of this more extended study, the root-mean-square displacements of the crystal atoms at $T=100°$K are 0.098 and 0.050A for orientation angles of 0° and 90°, respectively. At the melting point of zinc it is likely that the root-mean-square displacement in a given direction is not more than 8 percent of the axial distance in the same direction. The atomic structure factors at a scattering angle of 90° are somewhat larger than would be expected on quantum-theoretical grounds. At large scattering angles the curves of the intensity of the scattered rays approach each other irrespective of temperature or orientation, the intensity approaching that of x-rays scattered from a gas of zinc atoms.

1. INTRODUCTION

THE senior author and others[1] have investigated the atomic structure and vibrations in single zinc crystals at various temperatures and angles of orientation by means of diffuse scattering. However, although temperatures of 100°, 200°, 298°, 370° and 550°K and orientations of 3° and 90° were used, only one angle of scattering—namely, 30°—was used for temperatures other than 298°K. Further, even at room temperature the scattering angles were restricted to the range 15° to 40°. Hence, it was believed desirable to extend the investigation to a greater range of scattering angles.

In order to confine the present investigation to reasonable limits, the scattering angles used were in the range 15° to 90°, the temperatures were 100°K and 298°K, and the crystal orientations were nearly 0° and nearly 90°. With the exception of a cryostat for the low temperature work which has been described elsewhere,[2] the apparatus and method used were essentially those of the previous papers. The spectral distribution was that shown in Fig. 2 of Jauncey and Bruce's paper.[1]

2. EXPERIMENTAL RESULTS

We make use of the experimental quantity[3]

$$(S\rho/\mu)_{\text{exp}} = \frac{4R^2Wm^2c^4}{ANZe^4(1+\cos^2\phi)} \frac{D(\phi,\theta)}{D_0u(\phi,\theta)}, \quad (1)$$

[1] G. E. M. Jauncey and W. A. Bruce, Phys. Rev. **51**, 1067 (1937); W. A. Bruce and E. M. McNatt, Phys. Rev. **51**, 1065 (1937). See these papers for earlier references.

[2] E. M. McNatt, Rev. Sci. Inst. **10**, 42 (1939).

[3] G. E. M. Jauncey and W. A. Bruce, Phys. Rev. **50**, 413 (1935); G. E. M. Jauncey and W. D. Claus, Phys. Rev. **46**, 941 (1934).

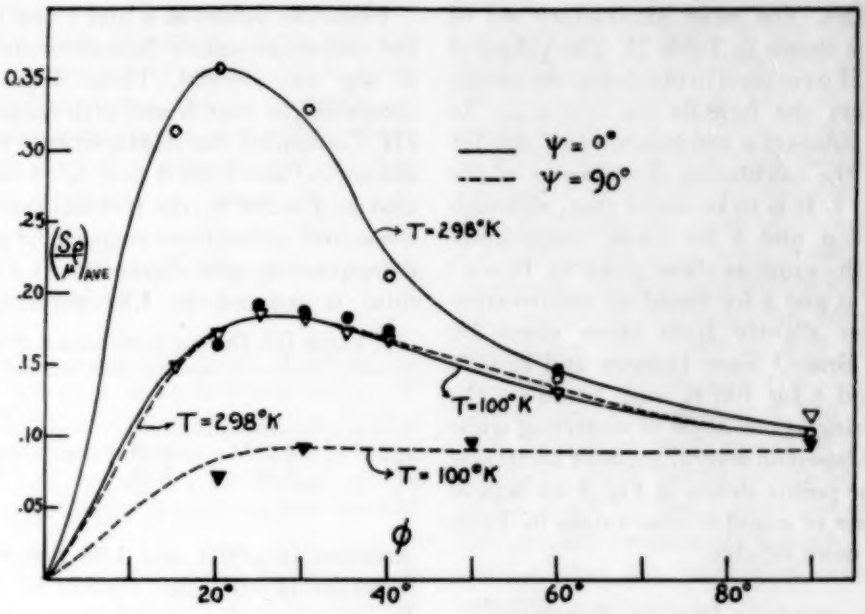

FIG. 1. Diffuse scattering of x-rays of average wave-length 0.44A from single zinc crystals.

where $D(\phi, \theta)$ and D_θ are, respectively, the ionization currents produced by the scattered and the primary rays, and where

$$u(\phi, \theta) = \frac{2 \sin (\phi - \theta)}{\sin (\phi - \theta) + \sin \theta}, \qquad (2)$$

ϕ is the scattering angle, θ is the angle between the primary rays and the surface of the crystal, R is the distance of the ionization chamber window from the axis of the spectrometer, A is the area of the chamber window, W the atomic weight of the crystal, and N, Z, e, and m have their usual meanings.

The experimental values of $(S\rho/\mu)_{exp}$ are shown as points in Fig. 1. The white circles represent values for the orientation angle $\psi = 0°$, $T = 298°$K, the black circles represent values for $\psi = 0°$, $T = 100°$K, the white triangles represent values for $\psi = 90°$, $T = 298°$K, and the black triangles values for $\psi = 90°$, $T = 100°$K.

The theoretical quantity $(S\rho/\mu_1)_{th}$ has previously been defined.[4] This quantity is a function of the true atomic structure factor and of the components of the atomic vibrations in a direction which bisects the angle between the direction of the scattered rays and the backward direction of the primary rays. The angle between the direction of these components and the c axis of the zinc crystal is the orientation angle ψ. According to Zener[5] the mean square of the displacements due to these components is related to the orientation angle ψ by

$$\langle u_\psi^2 \rangle_{Av}^{\frac{1}{2}} = \{(a \cos^2 \psi + b \sin^2 \psi)/8\pi^2\}^{\frac{1}{2}}, \qquad (3)$$

where $a/8\pi^2$ and $b/8\pi^2$ are the mean square displacements due to the components of the vibrations in the directions $\psi = 0°$ and $\psi = 90°$, respectively. Bruce[6] has described the method of analysis for determining the true atomic structure or f values from the measurements of the diffuse scattering. The f values shown in Table I for the range $(\sin \frac{1}{2}\phi)/\lambda = 0.1$ to 1.0 A^{-1} are due to Bruce.[6] The f values for $(\sin \frac{1}{2}\phi)/\lambda$ above 1.0 A^{-1} were obtained by us with the method of analysis described by Bruce.[6] It is also necessary to know

TABLE I. *True atomic structure factors for zinc.*

$(\sin \frac{1}{2}\phi)/\lambda$	0.1	0.2	0.3	0.4	0.5	0.6	0.8	1.0	1.3	1.6	1.9	2.2
f for $\psi = 0°$	27.0	23.5	20.2	17.0	14.4	12.5	9.5	7.3	5.5	4.5	3.8	3.5
f for $\psi = 90°$	28.4	25.9	21.5	18.2	14.9	"	"	"	"	"	"	"

[4] G. E. M. Jauncey and W. A. Bruce, Phys. Rev. **51**, 1062 (1937).

[5] C. Zener, Phys. Rev. **49**, 122 (1936).

[6] W. A. Bruce, Phys. Rev. **53**, 802 (1938).

the ΣE_r^2 values. The most satisfactory set of these values is shown in Table II. The values of Tables I and II were used in obtaining the curves of Fig. 1 from the formula for $(S\rho/\mu_1)_{th}$. In addition, the values of a and b shown in Table III were used in the calculation of ordinates of the curves in Fig. 1. It is to be noted that, although the values of a and b for room temperature (298°K) are the same as those given by Bruce,[6] the values of a and b for liquid-air temperature (100°K) differ slightly from those given by Jauncey and Bruce.[1] Since Jauncey and Bruce's value of a and b for 100°K were based on the diffuse scattering at one angle of scattering while our values are based on several angles of scattering as seen by the points shown in Fig. 1 we believe that our values of a and b—the values in Table III—are the more reliable.

3. Displacements Due to Thermal Vibrations

We feel that the experimental points shown in Fig. 1 fall reasonably well upon the theoretical curves shown in the same figure. Further, the experimental points fall pretty well on the theoretical curves out to a scattering angle of 90°. This causes us to feel that the values given in Tables I, II, and III are reasonably reliable. We should point out, however, that in calculating the curves of $(S\rho/\mu_1)_{th}$ for Fig. 1 we have not made correction for the Compton effect at large scattering angles such as 90°. Such a correction would lower each curve by about 0.008 in the units shown on the scale of ordinates of Fig. 1. However, the intensity of the diffuse scattering at $\phi=90°$ is small so that the error in the experimental points at this angle is somewhat large and of the same order as the correction for the Compton effect.

Table II. *Values of ΣE_r^2 for zinc.*

$(\sin\frac{1}{2}\phi)/\lambda$	ΣE_r^2	$(\sin\frac{1}{2}\phi)/\lambda$	ΣE_r^2
0.0	30.0	0.8	6.3
0.1	24.8	0.9	6.2
0.2	19.0	1.0	5.2
0.3	14.7	1.3	3.2
0.4	12.5	1.6	2.5
0.5	10.4	1.9	2.2
0.6	9.4	2.2	2.0
0.7	7.3		

From the values of a and b can be calculated the root-mean-square displacements of the atoms in the zinc crystal. These displacements are shown in the fourth and fifth columns of Table III. Comparing the displacements with the axial distances,[7] $a_0=2.657$A and $c_0=4.948$A, we note that at $T=298$°K, the thermal displacements in the a_0 and c_0 directions are each 3.5 percent of the corresponding axial distances. At $T=100$°K, the ratio is reduced to 1.88 percent for the a_0 direction ($\psi=90°$) and 1.98 percent for the c_0 direction ($\psi=0°$). At $T=550$°K, Jauncey and Bruce[1] obtained $a=6.20$A from which the root-mean-square displacement is 0.280A or 5.65 percent of the c_0 distance ($\psi=0°$). At the melting point (692°K) it does not seem likely that the ratio of displacement to axial distance will exceed 8 percent.

Table III. *Thermal displacements of zinc atoms.*

T	a	b	$\langle u_\psi^2\rangle_{Av}^{\frac{1}{2}}$ $\psi=0°$	$\psi=90°$
100°K	0.75A²	0.20A²	0.098A	0.050A
298	2.34	0.68	0.172	0.093

4. Structure Factors at Large Angles

In an element like zinc ($Z=30$) we believe that at $(\sin\frac{1}{2}\phi)/\lambda=2.2\ A^{-1}$ the contributions to the atomic structure factor come only from the K and L electrons. At this value of $(\sin\frac{1}{2}\phi)/\lambda$, $f=3.5$, and $\Sigma E_r^2=2.0$. If as an approximation we assume that the contribution of each K electron to f is E_K and that of each L electron is E_L, we then have the two equations

$$2E_K+8E_L=3.5, \tag{4}$$

$$2E_K^2+8E_L^2=2.0. \tag{5}$$

Solving these we obtain $E_K=0.905$ and $E_L=0.211$. For a hydrogen-like atom

$$E_K=1/(1+4\pi^2\gamma_K^2x^2)^2, \tag{6}$$

where $x=(\sin\frac{1}{2}\phi)/\lambda$ and γ_K is a parameter. Putting $E_K=0.905$ and $x=2.2$ in (6), we obtain $\gamma=0.0162$A. The quantity γ_K corresponds to the radius of the K orbit in the Bohr model of the atom. For $Z=30$, the radius of the Bohr model is $0.53/30=0.0177$A.

[7] See R. W. G. Wyckoff, *The Structure of Crystals* (Chemical Catalog Co., 1931), second edition, p. 207.

A similar expression to (6) can be worked out for the L electrons. However, there are two types of L electrons, the $2s$ and the $2p$ electrons. The wave functions for the L electrons are given by quantum mechanics.[8] From these the E_r value for each kind of L electron may be calculated from the formula

$$E_r=\int_0^\infty u(r)\frac{\sin kr}{kr}dr, \tag{7}$$

where $k=(4\pi \sin \frac{1}{2}\phi)/\lambda$ and $u(r)dr$ is the probability of the electron being between spheres of radii r and $r+dr$. The formulas for the E_r's so obtained contain a parameter γ. If it is assumed that γ is the same for each type of electron, the formulas may be added so as to give

$$f_L=2E_{2,0}+6E_{2,1}=8(1-y)(1-y/2)(1+y)^{-4}, \tag{8}$$

where

$$y=(16\pi^2\gamma_L^2 \sin^2 \tfrac{1}{2}\phi)/\lambda^2. \tag{9}$$

Now at $(\sin \frac{1}{2}\phi)/\lambda=2.2$, $f_L=8\times 0.211=1.688$. Solving (8) for y, we obtain $y=0.30$. From (9) this gives $\gamma_L=0.020$A. The radius of the L orbit in the Bohr model of a hydrogen-like atom ($Z=30$) is $(4\times 0.53)/30=0.071$A. With a screening constant of about 6 this radius would be $(4\times 0.53)/(30-6)=0.088$A. The discrepancy between $\gamma_L=0.020$A and 0.071 or 0.088A is too great. Putting it another way, if we make $\gamma_L=0.088$A in (9) and then calculate from (8), we obtain $f_L=0.232$ so that $f=f_K+f_L=2.140$. Our experimental value $f=3.5$ is thus considerably larger than what would seem to be a reasonable value of f on theoretical grounds. We have carefully repeated the diffuse scattering experiment at $\phi=90°$ several times but we consistently obtain values of $(S\rho/\mu)_{exp}$ which necessitate high values of f. Our results require that f decrease more slowly at high values of $(\sin \frac{1}{2}\phi)/\lambda$ than would otherwise be expected. Either the K or the L electrons or both are on the average concentrated more closely to the nucleus than on theoretical grounds we had expected.

In Fig. 1 it is interesting to note that all curves and points approach each other closely at $\phi=90°$. At large angles the effect of the atomic vibrations becomes negligible and the zinc crystal scatters x-rays in the same way as gaseous zinc atoms would scatter the rays.

In conclusion we wish to thank Mr. J. E. Nafe for assistance in the calculation of the curves in Fig. 1.

[8] See L. Pauling and E. B. Wilson, *Introduction to Quantum Mechanics* (McGraw-Hill Book Co., 1935), pp. 134, 135.

MARCH 1, 1939 PHYSICAL REVIEW VOLUME 55

An Attempt to Observe the Absorption of Neutrinos

H. R. CRANE
University of Michigan, Ann Arbor, Michigan
(Received January 10, 1939)

IT HAS been quite conclusively demonstrated[1] that the presence of neutrinos cannot be detected by an ionization effect, of the kind which results from the passage of charged particles, neutrons or gamma-rays through matter. At least one possibility of detecting them remains, however, and that is by a process which is the reverse of the K-electron capture process. An example of this is

$$Cl^{35}+\mu \rightarrow S^{35}+e^+.$$

The product S^{35} is a radioactive isotope (as would be true of the product in general), and decays back to Cl^{35} with the emission of a negative electron and a neutrino:

$$S^{35}\rightarrow Cl^{35}+e^-+\mu.$$

Adding the equations we see that the energy of

[1] M. E. Nahmias, Proc. Cambridge Phil. Soc. **31**, 99 (1935).

the neutrino producing the transformation must be greater than $2mc^2+W_0$, where W_0 is the upper limit of the beta-ray spectrum of the radioactive isotope produced. The process is a cyclic one, in which nothing but the creation of electron pairs is accomplished.

A rough estimate for high energies on the basis of the Fermi theory of the cross section for the above effect has been made for me by Professor G. Breit, and is $\sigma \sim 10^{-46}(E_\nu/mc^2)^2$. This indicates that neutrinos of cosmic-ray energies are readily absorbed, but that those of only a few Mev will not be absorbed in a detectable amount. It is possible to perform an experiment which will test for a cross section as small as 10^{-38} cm^2, and it has seemed to me worth while making such a test, in spite of the fact that the theory predicts a much smaller cross section. The experiment is of interest especially because the results have an application in astrophysics.

S^{35} is a radioactive isotope whose half-life is 80 days and whose beta-ray spectrum has an upper limit of about 0.3 Mev.[2] The minimum energy of neutrino which can transform Cl^{35} into S^{35} is therefore 1.3 Mev, a value well within the range of energy of neutrinos emitted from mesothorium and its products. In an attempt to transform Cl^{35} into S^{35} I placed a capsule containing one mC of MsTh and its products in the center of a bag containing three pounds of NaCl. After 90 days of irradiation I extracted the sulphur[3] and measured its activity in an ionization chamber which was capable of detecting the emission of 10 electrons per second. No measurable activity was found. By taking into account the large factor by which the sulphur was concentrated in the chemical separation, it appears that a cross section of 10^{-30} cm^2 for the absorption of neutrinos by Cl^{35} could have been detected. This is based upon the estimate that 3×10^7 neutrinos of energy greater than 1.3 Mev (the threshold energy for the transformation) are emitted per second from the source used.

The way in which this result applies to an astrophysical question is as follows. On the basis that nuclear transformations of the familiar kind constitute the energy source, and that hydrogen is the main building material, we suppose that a star generates about six percent of its energy in the form of neutrinos. When a proton is added to a nucleus about eight Mev energy is liberated, on the average. Since in all the nuclei built up the atomic weight is roughly twice the atomic number, we can assume that at least half the proton additions must have been followed by the emission of a positron and a neutrino. If the average energy of the neutrinos is taken as one Mev, we have about six percent for the fraction of the energy which is generated in the form of neutrinos. Although calculations of the energy flux or heat transport within a star have not reached this degree of refinement, it is nevertheless interesting to know whether the neutrinos escape from the center of the star without further collision with matter, or whether they constitute a rapid means of transport of part of the star's energy from the core to the outer regions.

The question of whether the absorption process under discussion is great enough to prevent the escape of neutrinos from the sun can be decided by performing the experiment described, with 1000 mC of radioactive material, either mesothorium or radium (with products). This will detect a cross section of 10^{-33} cm^2. In a column of the sun's matter one cm^2 in cross section, extending from the center to the surface, there are about 2×10^{33} atoms (average atomic weight assumed to be that of air). There are considerably less than 2×10^{33} atoms which are as favorable as Cl^{35} for the neutrino absorption process. We can therefore say with some confidence that if the process is not detected in the laboratory, it will not be of importance in the question of the escape of neutrinos from the sun.

[2] E. B. Andersen, Zeits. f. physik. Chemie **32**, 237 (1936); M. S. Livingston and H. A. Bethe, Rev. Mod. Phys. **9**, 359 (1937).

[3] The salt was dissolved in water and H_2O_2 added to oxidize the sulphur (which may have existed in various degrees of oxidation) to the sulphate form. The sulphate was precipitated as barium sulphate. No sulphate carrier was added because the NaCl already containd a trace of sulphate as an impurity.

LETTERS TO THE EDITOR

Prompt publication of brief reports of important discoveries in physics may be secured by addressing them to this department. Closing dates for this department are, for the first issue of the month, the eighteenth of the preceding month, for the second issue, the third of the month. Because of the late closing dates for the section no proof can be shown to authors. The Board of Editors does not hold itself responsible for the opinions expressed by the correspondents.

Communications should not in general exceed 600 words in length.

The East-West Asymmetry of the Cosmic Radiation at Very High Elevations Near the Equator

In order to obtain further evidence as to the nature of the primary cosmic rays associated with the soft component we have made a series of balloon flights near the equator with directionally selective recording instruments for determining the east-west asymmetry at very high elevations. The asymmetry at sea level leads almost inevitably to the conclusion that the primaries producing the hard component must be heavy positive particles such as protons.[1] On the other hand the success of the multiplicative theory in accounting for the transition effect in the upper atmosphere is circumstantial evidence that the primaries of the soft component are electrons. Such an electron component, if it is to satisfy the condition of an equilibrium of potential at the cosmic-ray source and at the same time preserve the neutrality of interstellar space, must consist of an equal number of positives and negatives and there would be no asymmetry of the soft component. If, on the other hand, the primaries of the soft component were protons a very considerable asymmetry would be expected; a western intensity of the order of eight times the eastern can be predicted at the elevations attained on these flights if one makes use of an extrapolation of the energy distribution of the primary rays deduced from the latitude effect.[2] Thus comparatively crude asymmetry measurements should enable one to distinguish between primary protons and electrons.

Each instrument carried by the balloons consisted of a triple coincidence train of Geiger-Mueller counters inclined 60° from the vertical, a barograph and a radio transmitter. The signals were automatically recorded on a paper tape at the receiving station and it was unnecessary to recover the balloons. Cosmic-ray coincidences were transmitted as "dots" whereas the barometric pressure was determined from the spacing of a pair of "dash" signals keyed at ten-second intervals by the rotation of a small motor.[3] A third contact from the motor was in series with a half-shaded photo-cell and this signal was transmitted only on those cycles when the photo-cell was exposed to the direct rays of the sun, thus indicating the orientation of the counter train. The instrument was carried by two strings of balloons attached to either end of a long horizontal bar and the entire rigging was rotated in azimuth by a pair of vanes acted upon by the air currents associated with the ascent. The instrument turned somewhat irregularly at speeds varying from one-half to three revolutions a minute at the take off and at lower speeds at the top of the flight. Ten flights of this type were sent up from the Barro Colorado Island Laboratory of the Institute for Research in Tropical America, located in the Panama Canal Zone, and complete records were obtained from five of these. The results are summarized in Table I, which contains the data from the portions of the records for which the atmospheric depth was less than one and one-half meters of equivalent water. At this depth the cosmic radiation entrant from the chosen zenith angle has its intensity maximum. The numbers of counts for each interval of the record have been corrected for the variation of intensity with elevation and the figures represent an average of the counting rates for the upper portion of the flight, the minimum depths of which are indicated in the table.

TABLE I. *Data from counters at atmospheric depths less than one and one-half meters of equivalent water.*

Flight Number	Minimum Depth Meters of Water	East			West			r_w/r_e
		Counts	Time Rate Min.	r_e	Counts	Time Rate Min.	r_w	
110	0.40	1091	14.6	75	1685	18.5	91	1.21
112	0.45	133	5.0	26.6	283	7.2	39.4	1.54
113	0.60	254	9.1	28	409	12.4	33	1.18
115	0.50	472	11.8	40	973	18.3	53.2	1.33
B	0.33	478	13.3	36	736	18.0	41	1.14
Total		2428	53.8	45	4086	74.4	55	1.22

The ratios of the western to eastern intensities are given in the last column of the table from which it is noted that the average western excess is 22 percent. This is not as great as would have been expected if the primaries were all protons but indicates that about ten percent of the high elevation intensity is produced by unbalanced positives. This may very well represent the part of the high elevation intensity attributable to the hard component. The soft component would then be made up of equal numbers of positive and negative electrons.

These studies have been carried out under a grant from the Carnegie Institution of Washington. We wish also to acknowledge the cooperation of Mr. James Zetek, Director of the Barro Colorado Laboratory, and of Colonel S. B. Akin of the U.S.A. Signal Corps.

T. H. JOHNSON
J. G. BARRY

Bartol Research Foundation of the Franklin Institute,
Swarthmore, Pennsylvania,
February 14, 1939.

[1] T. H. Johnson, Phys. Rev. **54**, 385 (1938).
[2] T. H. Johnson, Rev. Mod. Phys. **10**, 193 (1938).
[3] T. H. Johnson and S. A. Korff, Rev. Sci. Inst. **11**, 82 (1939).

Electrical Discharge Between a Stationary and a Rotating Electrode

A visual and photographic study has been made of electrical discharges between a stationary and a rapidly rotating electrode in dry air at reduced pressure. The rotating electrode was a 4″ solid tapered disk made of Duralumin ST14 mounted on the flexible shaft of an inverted vacuum-type ultracentrifuge, which has been previously described.[1] The usual metal vacuum chamber was replaced by one of glass, with a brass electrode mounted in the side of the wall, as shown in the photographs. The gas pressure could be varied from atmospheric down to the vapor pressure of the vacuum-pump oil, and the rotational speed of the electrode was limited only by the bursting strength of the rotor in the gas pressure range used (maximum peripheral speed of 7.5×10^4 cm/sec.). Contact to the rotor was made outside the vacuum chamber by dipping the end of the supporting shaft into a metal cup containing concentrated $CuSo_4$. Fig. 1 shows nonoscillating discharges of a 0.5-microfarad condenser with a spark gap (2.8 mm), 350-ohm resistance, and the two electrodes in series. The air pressure in the vacuum chamber was 1.4 cm Hg and the periphery of the rotor was moving 4×10^4 cm/sec. In addition to the light from the discharge, the apparatus was illuminated by auxiliary light to bring out the details of the electrodes and vacuum chamber. Fig. 1A shows a single discharge when the rotating electrode was anode, while Fig. 1B shows a single discharge when the rotating electrode was cathode.

In Fig. 1B it will be observed that the luminous column is carried around the periphery of the rotor. For a given discharge circuit and gas pressure, the length of this column is approximately proportional to the rotational speed. For example, we have observed this length to increase from a very slight displacement to approximately the circumference of the rotor as the rotational speed is increased. After stopping the rotor, it was found to have roughly circular pitts on its surface, which we interpret as cathode spots of the single discharges. None of the pitts were elongated into lines, indicating that the cathode spot remained fixed on the rotor surface as it moved.

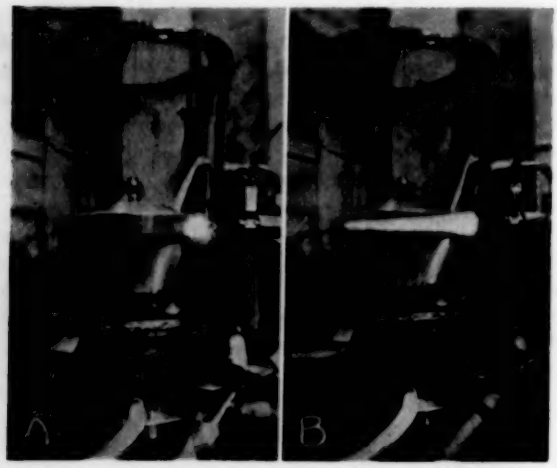

FIG. 1. Discharge between a stationary and rapidly rotating electrode. A, Rotating electrode as anode. B, With rotating electrode as cathode.

On the other hand, when the rotating electrode was the anode, only a comparatively small displacement was observed. While a more detailed report of these experiments will be made later, it is apparent that the difficulty of moving the cathode spot on the rotor surface is much greater than the resistance to the extension of the discharge length in this type of discharge.

J. W. BEAMS
L. B. SNODDY

Department of Physics,
University of Virginia,
Charlottesville, Virginia,
February 4, 1939.

[1] J. W. Beams and F. W. Linke, Rev. Sci. Inst. **8**, 160 (1937); J. App. Phys. **8**, 795 (1937).

On the Shape and Stability of Heavy Nuclei

The surface energy of a nucleus has its minimum value for the spherical shape if nuclear matter is assumed to behave like an incompressible fluid. Under the same assumption, the Coulomb energy is larger for the spherical shape than for any nearly spherical distribution. A heavy nucleus in its normal state will take the form of a sphere if for any small departure from sphericity the increase in surface energy is greater than the decrease in Coulomb energy.

To obtain a quantitative condition for the stability of the spherical shape I calculate the surface and Coulomb energies of a nucleus bounded by the ellipsoidal surface

$$x^2+y^2+(z/a)^2=R^2/a^{\frac{1}{3}}. \tag{1}$$

A sphere of radius R has a volume equal to that enclosed by the surface (1). For the sphere the energies are

$$E_s^0=\gamma A^{\frac{2}{3}}\ \text{(surface)}, \tag{2}$$

$$E_c^0=\frac{3}{5}\frac{Z^2e^2}{R}\ \text{(Coulomb)}.$$

The calculation yields

$$E_s=E_s^0\{1+8/45\ (a-1)^2+\cdots\}, \tag{3}$$
$$E_c=E_c^0\{1-4/45\ (a-1)^2+\cdots\}.$$

A necessary condition for stability against small departures from the spherical shape is

$$2E_s^0/E_c^0>1. \tag{4}$$

The quantities γ and R have been determined by fitting a semi-empirical energy formula[1] to the experimental mass defects[2] in the mass range $100\leqq A\leqq238$. One finds

$$\gamma=26\ mc^2, \tag{5}$$
$$R=1.39\times10^{-13}A^{\frac{1}{3}}\ \text{cm}$$

and

$$E_c^0=1.22\ Z^2/A^{\frac{1}{3}}mc^2, \tag{6}$$
$$2E_s^0/E_c^0=42.6\ A/Z^2.$$

Values assumed by the quantity $2E_s^0/E_c^0$ are given in Table I. The stability condition is satisfied for all known nuclei.

TABLE I.

Nucleus	$_{24}C^{50}$	$_{44}Ru^{100}$	$_{62}Sm^{150}$	$_{80}Hg^{200}$	$_{92}U^{238}$
$2E_s^0/E_c^0$	3.70	2.20	1.66	1.33	1.20

Recently several laboratories[1] have reported experiments showing that the uranium nucleus when activated by the capture of a neutron can explode into two heavy parts (possibly barium and krypton) and possibly a number of light particles (neutrons). The results stated in Table I suggest that the activation energy required to enable the uranium isotope to pass through the potential energy hill which stabilizes the state of spherical symmetry may well be only a few million volts. According to this picture the natural uranium isotopes and other heavy nuclei should explode occasionally when activated by bombardment with energetic gamma-radiation or charged particles.

EUGENE FEENBERG

New York University,
Washington Square College,
New York, New York,
February 14, 1939.

[1] H. A. Bethe and R. F. Bacher, Rev. Mod. Phys. **8**, 82 (1936), Eq. (182).
[2] A. J. Dempster, Phys. Rev. **53**, 869 (1938).
[3] O. Hahn and F. Strassmann, Naturwiss. **27**, 11 (1939). Also reported by Meitner and Frisch and verified at Columbia University and elsewhere according to current newspaper accounts.

Ferromagnetic Anisotropy in Nickel-Iron Crystals. Evidence for Superstructure near Ni_3Fe

Evidence for the existence of superstructure in nickel-iron alloys at about Ni_3Fe has been offered by Kaya.[1] Long distance order has not been found in this range by Haworth.[2] Precise measurements, herein reported, on the ferromagnetic anisotropy of single-crystal spheroids of critical compositions, seem best explained by short distance order.

The method used is that developed in this laboratory,[3] with changes in apparatus and technique which permitted greater precision.

A spheroid with 75 percent by weight of nickel and 25 percent of iron was, as nearly as could be measured, magnetically isotropic when rapidly cooled in vacuum after about half an hour at 750°C, as shown in curve A in Fig. 1. After reheating this spheroid to 600°C, lowering its temperature 20° a day for 5 days and to 450° in the next 15 days, it had, at room temperature, the anisotropy shown in curves B. Five days more at 430°C produced no further change. A second heating to 750°C, again followed by rapid cooling, restored the isotropic state (curve A).

A spheroid with 70 percent by weight of nickel and 30 percent of iron was similarly treated. In the rapidly cooled state the direction of easiest magnetization was [100], followed by [111] and [110] in that order. In the state following 22 days baking between 500°C and 430°C the direction of easiest magnetization was [111], followed by [110] and [100] in that order. It is therefore probable that at some rate of cooling almost complete isotropy could be established in crystals of this composition.

The two specimens just mentioned were from stock kindly furnished by the Bell Telephone Laboratories some

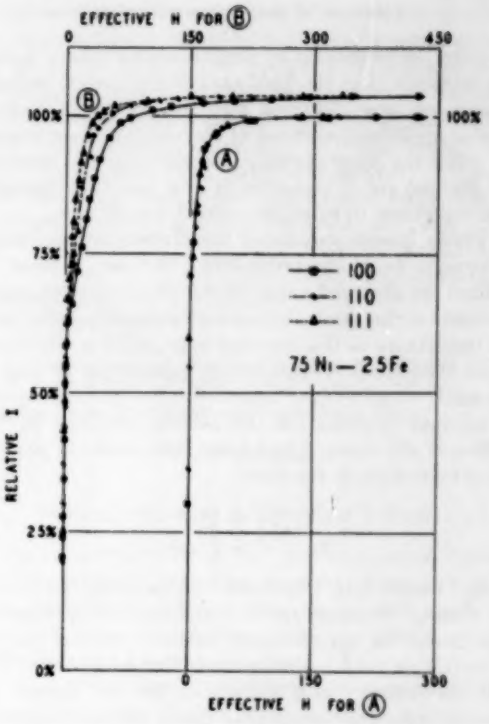

FIG. 1

years ago. The spheroids of J. D. Kleis were made from this stock. The results he reported[4] are similar to those here reported for quickly cooled specimens. Measurements on other compositions are in progress.

Besides the changes in directional properties we have to report that the saturation magnetization for all directions is raised in this range of composition by low temperature baking. The change in the 75 percent spheroid was about three percent, in the 70 percent spheroid about two percent. The reversibility of this change has been checked in the 75 percent spheroid.

It is noted that the change in anisotropy is consistent with the effect of ordering calculated by one of us.[5] The occurrence of zero anisotropy in the neighborhood of 75 percent nickel was consistent with dependence of the first anisotropy constant (K_1) almost exclusively upon "quadrupole" magnetic interaction, and this term is decreased (algebraically) in this region, by passing from disorder to order. A change of K_1 from zero to a negative value was therefore to be expected at the transition point for disordered states.

L. W. MCKEEHAN
E. M. GRABBE

Sloane Physics Laboratory,
Yale University,
New Haven, Connecticut,
February 11, 1939.

[1] S. Kaya, Hokkaido Imp. Univ., J. Fac. Sci. **2**, 29–53 (1938).
[2] F. E. Haworth, Phys. Rev. **54**, 693–698 (1938).
[3] L. W. McKeehan, Rev. Sci. Inst. **5**, 265–268 (1934); L. W. McKeehan, R. G. Piety and J. D. Kleis, Rev. Sci. Inst. **7**, 494–497 (1936).
[4] J. D. Kleis, Phys. Rev. **50**, 1178–1181 (1936).
[5] L. W. McKeehan, Phys. Rev. **52**, 18–30 (1937).

Lifetime of the Yukawa Particle

Recent investigations by various authors[1] have made it very probable that the hard rays of the cosmic radiation (mesotrons), now identified with the particle of Yukawa[2] of mass $\mu \sim 200m$ (m = mass of the electron), are unstable and will decay spontaneously into electrons and neutrinos. The lifetime for a mesotron at rest has been estimated from experience to be of the order $2\text{–}4\times10^{-6}$ sec.

Yukawa himself calculated the lifetime on the basis of his ideas to be of the order 0.25×10^{-6} sec., a result not far from the observed value. However, the present author[3] obtained on the same assumptions a much smaller value. The importance of this question may justify a restatement of the theoretical result and an explanation of this difference.

The final formulae for the lifetime obtained by both authors is the same, apart from differences in notation. It can be written in the form

$$\tau = \frac{G^2}{\hbar c} 4\pi^2 \left(\frac{m}{\mu}\right)^4 \frac{\hbar}{\mu c^2} \frac{1}{G_F^2} . \qquad (1)$$

In this formula $\hbar$, m, c have the usual meaning, and μ is the rest mass of the mesotron. G is the constant of dimension of a charge in the potential between nuclear particles $V(r) = (G^2/r)e^{-r\mu c/\hbar}$ following from Yukawa's theory. $G^2/\hbar c$ is of the order[3, 4] μ/M (M = mass of the proton) but probably somewhat larger than this quotient. The lifetime τ is therefore essentially proportional to μ^{-4}. G_F finally is the constant in Fermi's theory of β-decay, normalized to be a pure number. The form of interaction assumed for the coupling between proton, neutron and the electron neutrino field is

$$G_F mc^2(\hbar/mc)^3(\psi_N^* \beta \psi_P)(\varphi_\nu^* \beta \varphi_e) + \text{c.c.}$$

(ψ_N, ψ_P, φ_ν, φ_e being the wave functions of neutron, proton, neutrino and electron, respectively). This leads to the probability for emission of an electron of energy ϵ

$$w(\epsilon)d\epsilon = |M|^2 \frac{G_F^2}{(2\pi)^3} \frac{mc^2}{\hbar} \frac{(\epsilon_0 - \epsilon)^2(\epsilon^2 - mc^2)^{\frac{1}{2}}\epsilon d\epsilon}{(mc^2)^5} ,$$

where ϵ_0 is the maximum energy of the emitted electrons and M a matrix element from the motion of the heavy particles inside the nucleus.

The discrepancy in the calculated lifetimes comes from the different values used for the constant G_F. As discussed by Bethe and Bacher[5] and by Nordheim and Yost,[6] the experimental value of G_F depends quite appreciably on the group of elements which are taken for comparison, the difference being due in all probability to the matrix element M, which is smaller than unity for heavy elements but can be expected to be unity for light positron emitters. The value for G_F used by Yukawa (0.87×10^{-12} in our units) corresponds to the heavy natural radioactive elements, while the value deduced for the light positron emitters[6] is $G_F = 5.5\times10^{-12}$. It seems beyond doubt that this later value has to be taken for our purpose.

With the present most probable values $G^2/\hbar c = 0.3$; $\mu = 200m$; $G_F = 5.5\times10^{-12}$, we obtain from (1) $\tau = 1.6\times10^{-9}$ sec., i.e., a value about 10^{-3} times too small. A decrease in the assumed value for μ to $150m$ would increase τ only by a factor of order 3.

In view of this definite discrepancy the question arises whether any modifications of the theory could give a better result. It is to be noted firstly that the introduction of the Konopinski-Uhlenbeck form of the β-decay theory would only make matters worse as it would introduce roughly another factor $(m/\mu)^2$. A real improvement can only be expected by a complete reformulation of the theory. One possible suggestion would be to assume that the disintegration of a free mesotron is in first order approximation a forbidden transition, while in nuclei it is made allowed by the influence of the other nuclear particles.

L. W. NORDHEIM

Duke University,
Durham, North Carolina,
February 14, 1939.

[1] H. Euler and W. Heisenberg, Ergebn. d. Exakt. Naturwiss. (1938); P. Blackett, Phys. Rev. **54**, 973 (1938); P. Ehrenfest and A. Freon, J. d. Phys. **9**, 529 (1938); T. H. Johnson and M. A. Pomerantz, Phys. Rev. **55**, 105 (1939).
[2] H. Yukawa and others, I–IV, Proc. Phys. Math. Soc. Japan **17**, 58 (1935); **19**, 1084 (1937); **20**, 319, 720 (1938).
[3] L. W. Nordheim and G. Nordheim, Phys. Rev. **54**, 254 (1938).
[4] R. Sachs and M. Goeppert-Mayer, Phys. Rev. **53**, 991 (1938).
[5] H. Bethe and R. Bacher, Rev. Mod. Phys. **8**, 82 (1936).
[6] L. W. Nordheim and F. Yost, Phys. Rev. **51**, 942 (1937). It has to be noted that the formula for τ_0 on p. 943 should be $\tau_0^{-1} = (G_F^2/(2\pi)^3) \times (mc^2/\hbar)$. The value of G_F is then determined from the empirical value $\tau_0^{-1} \leqq 10^{-4}$.

The Scattering of Cosmic Rays by the Stars of a Galaxy

The problem dealt with in this note may be formulated in the following way: imagine a galaxy of N stars, each carrying a magnetic dipole of moment μ_n ($n = 1, 2, \cdots N$) and assume that the density, defined as the number of stars per unit volume, varies according to any given law, while the dipoles are oriented at random because of their very weak coupling. Under this condition the resultant field of the whole galaxy almost vanishes. Let there be an isotropic distribution of charged cosmic particles entering the galaxy from outside. Our problem is to find the intensity distribution in all directions around a point within the galaxy. Its importance arises from the fact that if the distribution should prove to be anisotropic a means would be available for determining whether cosmic rays come from beyond the galaxy, independent of the galactic rotation effect already considered by Compton and Getting.[1]

Suppose we consider a particle sent into an element of volume dV of scattering matter in a direction given by the vector R. Let the probability of emerging in the direction R' be given by a scattering function $f(R, R')$ per unit solid angle. Conversely a particle entering in the direction R' will have a probability $f(R', R)$ of emerging in the direction R. Let us assume that the scatterer (magnetic field of the star) has the reciprocal property so that $f(R, R') = f(R', R)$. In our case this property is satisfied provided the particle's sign is reversed at the same time as its direction of motion. That is, the probability of electron's going by any route is equal to the probability of positrons going by the reverse route. If it has the reciprocal property for each element of volume it will also have it for

any extended distribution of matter, that is, $F(R, P; R', P') = F(R', P'; R, P)$, where $F(R, P; R', P')$ is the probability that a particle going in the direction R at the point P will emerge in the direction R' at the point P'. This is because the probability of following any route is equal to the probability of following the reverse route, through the same elements of volume. Thus the probability of a certain end result from a number of possible routes will equal the probability of the reversal of the result occurring through the reverse routes.

In our case the scatterer (star) is to a large extent nonabsorbing and noncapturing. The former is true except for particles colliding with the star, which can only happen when their energy is sufficiently great, and the latter is true except for particles which follow asymptotic or periodic orbits in the magnetic field of any one of the N stars. These orbits, however, almost certainly form a set of zero measure in the manifold of all possible orbits,[2] that is, they occur only exceptionally. Thus, while a dipole magnetic field can imprison charged particles starting from a point within it and can also keep them away if starting from infinity, depending on their energy and angular momentum, it can only exceptionally capture such particles starting from infinity. In our case, therefore, all particles starting in a direction R at a point P, sufficiently far from all neighboring stars, have only a small chance of being either absorbed or captured in a periodic orbit (of finite or infinite period), so that the great majority of them will emerge at infinity. For almost all particles, therefore, the probability of emerging at infinity must be unity, or

$$\int_{R'} F(R, P; R', \infty)dR' = 1 \qquad (1)$$

almost always.

Now consider a beam of particles at infinity whose intensity in a direction R' is $I_\infty(R')$. The intensity at P observed in the direction R will be

$$I_p(R) = \int_{R'} F(R', \infty; R, P) I_\infty(R') dR'. \qquad (2)$$

Using (1) and assuming an isotropic distribution at infinity such that $I_\infty(R')$ is a constant (independent of R'), we find that Eq. (2) becomes

$$I_p(R) = I_\infty \int_{R'} F(R, P; R', \infty)dR' = I_\infty \qquad (3)$$

by (1). Therefore the intensity in any direction at P is the same and the distribution is isotropic at P if it is isotropic at infinity.

From the remark made previously, it is clear that if the distribution of positive and negative particles at infinity is isotropic, it will also be isotropic at any point P, except for small irregularities due to absorption by collision and by capture into periodic orbits. We conclude that particle scattering by magnetic fields of the stars is unable to contribute anything to the solution of the problem whether or not cosmic particles come from beyond our galaxy. The considerations developed in this note clearly hold so long as the scattering centers satisfy the conditions of being nonabsorbing and noncapturing, irrespective of the law of force which is responsible for the scattering. It need hardly be emphasized that they apply only to the case in which there is no resultant magnetic field for the whole galaxy, such as would exist if the dipoles were oriented along preferential directions. In this case particles would either be imprisoned if born within the galaxy, or kept out, if coming from outside, depending on their energy and angular momentum. The reciprocal property of paths would then break down in general, but would still hold for any allowed direction at any point within the galaxy.

M. S. VALLARTA
R. P. FEYNMAN

Massachusetts Institute of Technology,
Cambridge, Massachusetts,
February 15, 1939.

[1] A. H. Compton and I. A. Getting, Phys. Rev. **47**, 817 (1935). M. S. Vallarta, C. Graef and S. Kusaka, Phys. Rev. **55**, 1 (1939).
[2] See the discussion by E. J. Schremp, Phys. Rev. **54**, 153 (1938); and forthcoming papers by O. Godart and by A. Bančs, Jr.

Nuclear Excitation of Indium by X-Rays

It has been shown recently[1, 2] that the stable nucleus In^{115}, when excited by fast neutrons or protons, may be left in a metastable excited state, designated by In^{115*}, from which it decays, emitting negative electrons, with a half-life time of 4.1 hours.

We have now observed that the same metastable state can be excited when indium is irradiated by x-rays. The x-rays were produced by bombarding a 2-mm thick lead target with electrons from an electrostatic generator. A thick indium foil, 1 inch in diameter, was placed directly behind the lead target. After 30 minutes irradiation at an electron energy of 1.73 Mev and a current of 10 μa, the indium foil showed an initial activity, recorded on a Geiger-Müller counter, of 45 counts per minute. The activity decayed with a period of approximately 4 hours. The walls of the counter reduced the intensity of the rather soft β-rays to about one-half. Until more is known about the effective x-rays, no well-defined cross section can be deduced from these data.

By varying the bombarding voltage it was established that the effect has a threshold at 1.35 ± 0.1 Mev. This result might be interpreted by assuming that In^{115} has at that energy an excited state which combines both with the ground state and the metastable excited state.

In a note which has just become known to us Pontecorvo and Lazar[3] also report the excitation of indium by x-rays. In their experiments the x-rays were produced with an impulse generator working at a peak voltage of 1850 kv.

GEORGE B. COLLINS
BERNARD WALDMAN
EDWARD M. STUBBLEFIELD

Department of Physics,
University of Notre Dame,
Notre Dame, Indiana.

M. GOLDHABER

Department of Physics,
University of Illinois,
Urbana, Illinois,
February 15, 1939.

[1] Goldhaber, Hill and Szilard, Phys. Rev. **55**, 47 (1939).
[2] Barnes and Aradine, Phys. Rev. **55**, 50 (1939).
[3] Pontecorvo and Lazar, Compte rendus **208**, 99 (1939).

Electro-Optical Effects in Colloids

Recently the writer has repeated a few of Krishnan's experiments on the scattering of light in colloids. Most of his interesting results could be confirmed, but for the case of graphite sols our conclusions differ in one point. Contrary to his statement[1] the increase of the depolarization factor ρ_h in a magnetic field parallel to the direction of the incident light is due to a decrease of the component H_h while V_h remains constant. With this correction comparison with the theoretical predictions for the scattering in a strained glass[2] is somewhat improved. Changes of the depolarization factors which are similar to those for a graphite sol in a magnetic field can be produced also by electric fields. This effect is particularly large for a colloid of lead carbonate.

Since these effects depend on the anisometric form of the micelles it was expected that they should occur also in the sols of bentonite. However, neither a magnetic nor an electric field produces any noticeable changes of the scattering in these colloids if the incident light vibrates parallel or normal to the applied field. But a peculiar change of the Tyndall effect is observed when the incident light is polarized at 45° to the electric field. Observations normal to the plane of vibration of the incident light reveal a series of equi-distant dark regions along the path of the light beam. For observation normal to the plane of polarization these regions are light. The strayations are not visible in observations parallel or normal to the electric field. The distance between the regions decreases rapidly with increasing field strength and approaches a minimum value of about 2 cm for a field of 70 volt/cm a.c. in a sol with small particles (10 $\mu\mu$).

The origin of this effect is due not to a change of the scattering properties of the sol but to a change of the incident light. It is caused by an unusually large electro-optical effect in the bentonite sols. The scattering phenomenon is analogous to that used in the well-known demonstration experiment in which polarized light is passed through a sugar solution which contains some scattering matter, but in our experiment the effects are due to ordinary and not to circular birefringence.

Investigations of the transmitted light verify this conclusion. For fields up to 40 volt/cm a.c. this "Kerr" effect follows the law $\Delta n = n_0 K E^2$. The "Kerr" constant K is extremely large. For a concentrated sol we found $K = 1.2\ 10^{-3}$, i.e., the effect is 10^6 times larger than in nitrobenzene, 100 times larger than in Rochelle salt and 10 times larger than in the colloidal solutions of vanadium pentoxide.[3] For larger fields the birefringence approaches a saturation value which is so large that the two light components have a phase shift of 90° per cm. For d.c. voltage K is about twice as large as for 60-cycle a.c. An effect of the same order of magnitude exists also for high frequency fields (10^6 cycles).

It should be pointed out that the electro-optical effect in these colloids differs from the ordinary Kerr effect insofar as the birefringence does not vary with the period of the field but remains constant. When the field is removed the birefringence disappears gradually with a relaxation time of about 0.1 to 1 sec., depending on the concentration. In very viscous solutions it persists for hours. The relaxation time is of the same order of magnitude as in the experiments on streaming birefringence.[4] It appears therefore most probable that both effects have the same origin.

I am indebted to Professor Hauser and Dr. Le Beau for supplying the bentonite colloids.

HANS MUELLER

Massachusetts Institute of Technology,
Cambridge, Massachusetts,
February 13, 1939.

[1] R. S. Krishnan, Proc. Ind. Acad. Sci. **7**, 91 (1938).
[2] H. Mueller, Proc. Ind. Acad. Sci. **8**, 267 (1938).
[3] J. Errera, W. Overbeck and H. Sack, J. chim. Phys. **32**, 681 (1935).
[4] I. Langmuir, J. Chem. Phys. **6**, 873 (1938).

Note on Reduction for the Rotation Group

The reduction of a product representation of the rotation group into irreducible representations is important in many physical problems. If U_m, $V_{m'}$ form the basis vectors of irreducible representations of rank $2j+1$, $2j'+1$, respectively (m running from j to $-j$, m' from j' to $-j'$), then the products $U_m\ V_{m'}$ can be combined to form basis vectors $W_M{}^J$ of irreducible representations of rank $2J+1$. J has values decreasing from $j+j'$ by integers to $|j-j'|$ and $M=m+m'$.

A simple method of carrying out this reduction is given in van der Waerden's *Die Gruppentheoretische Methode in der Quantenmechanik*.[1] The connection between the vectors U, V, W is there given by

$$W_M{}^J = \rho_J \Sigma_m C_{m,\,m'}{}^J U_m V_{m'}, \tag{1}$$

$$C^J{}_{m,\,m'} = \Sigma_\nu (-)^\nu \frac{[(j+m)!(j-m)!(j'+m')!(j'-m')!(J+M)!(J-M)!]^{\frac{1}{2}}}{(j-m-\nu)!(j+m-\lambda+\nu)!(j'+m'-\nu)!\times(j'-m'-\lambda+\nu)!\nu!(\lambda-\nu)!}, \tag{2}$$

$$m' = M-m \qquad \lambda = j+j'-J.$$

The coefficients ρ_J are not determined by van der Waerden's argument. But it is often useful to have the matrix connecting the W's with the UV's unitary. Suitable values of ρ_J can be found as follows:

A necessary condition that the transformation be unitary is

$$\Sigma_m (\rho_J C^J{}_{m,\,M-m})^2 = 1. \tag{3}$$

We evaluate this for the particular case $M=J$. In the series (2), the only term that contributes for this case is $\nu = j-m$ and we find

$$C^J{}_{m,\,J-m} = (-)^{j-m} \frac{[(2J)!]^{\frac{1}{2}}}{(2j-\lambda)!(2j'-\lambda)!} \times \left[\frac{(j+m)!(j'+m')!}{(j-m)!(j'-m')!}\right]^{\frac{1}{2}}. \tag{2a}$$

m can take on values from $j-\lambda$ up to j. With $\sigma = j-m$ as summation index (3) becomes

$$\frac{(2J)!}{[(2j-\lambda)!(2j'-\lambda)!]^2}\rho_J^2\sum_{\sigma=0}^{\lambda}\frac{(2j-\sigma)!(2j'-\lambda+\sigma)!}{\sigma!(\lambda-\sigma)!}=1. \quad (4)$$

The summation over σ can be carried out, either by expressing it as a hypergeometric function, or just by using properties of binomial coefficients. Its value comes out to be

$$(2j-\lambda)!(2j'-\lambda)!\binom{2j+2j'+1-\lambda}{\lambda}$$

and finally

$$\binom{2J}{2j-\lambda}\binom{2J+1+\lambda}{\lambda}\rho_J^2=1. \quad (5)$$

J. M. KELLER

Department of Physics,
University of California,
Berkeley, California,
January 26, 1939.

[1] B. L. van der Waerden, *Die Gruppentheoretische Methode in der Quantenmechanik* (Julius Springer, 1932). A different method, leading to a formally different—though of course equivalent—result is given by Eugen Wigner, *Gruppentheorie und ihre Anwendung auf die Quantenmechanik der Atomspektren* (Friedr. Vieweg and Sohn, 1931).

Disintegration of Uranium

We have observed the disintegration of uranium[1] by neutrons in a cloud chamber containing air, water vapor, and alcohol vapor at a total pressure approximately 15 cm of mercury. The uranium was introduced into the cloud chamber in the form of UO_3 on thin collodion foils. On 885 stereoscopic photographs we have observed 25 examples of two tracks representing heavy particles recoiling in opposite directions, apparently from the same point in the thin foil. The uranium alpha-particle tracks on the same photographs are very faint, and so are easily distinguishable from the heavy tracks. A series of photographs made under similar conditions but with the uranium out of the cloud chamber showed no heavy tracks.

Some of the heavy tracks have short branches associated with them, presumably representing recoil carbon, nitrogen or oxygen atoms, since the tracks are too dense to be protons. In most of these cases the track of the heavy particle is deflected imperceptibly. The accompanying photograph shows two heavy tracks with three short branches. In the branch near the end of the lower track the angle of the fork is measurable when the track is reprojected. If the ratio of masses between the heavy track and the spur were as small as six the heavy track would be deflected by 10°, an easily detectable amount. Thus, assuming that the fork is the track of something at least as heavy as carbon, the mass of the particle in the main track must be greater than 75 mass units.

The maximum range observed for the heavy particles was approximately three centimeters of standard air. We have a few photographs which might be interpreted as showing more than two particles in the disintegration. However, the evidence for such a phenomenon is very meagre. We are continuing the experiments using heavier gases in the cloud chamber in order to measure the mass of the heavy particles from their collisions with the gas atoms.

We wish to express our thanks to Professor E. O. Lawrence for his continued interest in this problem. This work was supported in part by a grant from the Research Corporation.

D. R. CORSON
R. L. THORNTON

Radiation Laboratory,
Department of Physics,
University of California,
Berkeley, California,
February 15, 1939.

[1] O. Hahn and F. Strassmann, Naturwiss. **27**, 11 (1939).

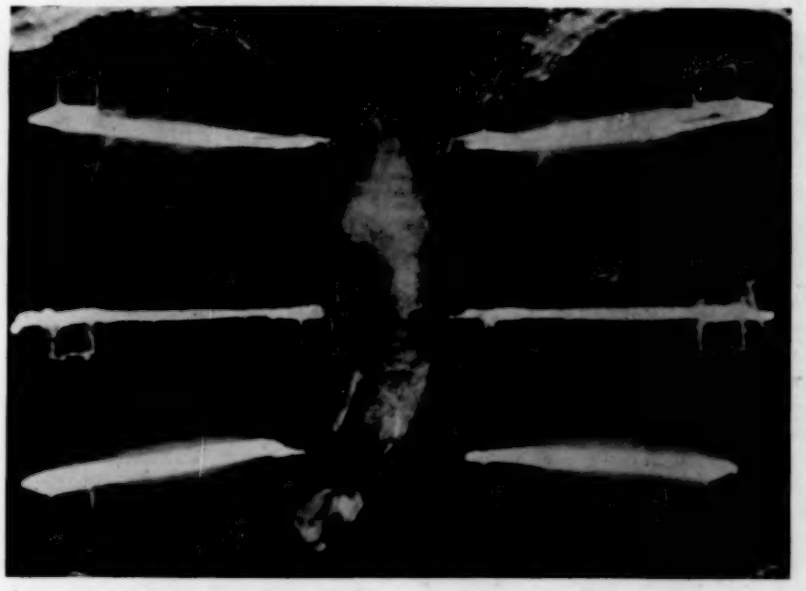

FIG. 1. Photograph showing heavy particles recoiling in opposite directions from uranium film under neutron bombardment.

Radioactive Recoils from Uranium Activated by Neutrons

It has been shown by Hahn and Strassmann[1] and immediately afterward by others[2] in this laboratory and elsewhere that the uranium nucleus under neutrom bombardment sometimes splits into parts with about half the atomic number of uranium, and thus produces radioactive isotopes in the middle of the periodic table. The range of the ejected radioactive particles can be measured by observing the distribution of the activity with depth in a layer of matter placed next to the uranium during bombardment.[3]

An experiment of this kind was done by placing a stack of thin (0.57 mg/cm²) Al foils in contact with a thin layer of UO_3 mounted on paper, and exposing to neutrons from the cyclotron. Then the activities of the separate foils were measured. The results are shown in Fig. 1 which gives

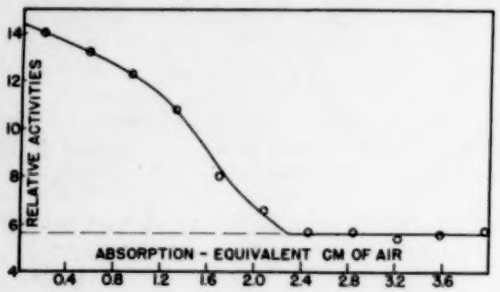

FIG. 1. Relative activities of aluminum foils plotted against the stopping power from the surface of the uranium sample in cm of air equivalent. The points are put at positions corresponding to the centers of the foils. The horizontal line represents the activity induced in the aluminum by the neutrons, and the curve shows the activity deposited by recoil from the uranium. The form of the curve near the end-point is not well determined by the data. The range may be estimated as 2.2±0.2 cm.

the relative activities at about two hours after the end of the bombardment. The horizontal line represents the "background" due to the activity induced in the Al itself. The last foil was omitted from the plot, since its activity is reduced about 30 percent by the recoil of the activated nuclei under the fast neutron impact, which drives some of them into the preceding foil. (The neutron source was to the right in the figure.) If the particles from the uranium had a homogeneous range, the distribution of activity would be rectangular. The observed shape can be explained either by supposing that there is a distribution of ranges, or by taking account of the finite size of the grains of UO_3. These grains have sizes ranging from about 40 microns down to 1/10 this or less. Since the mean diameter represents a stopping power of the order of the observed range, we can say that the results are not incompatible with an initially homogeneous range.

Another experiment was done to find out if there is any correlation between range and decay periods of the products. Cigarette papers of about one cm air equivalent stopping power were used instead of the Al foils. These were extracted with hydrochloric acid before use, and the UO_3 was mounted on filter paper, to avoid all mineral matter that would give extraneous activities. After bombardment, activity was found on the first three sheets of paper. The decay curve of the second sheet was followed for about 24 hours, and of the third for about 12 hours, and they were found to run parallel to that of the first sheet within the accuracy of the measurements. But the decay curve of the uranium sample (including the paper backing) showed quite striking differences from these. The uranium curve has a strong additional component of about 25 minutes half-life, which may be the substance identified by Hahn, Meitner and Strassmann[4] as a uranium isotope produced by resonance neutron capture, and also a long period (~2 day) which is strong compared with any activity of corresponding period in the recoil samples. (The intensity of activation is so great that the natural uranium activity can be neglected.) The ratio of the total activity on the paper sheets to the activity of the uranium sample is about $\frac{1}{6}$ at three hours after bombardment, when this ratio reaches its largest value. This means that at this time the total recoil activity from both sides of the UO_3 sample is about $\frac{2}{3}$ as great as the activity remaining in the uranium. Since a considerable part of the latter consists of the nonrecoiling activities mentioned above, it should be easy to make a complete separation of the recoils from the others by using a more finely divided uranium preparation. This work is being continued. By using thin inactive foils of organic material and a very thin layer of uranium, it should be possible to obtain a very accurate range curve of this method. The financial support of the Research Corporation is very much appreciated.

EDWIN MCMILLAN

Radiation Laboratory,
University of California,
Berkeley, California,
February 17, 1939.

[1] O. Hahn and F. Strassmann, Naturwiss. **27**, 11 (1939).
[2] These are too numerous to give individual references here.
[3] The same idea occurred to F. Joliot, who performed a similar experiment, and communicated the results in a letter to Professor E. O. Lawrence, received during the course of the above work. Joliot's result was reported at the January 30 meeting of the French Academy of Sciences. He found a recoil range of about 3 cm.
[4] L. Meitner, O. Hahn and F. Strassmann, Zeits. f. Physik **106**, 249 (1937).

Further Observations on the Splitting of Uranium and Thorium

Continuing a survey of the effects produced by bombarding uranium and thorium with neutrons we have measured the range of the energetic particles emitted. This was done by coating a movable plate with the substance to be investigated and observing the distance at which the particles could no longer be detected by an ionization chamber with a gauze front, connected to a pulse amplifier. The ranges found were 10.5±1 mm and 12.0±2 mm for the particles from uranium and thorium, respectively.

To test the possibility of the delayed emission of neutrons a boron-lined ionization chamber was placed a few centimeters from a lithium target used as a source of neutrons, both the chamber and the target being surrounded with paraffin. With this arrangement no pulses were observed after the deuteron bombardment was stopped. However, when a bottle containing about 100 grams of uranium nitrate was placed between the source

and the chamber, neutrons were observed as long as 1¼ minutes after the bombardment of the uranium, the initial intensity being about one neutron per second. The decay period of these neutrons was observed to be 12.5±3 sec.

Since delayed neutron emission could be due to photo-disintegration by gamma-rays we looked for and found a hard gamma-ray of approximately the same period. If these gamma-rays are the cause of the neutron emission, separate intensity tests showed that they must be at least 1000 times as effective as the lithium or fluorine gamma-rays produced by proton bombardment. No neutrons were observed with the same arrangement during proton bombardment of lithium or fluorine targets, although several photoneutrons per second were observed from a few grams of heavy water.

The period of the neutrons and gamma-rays is close to one of the beta-ray periods observed by Meitner, Hahn, and Strassmann.[1] It is possible that the gamma-ray emission follows the 10-sec. beta-ray emission observed by them, and causes or is accompanied by the emission of neutrons.

R. B. Roberts*
R. C. Meyer
P. Wang†

Department of Terrestrial Magnetism,
Carnegie Institution of Washington,
Washington, D. C.,
February 18, 1939.

* Carnegie Institution Fellow.
† Fellow of the China Foundation.
[1] L. Meitner, O. Hahn, and F. Strassmann, Zeits. f. Physik **106**, 249–270 (1937).

Presence of the Nitrogen Forbidden Line $^2P \rightarrow {}^4S$ in the Auroral Spectrum

I have recently reported the probable presence of the N I line $^2P \rightarrow {}^4S$ in the spectrum of diffuse aurorae.[1] A preliminary study of my plates had caused me to ascribe to this radiation a wave-length near 3470A, deduced from the approximate dispersion curve given by the N_2 bands of the second positive system. However, I had also at my disposal a plate with a comparison spectrum from a small luminescence lamp containing a mixture of neon and argon. The identification of all the lines appearing on the plate enabled me to make sure that the auroral radiation practically coincides with the neon line λ=3,466,575A, and also that, in the proper spectral region, my spectrograph is capable of distinguishing clearly lines only 3A apart. Under these conditions, I can affirm that the true wave-length of the line attributed to N I is: λ=3466.5±1A.

This value is in good accordance with the theoretical wave-length λ=3466.6A deduced from the ionization potential of N I (14.48 v, or 117,375 cm^{-1}, according to Hopfield). Besides, using Edlèn's still unpublished results concerning the excitation potentials of the N I levels, M. Nicolet[2] computes the value λ=3466.5A. On the other hand, J. Kaplan[3] now finds, for the line observed by him in the laboratory, the corrected wave-length λ=3466.3A, with an approximation of a few tenths of an angstrom. Thus, the best measurements of the lines found, near 3466A, in the afterglow and aurora spectra, indicate that their identity is highly probable, as well as the presence of ^2P nitrogen neutral atoms in the upper atmosphere.

According to B. Stepanoff,[4] the splitting of the ^2P level of N I would be nearly 2.15 cm^{-1}. It corresponds to a difference of one-fourth of an angstrom between the components of the line $^2P \rightarrow {}^4S$. Such a structure will be shown only by the interference method.

No night-sky radiation can be actually identified with the N I line λ=3466.5A, unless by assuming an error of 4 to 5A in the measurement of the strong sky line found at λ=3471A.

René Bernard

Institut de Physique Générale de l'Université de Lyon,
Lyon, France,
February 6, 1939.

[1] R. Bernard, Nature **141**, 1140 (1938).
[2] M. Nicolet, private communication.
[3] J. Kaplan, Phys. Rev. **54**, 541 (1938).
[4] B. Stepanoff, Phys. Zeits. Sowjetunion **8**, 353 (1935).

The Fission of Uranium*

This letter is a preliminary report of some of the experiments which we have undertaken on the fission process of the uranium nucleus by neutron bombardment.

The phenomenon was discovered by Hahn and Strassmann[1] who were led by chemical evidence to suspect the possibility of the splitting of the uranium nucleus into two approximately equal parts. Through the kindness of Professor Bohr we were informed of these results some days before receiving them in published form, as well as of the suggestion of Meitner and Frisch that the process should be connected with the release of energy of the order of 200 Mev.

It seemed worth while to attempt the detection of the fragments by their high ionization. The interior of a parallel plate ionization chamber was coated with a thin layer of uranium oxide. When this chamber was connected to a linear amplifier a large number of small pulses from the alpha-particles of uranium were observed, but when exposed to the bombardment of neutrons from the cyclotron or from a Rn-Be source very large pulses occurred in addition. From the ratio of the maxima of these large pulses to the maxima of those due to the alpha-particles it was estimated that the energies of the fragments of uranium range up to about 90 Mev. This value of the energy seems to be somewhat smaller than the theoretical expectation. If we assume that the energy release in the fission is approximately 200 Mev, and that the two fragments may have somewhat different masses, then fragments with energies up to 120 or 130 Mev might be expected in some cases. However, these values probably do not lie outside our experimental error since lack of linearity in the amplifier and incomplete collection of the ions might explain the difference.

After this experiment had been performed, Professor Bohr received a cable from Dr. Frisch stating that he had obtained the same results some days before.

A number of measurements have been made of the cross section for the fission process for neutrons of different energies. For this the interior of an ionization chamber

was coated, by electrolytic deposition, with a layer of uranium oxide of only 0.5 mm air equivalent, so that all the fission processes could be observed. In order to know the number of neutrons, a Rn-Be source of known intensity was utilized in a standard position inside a paraffin block.[2] In order to obtain the contributions of the thermal neutrons only, the difference in the number of fissions was measured with and without a cadmium absorber. These experiments gave a cross section of thermal neutrons for the fission process alone of about 2×10^{-24} cm^2. Fast neutrons from a Rn-Be source have instead an average cross section of about 0.1×10^{-24} cm^2.

By using a similar chamber with a thicker uranium oxide coating, the changes in the fission activity due to the interposition of cadmium and boron filters were determined and compared with those obtained when the same chamber was coated with boron instead of uranium. Within the limits of the experimental error the behavior for slow neutrons of the absorbers for the fission process and for the boron disintegration was the same. This suggests that the efficiency of slow neutrons for the fission process follows a $1/v$ law. As mentioned above, fast neutrons are relatively more efficient in producing the fission process than they are in the boron disintegration.

The validity of the $1/v$ law makes it probable that the levels of the compound nucleus are broadened by the short lifetime (probably not more than 10^{-17} sec.) of the fission process. There seems to be some contradiction between this result and the known fact that uranium has a sharp resonance for slow neutrons of about 25 ev that does not lead, however, to the fission but to the formation of U^{239}. As suggested by Professor Bohr a possible explanation is that the fission does not occur from U^{238} but from U^{235}, which is present in an amount of somewhat less than 1 percent.

The range of the fragments has been measured by allowing the fragments to enter a shallow ionization chamber 1.0 cm from the uranium through a grid. By varying the pressure the maximum range has been determined to be approximately 1.7 cm.

The recoil fragments from irradiated uranium have been collected upon a Cellophane foil placed next to it. After a ten-minute irradiation with slow neutrons from the cyclotron, the Cellophane foil showed an activity of about 400 counts per minute when wrapped around a counter. The decay of this activity indicated the presence of several periods which have not yet been analyzed. Interposition of an 0.0012 Cellophane foil between the uranium and the collecting foil showed that a small fraction of the recoil fragments passes through, in fair agreement with the range measurement. While these experiments were in progress we were informed by Professor Bohr that a similar experiment had been suggested by Miss Meitner.

We are indebted to Dr. J. Steigman, H. B. Hanstein and E. Haggstrom for their assistance in carrying out these experiments.

H. L. Anderson
E. T. Booth
J. R. Dunning
E. Fermi
G. N. Glasoe
F. G. Slack

Pupin Physics Laboratories,
Columbia University,
New York, New York,
February 16, 1939.

* Publication assisted by the Ernest Kempton Adams Fund for Physical Research of Columbia University.
[1] O. Hahn and F. Strassmann, Naturwiss. **27**, 11 (1939).
[2] E. Amaldi and E. Fermi, Phys. Rev. **50**, 899 (1936).

Proceedings of the New York State Section of the American Physical Society

Minutes of the Fall Meeting

University of Rochester, November 5, 1938

THE New York State Section of the American Physical Society met at the University of Rochester on Saturday, November 5, 1938. 183 persons registered, but nearly a hundred more were in attendance some time during the day.

The following papers were presented:

Morning Session

Color Photography. KENNETH C. E. MEES, *Eastman Kodak Company.*

Thermometers. BRADFORD NOYES, *Taylor Instrument Company.*

Afternoon Session

The Mechanism of Fluorescence. SAUL DUSHMAN, *General Electric Company.*

Preparation for College Physics. BRIAN O'BRIEN, *University of Rochester.*

The Cyclotron. LEE DUBRIDGE, *University of Rochester.*

In the business sessions, plans were made for completing minor revisions to the constitution and by-laws at the spring meeting. Seven additional charter members were enrolled, and twenty-five new members for 1939 paid their dues bringing the total membership up to 115.

Professor DuBridge and his associates demonstrated the cyclotron in operation, besides other experimental projects. Some members took advantage of the opportunity to visit the laboratories of either the Eastman Kodak Company, Bausch and Lomb Optical Company or the Taylor Instrument Company on Friday afternoon.

An informal dinner concluded the day followed by remarks by the Chairman, Dr. Wold and the Vice Chairman, Dr. Rayton. Announcement was made that the spring meeting would be held at Hamilton College, Clinton.

PAUL R. GLEASON
Secretary